

NISTIR 7355

**Development of a Fluorescence Based
Measurement Technique to Quantify
Water Contaminants at Pipe Surfaces
During Flow**

Mark A. Kedzierski

NIST

National Institute of Standards and Technology
Technology Administration, U.S. Department of Commerce

NISTIR 7355

Development of a Fluorescence Based Measurement Technique to Quantify Water Contaminants at Pipe Surfaces During Flow

Mark A. Kedzierski

U.S DEPARTMENT OF COMMERCE
National Institute of Standard and Technology
Building Environment Division
Building and Fire Research Laboratory
Gaithersburg, MD 20899-8631

September 2006



U.S. Department of Commerce
Carlos M. Gutierrez, Secretary

National Institute of Standards and Technology
William A. Jeffrey, Director

Development of a Fluorescence Based Measurement Technique to Quantify Water Contaminants at Pipe Surfaces During Flow

M. A. Kedzierski

National Institute of Standards and Technology

Bldg. 226, Rm B114

Gaithersburg, MD 20899

Phone: (301) 975-5282

Fax: (301) 975-8973

ABSTRACT

This paper provides a detailed account of the development of a fluorescence based measurement technique for measuring the mass of contaminant on solid surfaces in the presence of water flow. A test apparatus was designed and developed for the purpose of studying adsorption and desorption of diesel to and from a copper test surface in the presence of contaminated and fresh water flow, respectively. A calibration technique was developed to correlate the measured fluorescence intensity to the mass of diesel adsorbed per unit surface area (the excess surface density) and the bulk concentration of the diesel in the flow. Both bulk composition and the excess surface density measurements were achieved via a traverse of the fluorescent measurement probe perpendicular to the test surface. Two nominal bulk mass fractions (0.2 % and 0.3 %) were tested each for five different Reynolds numbers between zero and 7000. Measurements for a given condition were made over a period of approximately 200 h. The measured diesel excess surface density varied between zero and 0.02 kg/m^2 for the variation in the bulk mass fraction and Reynolds number of the flow. Normalized Freundlich constants were calculated for the various bulk mass fractions and Reynolds numbers.

Keywords: adsorption, contaminant, diesel, excess layer, fluorescence, measurement technique, sorption, water

LIST OF TABLES

ABSTRACT.....	4
EXPERIMENTAL APPARATUS AND UNCERTAINIES.....	9
TEST FLUIDS.....	11
MEASUREMENTS AND UNCERTAINTIES.....	12
<i>Fluorescence/Mass Calibration.....</i>	<i>12</i>
<i>Application of Calibration.....</i>	<i>15</i>
<i>Air Gap Calibration.....</i>	<i>17</i>
MEASUREMENT RESULTS	17
<i>Excess Layer Thickness.....</i>	<i>17</i>
<i>Freundlich Constants.....</i>	<i>19</i>
DISSCUSSION.....	20
CONCLUSIONS	20
NOMENCLATURE.....	22
<i>English Symbols.....</i>	<i>22</i>
<i>Greek symbols.....</i>	<i>22</i>
<i>English Subscripts.....</i>	<i>22</i>
<i>Superscripts</i>	<i>23</i>
REFERENCES.....	24
APPENDIX A: EXCITATION AND EMISSION WAVELENGTHS	38
APPENDIX B: DIESEL PROPERTIES.....	40
<i>Liquid Density.....</i>	<i>40</i>
<i>Kinematic Viscosity.....</i>	<i>40</i>
APPENDIX C: HYDROLYZED DIESEL.....	43
APPENDIX D: FLUORESCENCE TEMPERATURE DEPENDENCE.....	45
APPENDIX E: FLUORESCENCE CALIBRATION.....	46
APPENDIX F: LINEAR BEER LAW	51
APPENDIX G: UNCERTAINTIES	53
APPENDIX H: TABULATED MEASUREMENTS.....	55
APPENDIX I: SPECTROFLUOROMETER CHECK.....	81

LIST OF FIGURES

Fig. 1 Schematic of test loop.....	25
Fig. 2 Schematic of spectrofluorometer, test section, and linear positioning device.....	26
Fig. 3 Schematic of right angle spectrofluorometer.....	27
Fig. 4 Cross-sectional illustration of test section during contamination and flushing... 28	28
Fig. 5 Schematic of fluorescence/composition calibration jar	27
Fig. 6 Overall calibration of Beer-Lambert Bougher law for diesel on copper disk	30
Fig. 7 Demonstration of excess layer thickness measurement	31
Fig. 8 Effect of exposure time and flow rate on thickness of the diesel excess layer for a 0.2 % bulk freestream mass fraction.....	32
Fig. 9 Effect of exposure time and flow rate on thickness of the diesel excess layer for a 0.3 % bulk freestream mass fraction.....	33
Fig. 10 Diesel excess layer thickness as a function of Re for water/diesel (99.8/0.2).....	34
Fig. 11 Diesel excess layer thickness as a function of Re for water/diesel (99.7/0.3).....	35
Fig. 12 Normalized Freundlich constants for diesel adsorption to an oxidized Cu disk from diesel contaminated water.....	36
Fig. A.1 Emission and excitation spectra for diesel	38
Fig. A.2 Filtered excitation and emission spectra for diesel.....	39
Fig. B.1 Measured liquid density of diesel and fit.....	41
Fig. C.1 Fluorescent emission spectra for pure diesel and hydrolyzed reservoir test fluid.....	43
Fig. D.1 Temperature dependence of diesel fluorescence.....	45
Fig. E.1 Calibration of diesel fluorescence against diesel mass fraction for different runs	48
Fig. E.2 Filtered excitation and emission spectra for diesel	49
Fig. E.3 Calibration of diesel fluorescence intensity for fixed film thickness and air gap between quartz tube and liquid film	50
Fig. F.1 Absorbance of diesel for calibration measurements as a function of mass	52
fraction	52
Fig. G.1 Relative uncertainty of l_e for 95 % confidence level and $x_b = 0.2$ %	53
Fig. G.2 Relative uncertainty of l_e for 95 % confidence level and $x_b = 0.3$ %	54
Fig. I.1 Verification of spectrofluorometer wavelength with Mercury standard.....	82

LIST OF TABLES

Table B.1 Diesel liquid density measurements (file:DieDen.dat).....	42
Table B.2 Diesel #2 liquid kinematic viscosity measurements (Simplex, 2006).....	42
Table H.1.1 Diesel contamination on oxidized copper surface for $Re = 0$ and $x_b = 0.2\%$	55
Table H.1.2 Diesel contamination on oxidized copper surface for $Re = 1900$ and $x_b = 0.2\%$	56
Table H.1.3 Diesel contamination on oxidized copper surface for $Re = 3200$ and $x_b = 0.2\%$	57
Table H.1.4 Diesel contamination on oxidized copper surface for $Re = 4600$ and $x_b = 0.2\%$	58
Table H.1.5 Diesel contamination on oxidized copper surface for $Re = 7000$ and $x_b = 0.2\%$	59
Table H.1.6 Tap water flushing after $Re = 4600$ contamination tests at $x_b = 0.2\%$	60
Table H.1.7 Diesel contamination on oxidized copper surface for $Re = 0$ and $x_b = 0.3\%$	61
Table H.1.8 Diesel contamination on oxidized copper surface for $Re = 2000$ and $x_b = 0.3\%$	62
Table H.1.9 Diesel contamination on oxidized copper surface for $Re = 4000$ and $x_b = 0.3\%$	63
Table H.1.10 Diesel contamination on oxidized copper surface for $Re = 5000$ and $x_b = 0.3\%$	64
Table H.1.11 Diesel contamination on oxidized copper surface for $Re = 7000$ and $x_b =$ 0.3%	65
Table H.1.12 Tap water flushing after $Re = 5000$ contamination tests at $x_b = 0.3\%$	66
Table H.1.13 Tap water flushing after $Re = 7000$ contamination tests at $x_b = 0.3\%$	67
Table H.2.1 Diesel contamination on oxidized copper surface for $Re = 0$ and $x_b = 0.2\%$	68
Table H.2.2 Diesel contamination on oxidized copper surface for $Re = 1900$ and $x_b = 0.2\%$	69
Table H.2.3 Diesel contamination on oxidized copper surface for $Re = 3200$ and $x_b = 0.2\%$	70
Table H.2.4 Diesel contamination on oxidized copper surface for $Re = 4600$ and $x_b = 0.2\%$	71
Table H.2.5 Diesel contamination on oxidized copper surface for $Re = 7000$ and $x_b = 0.2\%$	72
Table H.2.6 Tap water flushing after $Re = 4600$ contamination tests at $x_b = 0.2\%$	73
Table H.2.7 Diesel contamination on oxidized copper surface for $Re = 0$ and $x_b = 0.3\%$	74
Table H.2.8 Diesel contamination on oxidized copper surface for $Re = 2000$ and $x_b = 0.3\%$	75
Table H.2.9 Diesel contamination on oxidized copper surface for $Re = 4000$ and $x_b = 0.3\%$	76
Table H.2.10 Diesel contamination on oxidized copper surface for $Re = 5000$ and $x_b = 0.3\%$	77

Table H.2.11 Diesel contamination on oxidized copper surface for $Re = 7000$ and $x_b = 0.3\%$	78
Table H.2.12 Tap water flushing after $Re = 5000$ contamination tests at $x_b = 0.3\%$	79
Table H.2.13 Tap water flushing after $Re = 7000$ contamination tests at $x_b = 0.3\%$ (file:flsh6c2.tb2).....	80
Table I.1 Calibration check of spectrofluorometer against Mercury lamp.....	881

INTRODUCTION

Since the signing of the Executive Order establishing the Office of Homeland Security, Federal agencies have been working on ways to improve the security of the general public. One way in which the National Institute of Standards and Technology (NIST) is doing its part is by helping the U.S. Environmental Protection Agency (EPA) devise ways to safeguard the nation's drinking water supply. EPA is conducting potable water research with NIST on six different efforts. This report describes one of those efforts designed to fundamentally understand the attachment and detachment mechanisms of contaminants to solid plumbing materials under dynamic water flow conditions. The results of this work provide EPA with an investigative tool to support the development of a response to water contamination events and a potential detection technique for timely warning of such events.

The purpose of this study is to apply a NIST fluorescence based measurement technique that was developed for measuring the mass of lubricant at the wall during boiling of refrigerants (Kedzierski, 2001) to measuring the mass of diesel on a copper pipe surface in the presence of flowing water/diesel mixture. In this way, we not only gain vital fundamental modeling information but we lay the groundwork for a possible early detection/monitoring system for sticky contaminants. Two major efforts have been focused toward the development of an in situ fluorescent measurement technique. First, a calibration technique was developed specifically for quantifying the amount of diesel on a copper pipe surface. Second, a water loop was designed and constructed consisting of a test chamber for subjecting small samples of pipe substrate materials to known concentrations of diesel/water solutions under controlled dynamic flow conditions. These two efforts have formed the foundation for future work that will focus on using the water loop and the calibration technique to measure the accumulation and removal of diesel as a function of free-stream diesel concentration and flow rate.

Commercial diesel was used rather than a chemically simpler surrogate in order to demonstrate the use of the technique with an actual potential contaminant. Diesel was also a desirable test contaminant because it has been found to exhibit a strong fluorescence. However, because of the complexity and the variability of diesel, the diesel for the project was restricted to a single batch. In this way, we can ensure the consistency of the properties of pure diesel¹ such as its liquid density and fluorescence characteristics.

EXPERIMENTAL APPARATUS AND UNCERTAINTIES

The standard uncertainty (u_i) is the positive square root of the estimated variance u_i^2 . The individual standard uncertainties are combined to obtain the expanded uncertainty (U), which is calculated from the law of propagation of uncertainty with a coverage factor. All measurement uncertainties are reported at the 95 % confidence level except where specified otherwise.

Figure 1 schematically shows the flow loop for measuring diesel on pipe substrates. The primary components of the loop are the pump, the reservoir, and the test chamber with the test section. The inside surfaces of the approximately 96 mm x 1.6 mm rectangular flow cross-section of the aluminum test chamber, shown in Fig. 2, were black anodized to

¹ "Pure diesel" is used here to denote that the particular batch of diesel, which will be consistently used throughout this project, is not mixed with water.

minimize stray light reflections. The channel was designed to have the same flow area as a 13 mm diameter copper tube. The test chamber had a circular cavity to accept the solid pipe test section. The height of the channel was 1.6 mm so that the probe could be flush to the top of the test section while maintaining proximity to the test surface for measurement purposes without being an obstruction to the flow. A centrifugal pump delivered the contaminated water to the entrance of the rectangular test chamber at room temperature. The pump head was removable so that it could be easily replaced in order to test a different contaminant. The flow rate was controlled and varied by varying the pump speed with a frequency inverter. A heat exchanger immersed in the reservoir was supplied with brine from a temperature-controlled bath to maintain the entrance temperature to the test chamber at ambient temperature (293.8 K). This was done to ensure that the diesel was at the same temperature as it was during the fluorescence calibration to avoid the temperature effect on fluorescence (Miller, 1981). An additional temperature-controlled bath was used to maintain the fluorescence standards at the same ambient temperature.

Residential copper pipe was used to plumb together the various components of the loop. Redundant volume flow rate measurements were made with an ultrasonic doppler and a turbine flowmeter with expanded uncertainties of $\pm 0.12 \text{ m}^3/\text{h}$ and $\pm 0.03 \text{ m}^3/\text{h}$, respectively. As shown in Fig. 1, three water pressure taps before and after the test chamber permit the measurement of the upstream absolute pressure and the pressure drops along the test section with expanded uncertainties of $\pm 0.24 \text{ kPa}$ and $\pm 1.5 \text{ kPa}$, respectively. Also, a sheathed thermocouple measured the water temperature at each end of the test chamber to within an uncertainty of $\pm 0.25 \text{ K}$. The dissolved oxygen level, the conductivity, and the pH, were monitored at the water reservoir with associated B-type uncertainties of $\pm 0.5 \%$, $\pm 50 \mu (\Omega\text{cm})^{-1}$, and ± 0.3 , respectively.

Figure 1 also shows the inlet and exit taps that were used to flush the test section with fresh tap water. In preparation for flushing, the test section was isolated with valves from the rest of the test loop. Then the fluid was drained from the test chamber and returned to the reservoir. Next, a tap water supply was connected to a test chamber port. The other test chamber port was connected to a filter to absorb any diesel before it was sent to a drain.

Figure 2 shows a view of the spectrofluorometer that was used to make the fluorescence measurements and the test chamber with the fluorescence probe perpendicular to the flattened pipe test surface. Figure 3 shows a simplified schematic of the right angle spectrofluorometer consisting of a xenon light source, an excitation and an emission monochromator, and an emission photomultiplier tube (detector). The spectrofluorometer was designed to accept $45 \text{ mm} \times 10 \text{ mm} \times 10 \text{ mm}$ fluorescent samples or cuvettes filled with fluorescent material. A special adapter with lenses and mirrors, which replaced the cuvette holder, was fabricated to remotely excite and measure fluorescence via a bifurcated optical bundle. Two optical bundles consisting of 84 fibers each originated from the spectrofluorometer. One of the bundles transmitted the excitation light, i.e., the incident intensity (I_0), to the test pipe surface. The other bundle carried the emission, i.e., the fluorescence intensity (F), from the test surface to the spectrofluorometer. The optical bundles originating from the spectrofluorometer merge transmitting and receiving fibers randomly into a single probe before entering the test section chamber. The sensor end of the

fluorescence probe is sheathed with a quartz tube to protect it from reacting with the contaminant in the test fluid.

As the name suggests, right angle spectrometry was designed to limit the interference of the excitation signal on the emission signal by orientating the detector perpendicular to the beam of the emission monochromator. Considering this, the parallel configuration of the excitation and emission at the measuring end of the bifurcated optical bundle as shown in Fig. 2 is not ideal but was necessary for this application. The parallel configuration allows the reflection of the excitation from the copper surface to be transmitted through the emission fiber optics and to the detector. This can be a serious limitation given that the reflected excitation can overwhelm the emission signal even if the emission wavelength (λ_m) and the excitation wavelength (λ_x) differ because: (1) the excitation intensity can be several orders of magnitude greater than that of the fluorescence emission, and (2) the filtering process of the emission monochromator is not complete enough to entirely remove the reflected wave. The filtering process of the monochromator supplies the detector with an intensity that is distributed about the desired wavelength but with relatively small tails at larger and smaller wavelengths. Consequently, if the excitation intensity is very large, the tails of the excitation distribution can be greater than the peak emission intensity. A successful remedy for reducing the interference of the excitation signal was to place a 10 nm bandwidth bandpass interference filters at the exit of the excitation monochromator and one before the entrance to the emission monochromator. Figure 3 schematically shows the placement of the bandpass interference filters.

The excitation wavelength and the emission wavelength were set to 434 nm and 485 nm, respectively, for all tests. As Appendix A details, the choice of these wavelengths ensured that a significant and measurable emission signal was obtained with no measurable overlap of the excitation and emission spectra.

TEST FLUIDS

A 2 % by mass diesel mixture was prepared with local Gaithersburg, MD tap water and the mixture was left to form a colloid for approximately 3 months to provide sufficient time for the diesel and the water to reach equilibrium. While the method of preparation may not reflect the most likely contamination scenario, the methodology does provide a consistent test fluid for examining the effect of flow rate on contamination because the flow rate is varied for fixed fluid properties. The measured dissolved oxygen level, the conductivity, and the pH, of the water at 24 °C before mixing with diesel were found to be, 86.4 %, 358 $\mu\Omega/\text{cm}$, and 7.04, respectively. Number 2 diesel fuel was used from a single batch throughout the experiment to avoid property variations that might be caused by batch variations due to it being a complex mixture of hydrocarbons. Appendix B provides the measured viscosity and density of the pure diesel liquid.

Because diesel is a complex mixture, its hydrolysis results in a dispersed phase of differing components that reside in separate regions of the colloid depending on the density, dispersion size, and hydrophobic nature of each component. If quiescent, the test reservoir had a stable Brownian suspension within the bulk water, which likely differed chemically from the dispersed phase that floated on top of the bulk liquid, and that which rested on the bottom of

the reservoir. The result of and the evidence for a chemical breakdown of the diesel is given in Appendix C, which shows that the peak fluorescence emission for the emulsified water diesel mixture taken from the reservoir exists at a wavelength that is 25 nm greater than that of pure diesel. Because of the hydrolysis of diesel, positive and/or negative bias errors are likely to occur in the mass measurement depending on the individual spectra of the fluorescing components of the hydrolyzed diesel. For example, a positive bias error may result because nonfluorescent components that contributed to the diesel mass during the calibration may not deposit on the surface. Likewise, a negative bias error may occur because the peak intensity of the fluorescent material on the test surface has shifted from that of the calibration.

The hydrolysis of the diesel and the configuration of the inlet and the outlet of the reservoir influence the flow in the test section. As shown schematically in Fig.1, the opening of the pump suction line in the reservoir is situated approximately 10 mm below the liquid-air interface. This design entrains the hydrolyzed diesel floating on the water surface with that in the bulk water, and on the bottom of the reservoir into the pumped flow. The return flow entering the bottom of the reservoir ensured good flow mixing. Figure 4 depicts the colloidal flow within the test section and the fluorescent measurement probe above it for the contamination and decontamination test conditions. The size of the droplets in the dispersed flow is exaggerated for illustration purposes. Both test conditions are shown to have an excess layer thickness (l_e) of undiluted hydrolyzed diesel adsorbed to the test surface. Because the molar mass of the diesel is unknown, the surface excess density (Γ) is defined in the work on a mass basis as (Kedzierski, 2001):

$$\Gamma = l_e(\rho_d - \rho_b x_b) \quad (1)$$

The density of liquid diesel is ρ_d . The density of the bulk mixture ρ_b is evaluated at the bulk mass fraction of the mixture (x_b). The surface excess density is roughly the mass of diesel attached per surface area. The Γ and l_e are the primary measurements of this study.

MEASUREMENTS AND UNCERTAINTIES

Fluorescence/Mass Calibration

Fluorescence as a means for detecting a contaminant has its advantages in that its absorption and fluorescence spectra are like a fingerprint that can be used in its identification. Consequently, by isolating the wavelength of light that the contaminant fluoresces, its intensity can be used to identify its mass. This is true even when the contaminant is mixed with another fluorescent or nonfluorescent substance as long as the fluorescent substance does not absorb and emit at the same wavelengths as the contaminant. For this reason, the tap water was examined and it was not found to fluoresce at any wavelength for any excitation wavelengths between the range of 200 nm and 800 nm. Consequently, interference from water is not possible via it contributing to the intensity of the fluorescence signal.

The calibration technique that was developed here for detecting the mass of diesel on a copper surface exposed to a flowing dilute mixture of diesel in water is introduced in the following. Two different calibration methods had to be combined due to the additional

complexity caused by immiscible liquids. Both calibration techniques were used to quantify different functional aspects of the Beer-Lambert-Bouguer law (Amadeo et al., 1971), which forms the basis of the calibration equation. The first method is essentially the same as the original NIST calibration method that was used to detect lubricants on boiling surfaces (Kedzierski, 2002). This methodology was used to obtain the relationship between diesel composition and fluorescence intensity for a fixed light path length (fixed probe height above the test surface).² The second method, that was developed in this study, relies on a perpendicular traverse of the flow stream with the measurement probe. To achieve this, a linear positioning device with a graduated knob was adapted to the quartz tube as shown in Fig. 2. The second method (traverse method) is used to calibrate the effect of contaminant thickness (path length) and the proximity of incident intensity. The traverse method is essential for splitting the total measured fluorescent intensity into two components: that from the diesel on the test surface and that from the diesel in the bulk flow stream. In this way, the mass of diesel on the test surface and the composition of the fluid stream are determined.

Figure 5 shows the vessel that was used in the first method to calibrate the fluorescence intensity received from the bifurcated optical bundle against the mass fraction of diesel. The lid of the 150 mL black, anodized, metal jar had a port for evacuation³ and filling of the test sample and a fitting to seal around the stainless tube that pierced the lid. The stainless tube had a quartz tube and a quartz bottom welded to its end and it was the same type that was used in the test chamber of Fig. 2. A disk of copper pipe material was placed on the bottom of the jar. By using the same material and surface roughness, the disk and the test pipe had the same reflective properties. Copper from a flattened pipe was evenly oxidized by electrolysis and soldered to the top of the calibration disk that had circumferentially machined grooves for sealing in the test chamber. The same disk was used as the calibration disk and the test surface to compensate for unknown surface effects. The distance between the top of the calibration disk and the bottom of the quartz tube was set with the aid of a 1.6 mm Teflon⁴ gauge disk and micrometer dial indicators. This fixes the path length of the fluorescence and the mass of fluorescent liquid below the probe. During calibration, the jar and the portion of the quartz tube above the lid were covered with black insulation to prevent the optical probe from receiving ambient light. The probe rested on the inside-bottom of the quartz tube.

Three jars were used to calibrate the mass fraction of diesel to the fluorescent intensity. Two jars were used as standards to set the lower (0) and upper (100) limits of the intensity signal on the spectrofluorometer. A jar that contained only pure water was used to zero the intensity. Because light intensities are additive, the zeroing ensured that the reflected

² The first method would have been sufficient had the bulk composition of the flow remained the same as it was charged in the reservoir. Due to the immiscibility of the two fluids, the bulk composition of the flow differs from that in the reservoir.

³ It has been found that weak evacuation of a vessel containing diesel does not measurably change its fluorescent characteristics.

⁴ Certain trade names and company products are mentioned in the text or identified in an illustration in order to adequately specify the experimental procedure and equipment used. In no case does such an identification imply recommendation or endorsement by the National Institute of Standards and Technology, nor does it imply that the products are necessarily the best available for the purpose.

excitation wave and other effects were not attributed to fluorescence. A second jar that contained pure diesel was used to set the intensity on the spectrofluorometer to 100. The third jar was used to measure and record the intensity of various mixtures of diesel and nonfluorescent n-decane of different concentrations. N-decane was used instead of water because it was miscible with diesel and also non-fluorescent. As an additional precaution, all raw-measured intensities (F_r) were numerically normalized by the intensity from the zero-jar (F_0) and the maximum-jar (F_{100}):

$$F = \frac{F_r - F_0}{F_{100} - F_0} \quad (2)$$

where the intensity of the contamination data was adjusted (see Appendix D) by no more than 0.3 % to account for the small (typically within ± 1 K) difference in temperature between the test section and the bath containing the maximum- and the zero-jars. The maximum correction for the flushing data was greater (1.5 %) than for the contamination measurements due to the colder temperature of the house tap water.

Evacuation of the jar was done to prevent fluorescence quenching by oxygen (Guilbault, 1967). N-decane was used because it is miscible with diesel. Calibration measurements proceed by successively adding or removing diesel in appropriately small increments. As shown in Appendix E, the fluorescence intensity was fitted linearly with respect to the diesel mass fraction to within a residual standard deviation of ± 1.2 %.

The second calibration method involved pure diesel alone and varying the thickness of the diesel below the quartz probe to determine the effect of the proximity of the incident light (I_o) and its path length (l). For these tests, the probe was traversed through the diesel and diesel thickness below the quartz probe was synonymous with the path length. As shown in Fig. 2, a linear positioning device with a graduated knob was used to locate the quartz tube relative to the test surface and thus measure the path length of the incident light through the diesel. The measured fluorescent intensity versus the path length was non-linear as shown in Appendix E. Given that the intensity versus mass fraction followed a linear relationship, the nonlinear aspect of the intensity versus l was due to the variation in the incident intensity with l . For this reason, further calibrations were done with fixed diesel film thickness and variable path lengths and it was observed that $\frac{1}{F} \frac{dF}{dl}$ was approximately constant for all ranges of the F and l traverse data for fixed diesel film thickness. This demonstrates the exponential dependence of I_o with the proximity of the probe to the diesel (l) and that this was the cause of the nonlinear calibration with respect to l . The I_o path length effect is known as excitation absorbance (Herman, 1998), which results from the diesel nearest to the light source receiving more excitation than the diesel that is further away.

The linear form of the Beer-Lambert-Bouguer law (Amadeo et al., 1971) was used to correlate the measured intensity of the fluorescence emission (F) to the mass of diesel:

$$F = 2.3I_o \epsilon c l \Phi \rightarrow [\epsilon c l \leq 0.05] \quad (3)$$

Here c is the concentration of the fluorescent diesel, which can be rewritten as a product of the bulk contaminant (diesel) mass fraction (x_b) and the bulk liquid mixture density (ρ_b) divided by the molar mass of the contaminant (M_c). Appendix F shows that the linear criteria for eq. (3) ($\varepsilon cl \leq 0.05$) is satisfied for 78% of the calibration data and the absorbance (εcl) did not exceed 0.063. In addition, the use of the full, nonlinear Beer-Lambert-Bouguer law did not reduce the residual standard deviation of the fit. Consequently, use of the linear form of the law is justified.

The mixture densities were calculated on a linear mass weighted basis. The quantum efficiency of the fluorescence (Φ), the extinction coefficient (ε), the intensity of the incident radiation (I_o), and the M_c are all unknowns that are lumped into two regression constants and an exponential term to give the regressed calibration of F against x_b for diesel as:

$$F = \frac{2.3I_o\Phi\varepsilon}{M_c}lx_b\rho_b = 1.04735 \left[\frac{\text{m}^2}{\text{kg}} \right] lx_b\rho_b e^{-209.23\text{m}^{-1}l} \quad (4)$$

Equation (4) shows that $2.3I_o\Phi\varepsilon M_c^{-1} = 1.04735 \left[\text{m}^2\text{kg}^{-1} \right] e^{-209.23\text{m}^{-1}l}$. The uncertainty of the calibration given in eq. (4) is approximately $\pm 0.2\%$ of F for the 95% confidence level.

Figure 6 shows that the resulting calibration for the flow conditions is linear. The regression of the same measurements against the Beer-Lambert-Bouguer law (Amadeo et al., 1971) gave a greater fit uncertainty suggesting that the linear fit is more appropriate.

Application of Calibration

Given that Γ and l_e are the primary measurements of this study, the main use of the calibration is to solve for these parameters. For the case where the diesel remains completely immiscible with water and has a strong affinity for metal surfaces, an excess layer of pure diesel will form on the pipe surface of thickness l_e .

Equation 3 can be rearranged to solve for the diesel excess layer thickness by setting the mass fraction, and the mixture density to reflect the properties of pure diesel:

$$l_e = \frac{F}{2.3I_o\Phi\varepsilon M_c^{-1}\rho_d} = A_0 + A_1l \quad (5)$$

As shown in Fig. 7, l_e can be regressed to eq. (5) using measurements of F for given values of path length (l) and plotted versus l . The two example F versus l data sets shown in Fig. 7 were obtained by moving the optical bundle closer to the test surface in order to vary the path length. As illustrated by the open circles, most of the resulting values of l_e for a given data set were directly proportional to l ; hence, a linear relationship with respect to l including fitting constants A_0 and A_1 is shown on the rightmost side of eq. (5). Although, eq. (5) can be used to calculate as many values of l_e as long values of F and l can be supplied, it is valid only for when the path length and the excess layer thickness coincide (for non-zero bulk

compositions) because it has been derived for pure diesel. This condition can be met by setting l to l_e in the rightmost portion of the eq. (5) and solving for l_e :

$$l_e = \frac{A_0}{1 - A_1} \quad (6)$$

For traverse data sets that are not linear for the full range of l , as illustrated by the open square symbols in Fig. 7, only the data that is approximately linear near the wall was used to generate constants A_0 and A_1 .

Equation 6 is necessary only for a non-zero bulk mass fraction (x_b). For flushing tests, where $x_b = 0$, eq. (5) is valid for all $l \geq l_e$. Consequently, the excess surface density of diesel for flushing tests is obtained from an average of the l_e obtained from eq. (5) and the traverse measurements.

As shown in Appendix G, roughly 85 % of the l_e measurements have a relative uncertainty of less than 25 % for the 95 % confidence level. For these measurements the average uncertainty of l_e is approximately ± 7 % of l_e . Overall, the average uncertainty of l_e was approximately $\pm 0.2 \mu\text{m}$.

The bulk mass fraction can be obtained by dividing the total fluorescence signal (F) into its components along the path length while assuming a uniform bulk mass fraction. The total intensity is the sum of that contributed by the bulk concentration ($F_l(x_m = x_b)$) for the entire path length and that in the diesel excess layer ($F_{l_e}(x_m = 1)$) minus the intensity that would have been due to the bulk concentration but did not occur because it was displaced by the excess layer ($F_{l_e}(x_m = x_b)$)

$$F = F_l(x_m = x_b) - F_{l_e}(x_m = x_b) + F_{l_e}(x_m = 1) \quad (5)$$

Substitution of eq. (4) into the components of the above equation and grouping like terms gives:

$$F = 2.3I_o\Phi\epsilon M_c^{-1} [lx_b\rho_b - l_ex_b\rho_b + l_e\rho_d] \quad (8)$$

Here ρ_d is the density of liquid diesel.

When the expression for the linearly mass fraction weighted ρ_b is substituted into eq. (8), its solution is quadratic in x_b with only one root that is less than or equal to 1.

$$x_b = \frac{1}{2} \left(\frac{1}{1 - \frac{\rho_d}{\rho_w}} \right) - \frac{1}{2} \sqrt{\left(\frac{1}{1 - \frac{\rho_d}{\rho_w}} \right)^2 - \frac{4 \left(\frac{F}{2.3I_o\Phi\epsilon M_c^{-1}} - l_e\rho_d \right)}{(l - l_e)(\rho_w - \rho_d)}} \quad (9)$$

where ρ_w is the density of liquid tap water. The average uncertainty of x_b was approximately ± 0.002 .

Air Gap Calibration

A secondary methodology was developed that relies on the gradient of F rather than its absolute value in order to confirm the measurement of l_e as obtained from eq. (5) or eq. (6). The advantage of a gradient approach would be the elimination of a bias error on the measurement of F if it existed. As shown in Fig. 4, part of the excitation is reflected from the diesel-air interface and is not available to induce fluorescence. Consequently, the calibration must be adjusted to account for the air gap during the drained test chamber measurements. Appendix E provides the derivation of the air-gap l_e and the result is given here as:

$$l_e = \frac{-0.0121 \text{m} \frac{dF_{\text{ag}}}{dl} M_c}{2.3 I_o \Phi \epsilon x_m \rho_m} = -0.01156 \frac{\text{kg}}{\text{m}} \frac{\frac{dF_{\text{ag}}}{dl} e^{209.23 \text{m}^{-1} l}}{x_m \rho_m} \quad (10)$$

MEASUREMENT RESULTS

Excess Layer Thickness

The test apparatus shown in Fig. 1 was used to submit an oxidized copper disk to exposure tests with two different bulk concentrations of diesel in tap water under varying flow conditions. More specifically, contamination measurements over an approximate 200 h time period were made for five different Reynolds numbers varying from 0 to 7000:

$$\text{Re} = \frac{4\dot{m}}{\mu_b p_w} \quad (11)$$

where the wetted perimeter of the channel was 195 mm, the viscosity of the mixed bulk flow (μ_b) was calculated using a nonlinear mixture equation, and the mass flow rate (\dot{m}) was obtained from the turbine meter. Flushing measurements were done for a fixed Re of approximately 5000. The range of Reynolds numbers result from using a range of volume flow rates that a half-inch diameter tube would experience in typical buildings. After each contamination tests, the test surface was cleaned with acetone and clean tap water. Appendix H provides tabulated measurements for both the raw and reduced data.

Figures 8 provides the measured diesel layer thickness as caused by an exposure to a flowing water/diesel (99.8/0.2) mixture, i.e., diesel at approximately 0.2 % bulk mass fraction (2000 ppm). The exposure time is the duration of exposure of the test surface to the flow starting from when the clean surface was first exposed to a particular flow condition. For all flow rates and exposure times, the average l_e for $x_b = 0.2$ % obtained from the eq. (6) methodology was approximately 2.3 μm .

Figure 9 provides the measured diesel layer thickness as caused by an exposure to a flowing water/diesel (99.7/0.3) mixture, i.e., diesel at approximately 0.3 % bulk mass fraction (3000 ppm). A much larger variability in the measurements is evident for the 0.3 % mass fraction than for the 0.2 % mass fraction condition. For all exposure times and Re, the average l_e for $x_b = 0.3$ % was approximately 7.4 μm , which is 5.1 μm (222 %) thicker than the average thickness observed for the 0.2 % mass fraction tests.

Figure 10 crossplots all of the excess layer measurements of Fig. 8 as a function of Re. Figure 10 shows that the maximum diesel excess layer thickness of approximately 8 μm occurred at a Re near 4800. For Re larger and smaller than 4800, the diesel excess layer was thinner. For example, the l_e for Re near 1900 and 3800 was approximately 1 μm , which is nearly eight times less than the maximum l_e . The l_e for Re greater than 6000 was approximately 3 μm . Figure 11 crossplots all of the excess layer measurements of Fig. 9 (the 0.3 % mass fraction tests) as a function of Re. Figure 11 shows that the maximum film thickness of approximately 26 nm occurred at a Re of approximately 4000. Consequently, a maximum for the diesel adsorption exists near a Re of 4000 for both freestream concentrations. The dashed lines given in Figs. 10 and 11 represent the maximum measured excess layer for each range of Re tests. The variation in Re for a given set of tests for “fixed” Re was caused by an approximate 1 % variation in the water temperature during startup and the an approximate 15 % variation in the water flow during the nearly 200 h test duration.

Filled symbols in Figs. 8 and 10, shown between 150 h and 200 h, represent l_e measurements that were made at the end of the exposure tests after the test section was drained using the air-gap technique as a secondary measurement technique. For the water/diesel (99.8/0.2), mixture all three of the drain checks were within ± 1.5 μm of the measurements that were made while the test fluid was flowing. For example, for the air-gap check obtained using eq. (10) for the Re near 7000 condition produced a l_e near 3 μm , while the last measurement made with eq. (6) produced a l_e near 3.7 μm . Similarly, eq. (6) produced a l_e of approximately 2 μm for both the no-flow and the 3200-Re tests, while the eq. (10) check resulted in 3.5 μm and 1 μm for l_e , respectively. For the water/diesel (99.7/0.3) mixture, all three of the drain checks for the flushing data were also within ± 1.5 μm of the measurements that were made while the test fluid was flowing giving 0.5 μm and -0.5 μm , respectively. However, the agreement between the empty and filled test chamber tests was not as good for the water/diesel (99.7/0.3) mixture for the 7000-Re contamination measurements. For example, the air-gap check for the Re near 7000 condition produced a l_e near 5 μm , while the last measurement made with eq. (4) produced a l_e near 2 μm .

Flushing tests done after the water/diesel (99.8/0.2) 4800-Re contamination tests are shown in Fig. 8. The flushing measurements start at an l_e near 6.5 μm , which agrees with the value of l_e at the end of the 4600-Re contamination tests, thus, confirming the repeatability of the measurement technique. The l_e decreased from approximately 6.5 μm to approximately 1.5 μm after flushing for approximately 55 h. This corresponds roughly to a 0.09 $\mu\text{m}/\text{h}$ removal rate and a 77 % reduction of the total diesel thickness over 55 h.

The flushing tests shown in Fig. 10 performed after the 5000-Re water/diesel (99.7/0.3) contamination tests, likewise start at approximately the same l_e (1.5 μm) as where the previous contamination test ended, again demonstrating good repeatability. After approximately 20 h of flushing, the 5000-Re contaminant thickness was reduced to approximately -0.5 nm. Given the uncertainty of the measurement, most all of the diesel has been removed by flushing with clean tap water. The removal rate achieved after the 5000-Re, 0.3 % mass fraction (3000 ppm) contamination tests (0.1 $\mu\text{m}/\text{h}$) agrees closely with that achieved for the flushing tests done after the 4600-Re, 0.2 % mass fraction (2000 ppm) contamination tests. This suggests a constant removal rate of approximately 0.1 $\mu\text{m}/\text{h}$ of diesel from a copper surface for a flushing Re of 5000 that is independent of initial thickness and original contamination concentration. No removal rate could be calculated for the flushing tests done after the 7000-Re water/diesel (99.7/0.3) because the tests produced an l_e near -0.5 nm for nearly all measurement times.

Freundlich Constants

For sorption systems, the Freundlich constant (K) relates the equilibrium solid-phase concentration (c_s) to the equilibrium concentration of the bulk liquid-phase (c_l) as (Schwarzenbach et al., 2003):

$$c_s = Kc_l^n \quad (12)$$

where the Freundlich exponent (n) determines the rate of sorption to the solid surface.

Equation 12 can be rewritten in terms of the excess surface density and the mass fraction of the bulk liquid as:

$$\Gamma = \frac{K}{a_s} \left(\frac{x_b \rho_b}{M_c} \right)^n = \hat{K} (x_b \rho_b)^n \quad (13)$$

where the constant a_s is the specific surface area of the solid defined as the surface area per mass of solid. Here K is normalized by the constant a_s and the molar mass of the contaminant raised to the n^{-1} power ($M_c^{n^{-1}}$) to give \hat{K} .

Because the present measurements do not sufficiently span the free stream concentration variable to accurately determine the Freundlich exponent, it was assumed that the diesel-water-copper system behaved as one with constant sorption free energies giving a linear isotherm with $n = 1$. Using this assumption, the normalized ‘‘Freundlich constants’’ were obtained by averaging measurements for a particular Re test for exposure times greater than 50 h in order to approach an equilibrium or steady state value for \hat{K} . All of the l_e measurements, for a given Re test, appeared to be nearly constant after 50 h of exposure. Consequently, it was assumed that a balance between diesel deposition and removal had been achieved.

Figure 12 shows the normalized Freundlich constant as a function of Re for the two different bulk concentrations of this study. The figure shows that \hat{K} varies between near zero to values approaching 0.015 m. For Re less than 4000, the \hat{K} behaves as expected with values for the 0.3 % bulk mass fraction being larger than those for the 0.2 % bulk mass fraction. However, for Re greater than 4000, the opposite behavior is observed, with \hat{K} 's for the 0.2 % mass fraction being larger than those for the 0.3 % mass fraction. Considering that a Re of 4000 is beyond the transition Re (from laminar to turbulent flow)⁵ and within the transition region, no explanation can be offered at this time for the crossover phenomenon.

DISCUSSION

Because of its derivation from thermodynamics, the Freundlich constant given in eq. (12) is associated with chemical and/or physical equilibrium between the liquid-phase and the solid-phase concentrations. The measured phenomenon of the present study cannot be expressed in terms of a solid-phase concentration. The solid is not soluble with respect to the contaminant. Rather, the contaminant is located at the solid surface. As a result, the normalized “Freundlich constant” given by eq. (13) (\hat{K}) may not necessarily represent thermodynamic equilibrium. The \hat{K} may be influenced by physical forces other than Van der Waals like flow and pressure forces. For this reason, the variation of the normalized Freundlich constant with respect to Re for fixed liquid-phase concentration is not prohibited by thermodynamics.

It is difficult to estimate the effect of the hydrolyzed diesel on the measurements, but it has likely introduced an unknown bias error to measurements. Future test with fresh diesel and water mixtures that have not had time to hydrolyze would reduce or eliminate the bias error.

CONCLUSIONS

A detailed account of the development of a fluorescence based measurement technique for measuring the mass of contaminant on solid surfaces in the presence of water flow has been provided. A test apparatus was designed and developed to use the fluorescent properties of diesel for the purpose of studying its adsorption and desorption to and from an oxidized copper test surface. A calibration technique was developed to measure both the mass of diesel adsorbed per unit surface area (the excess surface density) and the bulk concentration of the hydrolyzed diesel in the flow.

The measured diesel excess surface density that was adsorbed to the surface varied between zero and 0.02 kg/m² for Reynolds numbers between zero and 7000. A maximum for the diesel adsorption was observed near a Re of 4000 for both nominal bulk mass fractions of 0.2 % and 0.3 % diesel. For the most part, the thickness of the diesel excess surface density remained less than 10 μ m. The exception to these excess layer measurements was the 0.3 % bulk mass fraction with Re = 4000 measurements that peaked near 25 μ m.

In an effort to model the adsorption of diesel to copper, normalized Freundlich constants were calculated based on a linear isotherm and found to vary between near zero and 0.015 m.

⁵ The transition Re would be 2300 if the hydraulic diameter concept prevails, and 3000 (Schlichting, 1979) if the flow is considered to be one between infinite flat plates.

Most of the Freundlich constants were less than 0.005 m. In addition, flushing tests suggest a constant removal rate of approximately 0.1 $\mu\text{m}/\text{h}$ of diesel from a copper surface that is independent of initial thickness and original contamination concentration. The measurements show that most all of the diesel has been removed to within the uncertainty of the measurement procedure by flushing with clean tap water.

ACKNOWLEDGEMENTS

This work was funded by the U.S. Environmental Protection Agency (EPA) under contract #DW-13-92167701-0, with the guidance of project manager Mr. V. Gallardo. Thanks go to the following NIST personnel for their constructive criticism of the first draft of the manuscript: Dr. S. Treado, and Dr. P. Domanski. Thanks goes to the Mr. V. Gallardo of EPA for his constructive criticism of the second draft of the manuscript. Furthermore, the author extends appreciation to Mr. D. Wilmering for taking the measurements and conquering the difficult machining and design problems encountered in the project.

NOMENCLATURE

English Symbols

A	regression constants in eq. (5)
a_s	specific surface area, $\text{m}^2 \text{kg}^{-1}$
c	concentration, mol m^{-3}
F	fluorescence intensity
F_r	raw fluorescence intensity measurement
I_o	incident intensity, V
K	Freundlich constant, $\text{mol}\cdot\text{kg}^{-1}$
\hat{K}	normalized Freundlich constant, m
l	path length, m
l_e	thickness of excess layer, m
M_c	molar mass of contaminant, kg mol^{-1}
\dot{m}	mass flow rate, kg s^{-1}
Re	Reynolds number
n	Freundlich exponent
p_w	wetted perimeter of channel, m
T	temperature, K
U	expanded uncertainty
u_i	standard uncertainty
x	mass fraction of diesel

Greek symbols

β	coefficient of temperature dependence, K^{-1}
Γ	surface excess density, kg m^{-2}
ε	extinction coefficient
λ	wavelength, m
μ	dynamic viscosity, $\text{kg m}^{-1} \text{s}^{-1}$
ν	kinematic viscosity, $\text{m}^2 \text{s}^{-1}$
ρ	mass density of liquid, kg m^{-3}
Φ	quantum efficiency of fluorescence

English Subscripts

0	zero reference jar
100	maximum reference jar
a	ambient
ag	air gap
b	bulk
d	pure diesel
e	excess layer
i	inlet
l	liquid
l_e	excess layer
m	emission, mixture
ng	no air gap
o	outlet or exit

s solid surface
 T_b reference bath temperature
 T_T test section temperature
x excitation
w tap water

Superscripts

- average

REFERENCES

Amadeo, J. P., Rosén C., and Pasby, T. L., 1971, *Fluorescence Spectroscopy An Introduction for Biology and Medicine*, Marcel Dekker, Inc., New York, p. 153.

Guilbault, G. G., 1967, Fluorescence: Theory, Instrumentation, and Practice, Edward Arnold LTD., London, pp. 91-95.

Herman, B., 1998, *Fluorescence Microscopy*, 2nd ed., Springer-Verlag New York, Inc., pp. 69 –71.

Kedzierski, M. A., 2003, "Effect of Bulk Lubricant Concentration on the Excess Surface Density During R134a Pool Boiling with Extensive Measurement and Analysis Details," NISTIR 7051, U.S. Department of Commerce, Washington, D.C.

Kedzierski, M. A., 2002, "Use of Fluorescence to Measure the Lubricant Excess Surface Density During Pool Boiling," *Int. J. Refrigeration*, Vol. 25, pp.1110-1122.

Kedzierski, M. A., 2001, "Use of Fluorescence to Measure the Lubricant Excess Surface Density During Pool Boiling," NISTIR 6727, U.S. Department of Commerce, Washington, D.C.

Miller, J. N., 1981, *Volume Two Standards in Fluorescence Spectrometry*, Chapman and Hall, London, pp. 44-67.

Reader, J, Corliss, C. H., Wiese, W. L., and Martin, G. A., 1980, "Wavelengths and Transition Probabilities of Atoms and Atomic Ions", NSRDS-National Bureau of Standards #68, U.S. Department of Commerce, Washington.

Schlichting, H., 1979, Boundary-Layer Theory, McGraw-Hill, New York, pg. 591.

Schwarzenbach, R. P., Gschwend, P. M., and Imboden, D., M., 2003, Environmental Organic Chemistry, 2nd ed., Wiley, NJ, pp 281-283.

Simplex, 2006, <http://www.simplexdirect.com/FuelSupply/mainten04.html>

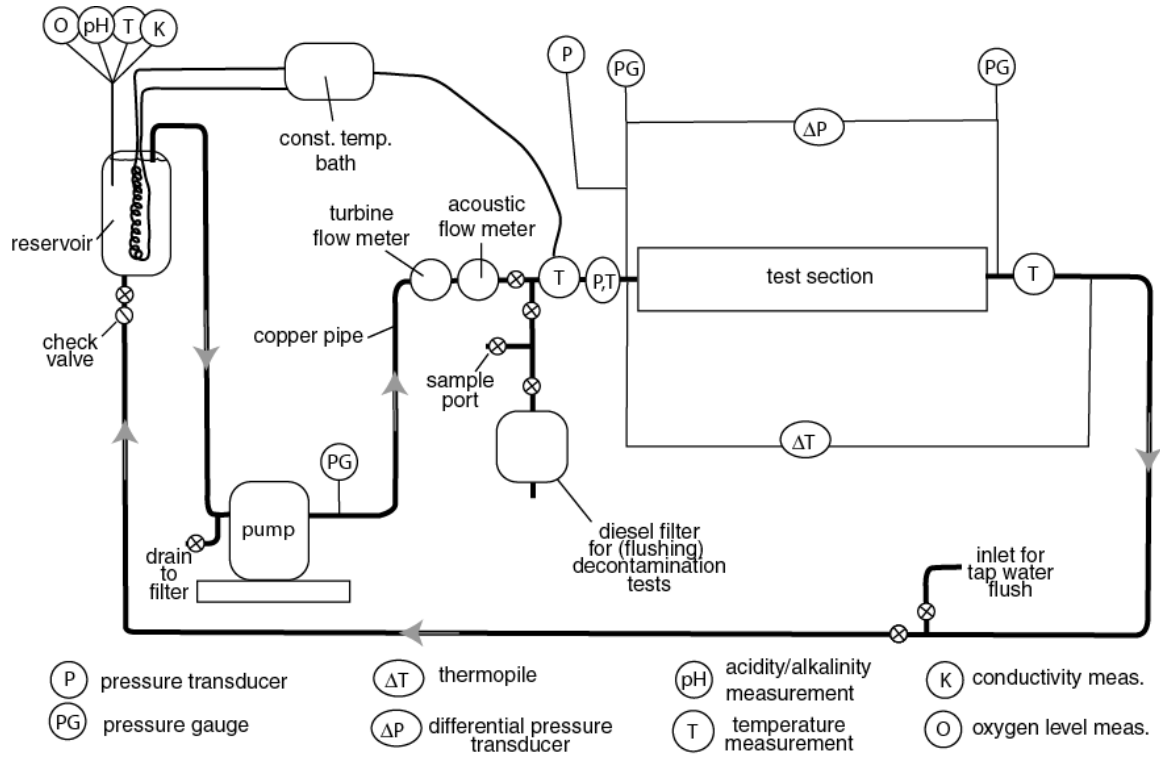


Fig. 1 Schematic of test loop

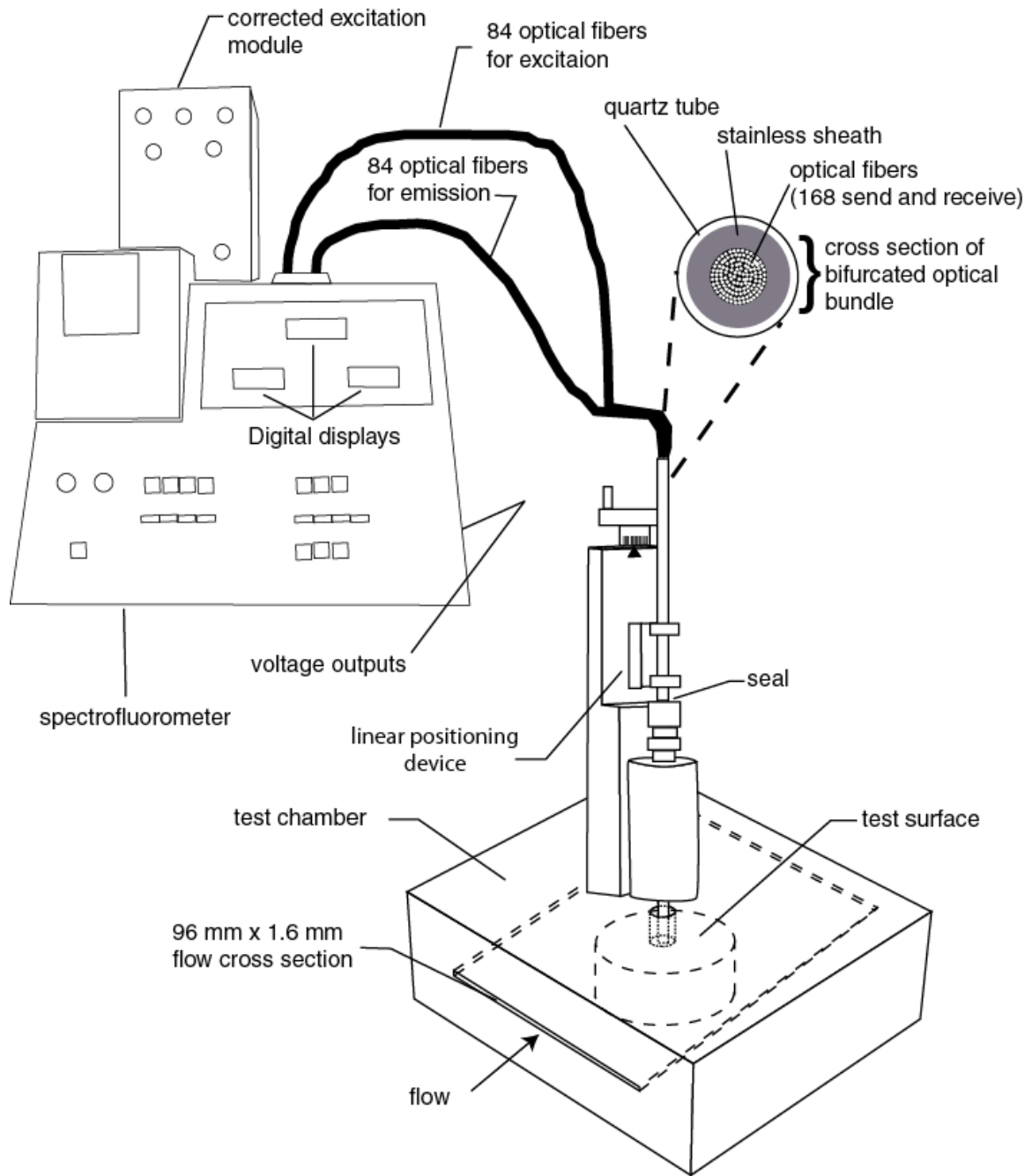


Fig. 2 Schematic of spectrofluorometer, test section, and linear positioning device

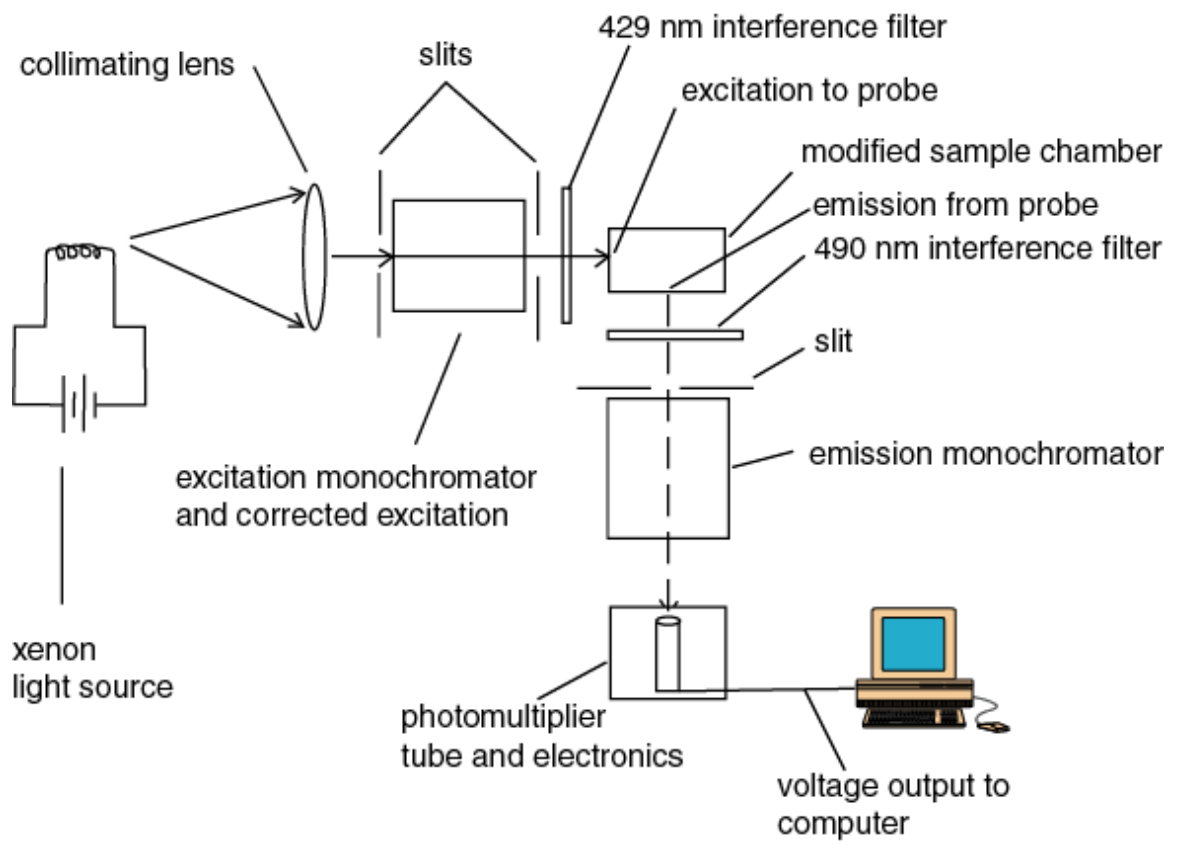


Fig. 3 Schematic of right angle spectrofluorometer

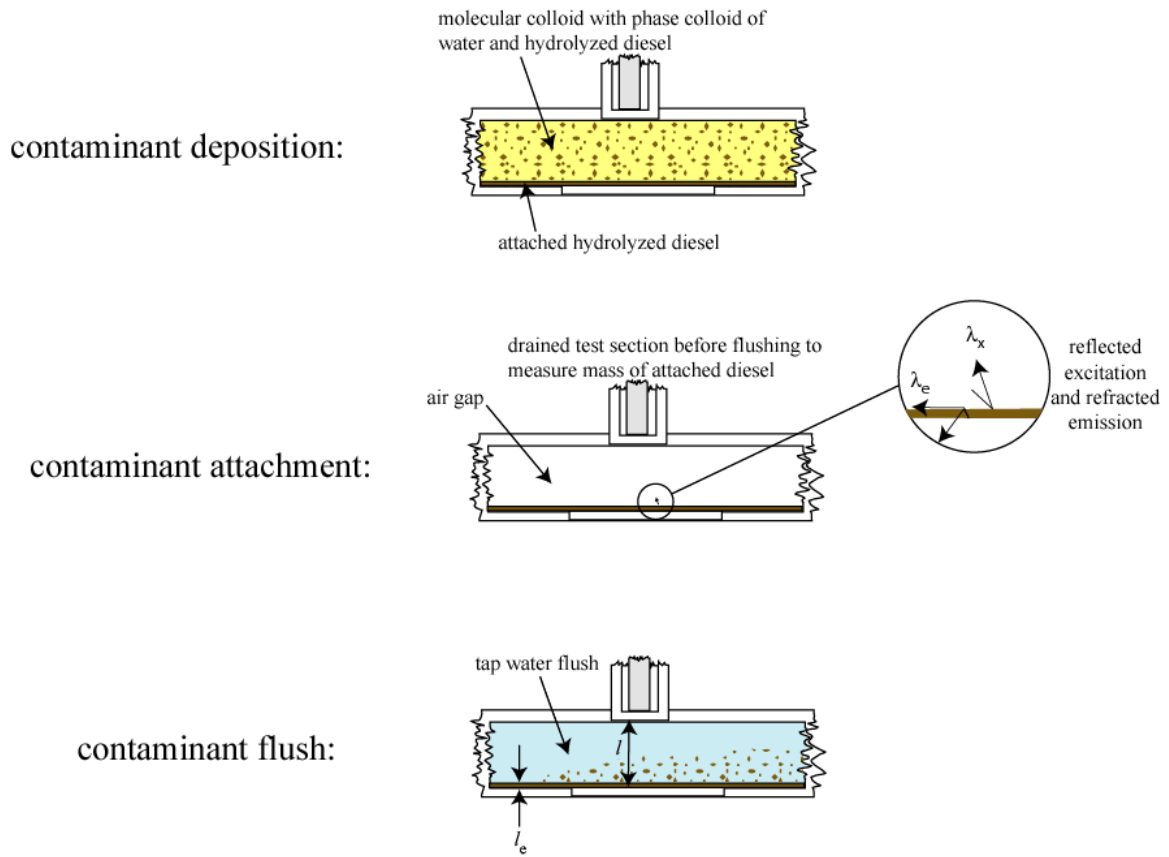


Fig. 4 Cross-sectional illustration of test section during contamination and flushing

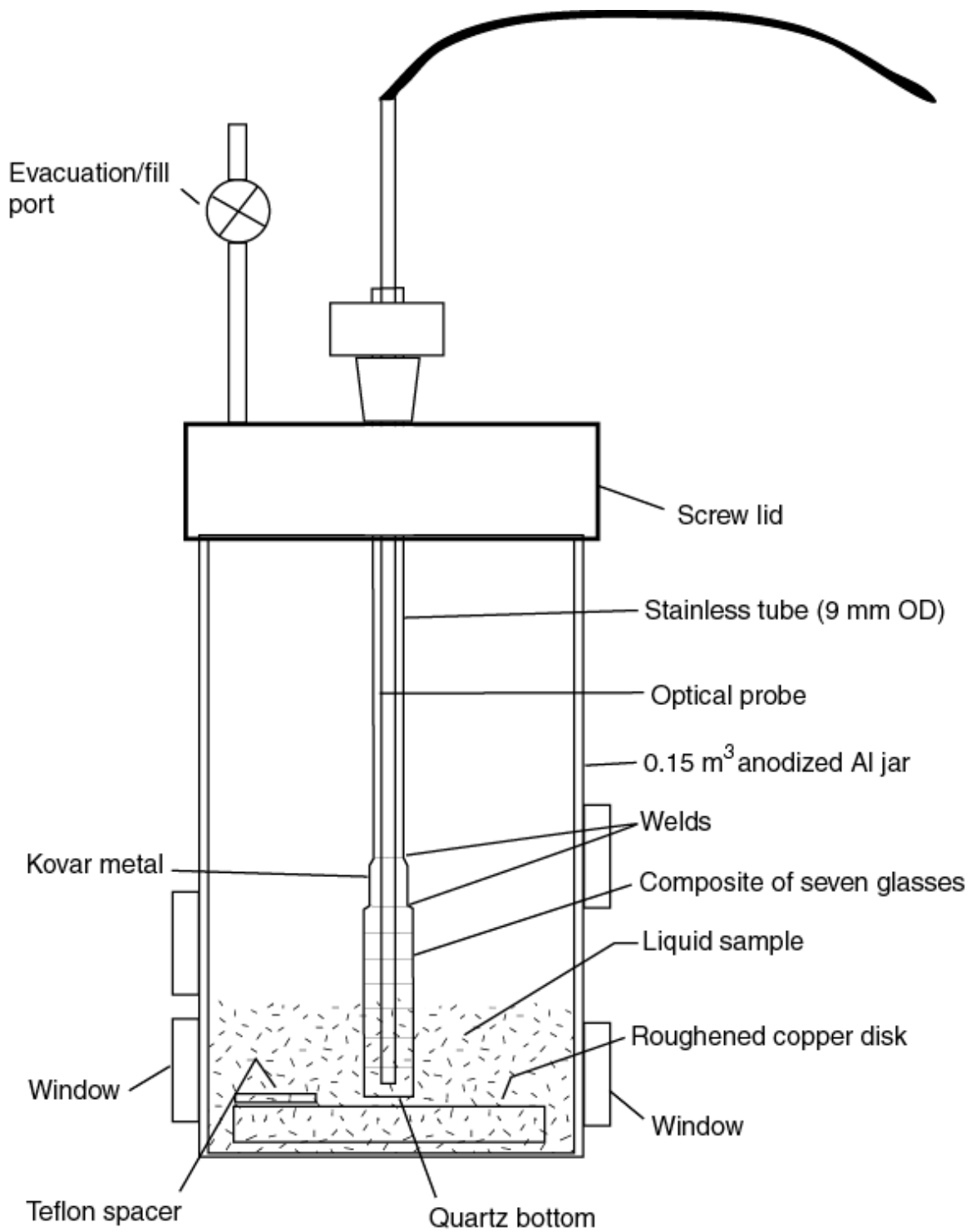


Fig. 5 Schematic of fluorescence/composition calibration jar

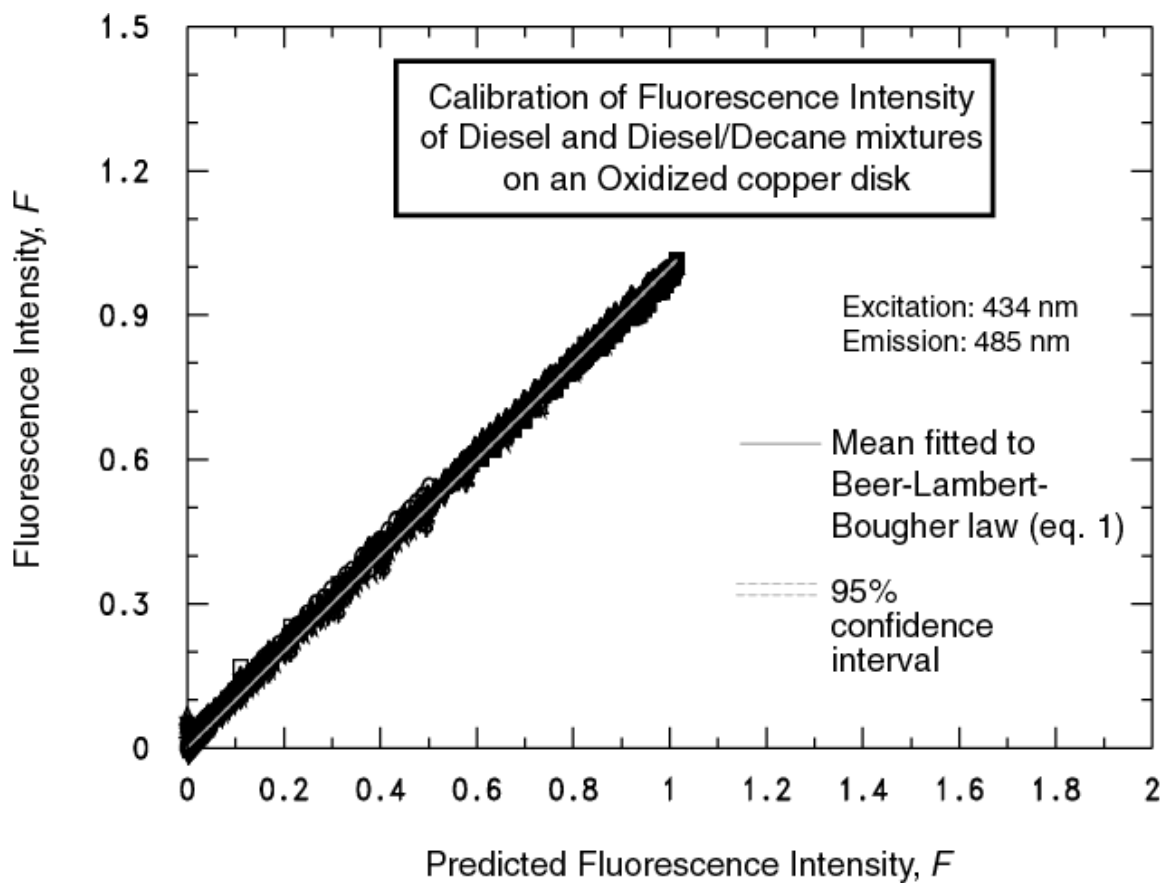


Fig. 6 Overall calibration of Beer-Lambert Bouguer law for diesel on copper disk

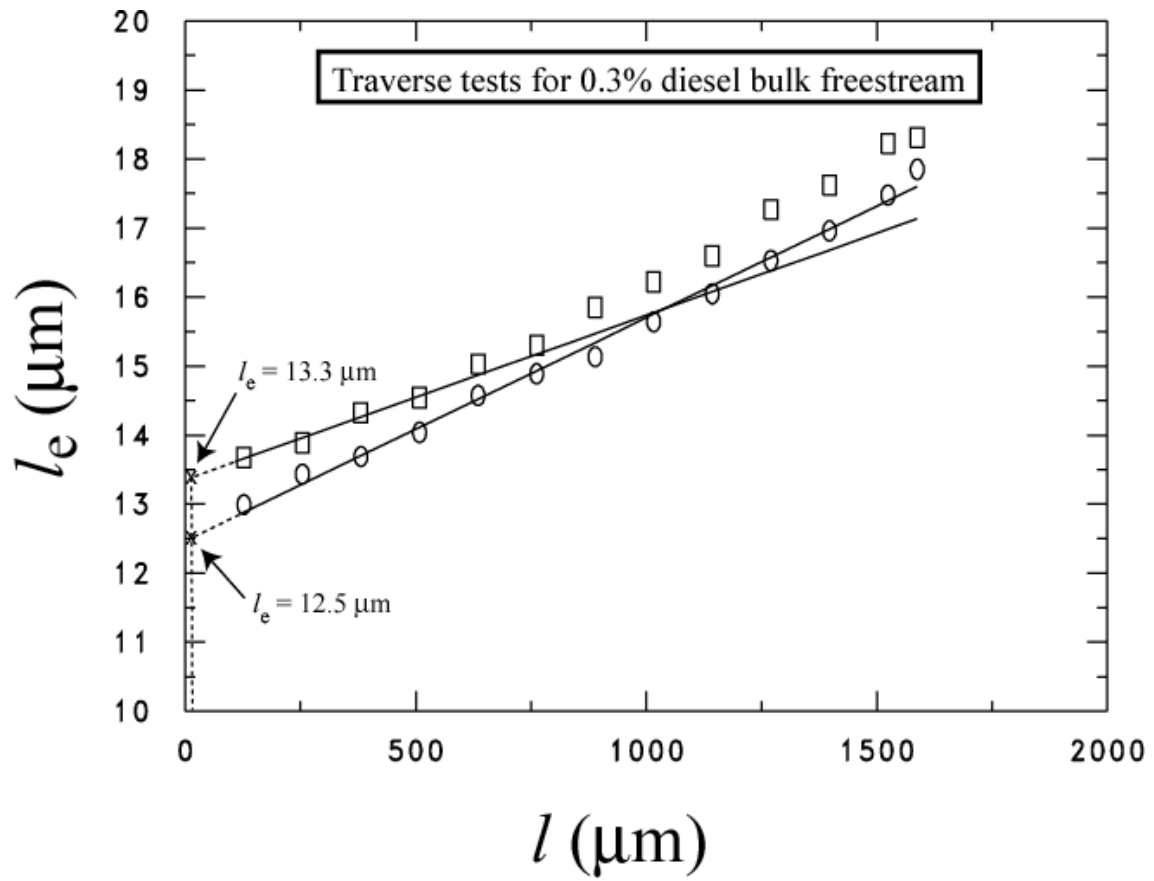


Fig. 7 Demonstration of excess layer thickness measurement

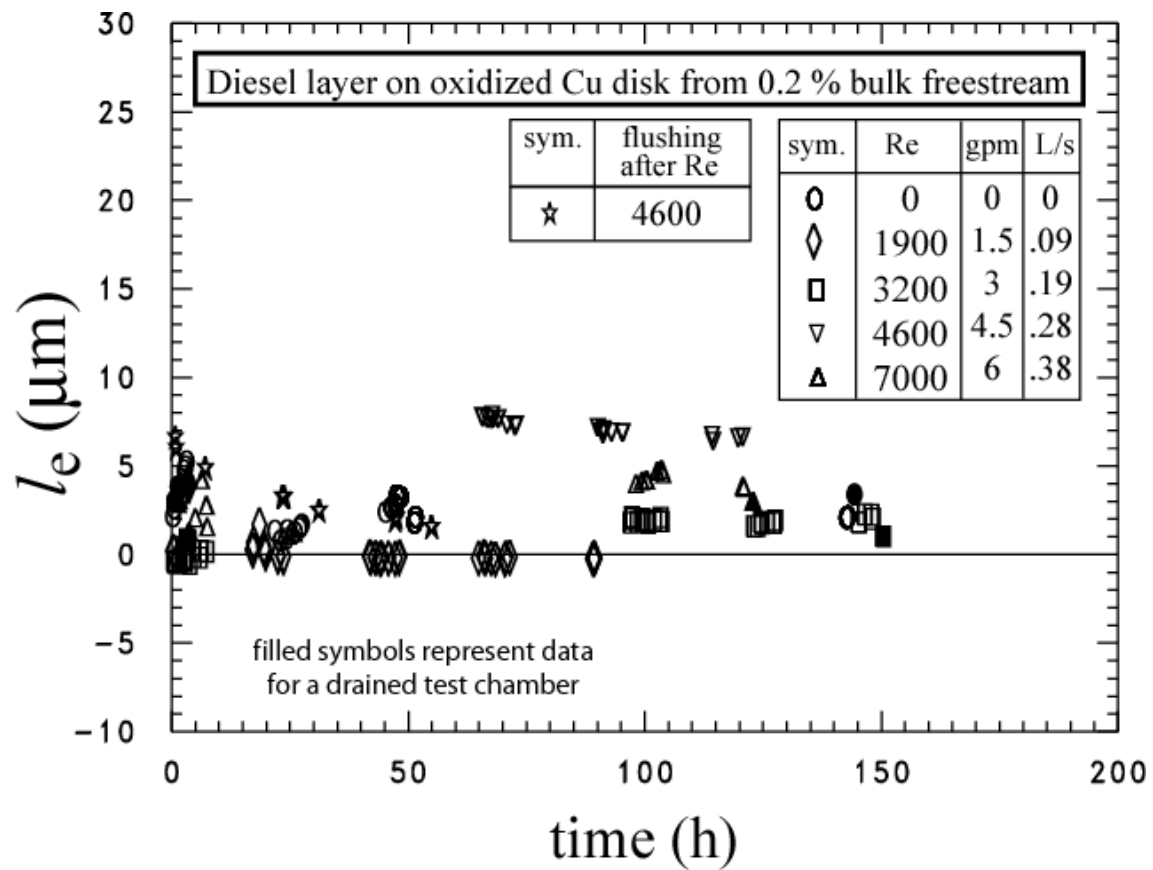


Fig. 8 Effect of exposure time and flow rate on thickness of the diesel excess layer for a 0.2 % bulk freestream mass fraction

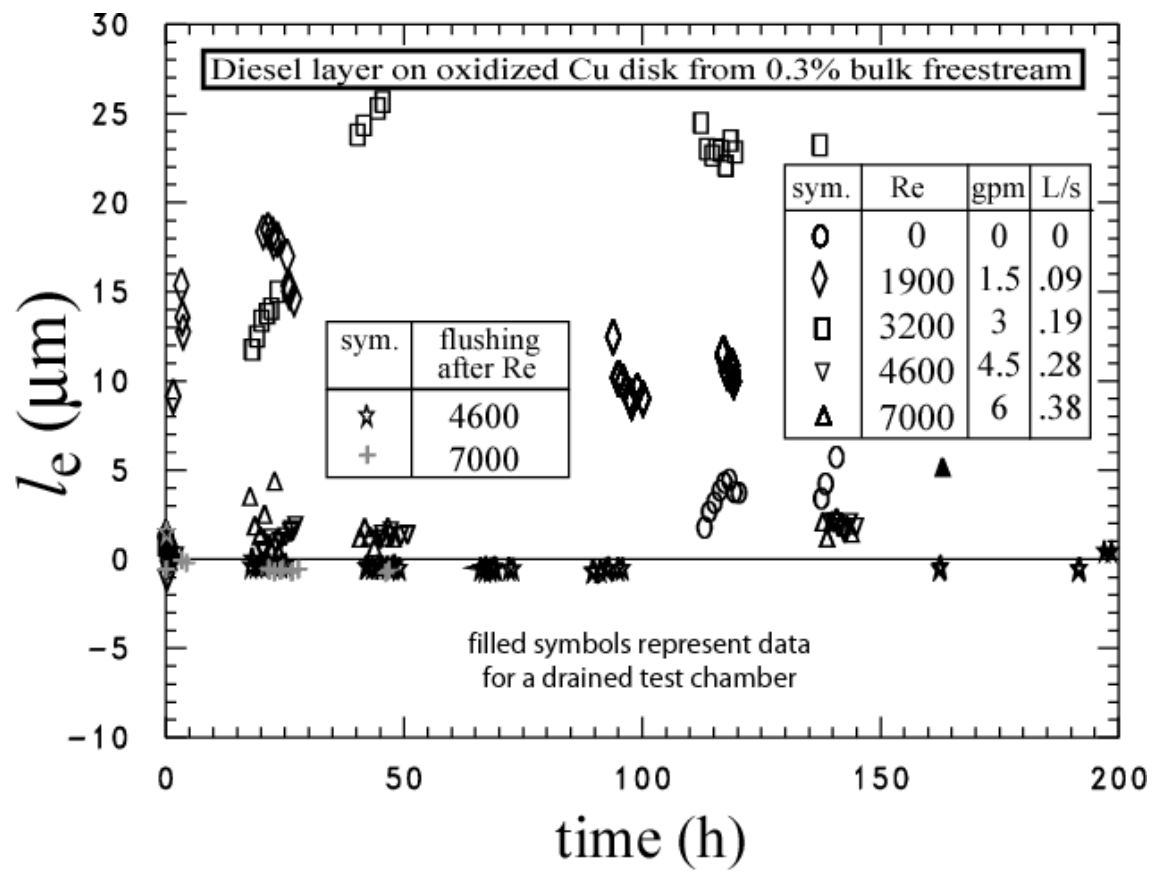


Fig. 9 Effect of exposure time and flow rate on thickness of the diesel excess layer for a 0.3 % bulk freestream mass fraction

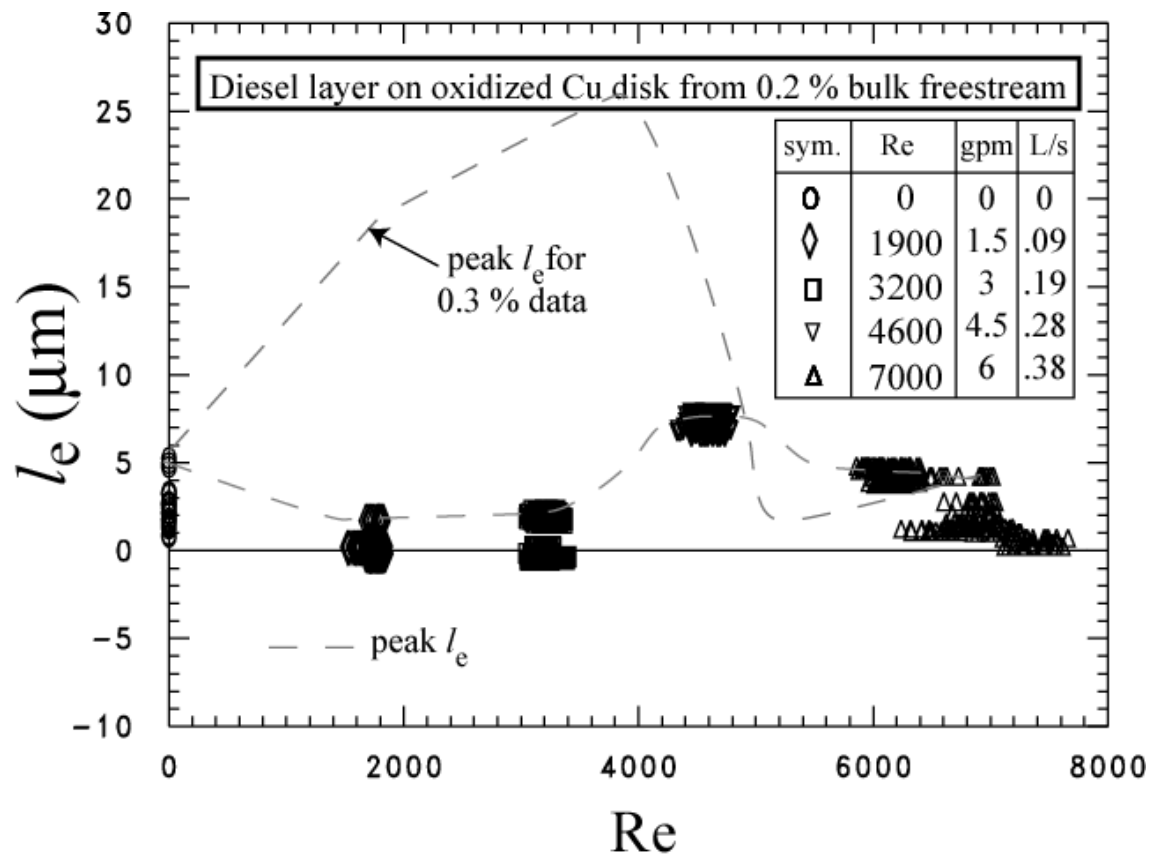


Fig. 10 Diesel excess layer thickness as a function of Re for water/diesel (99.8/0.2)

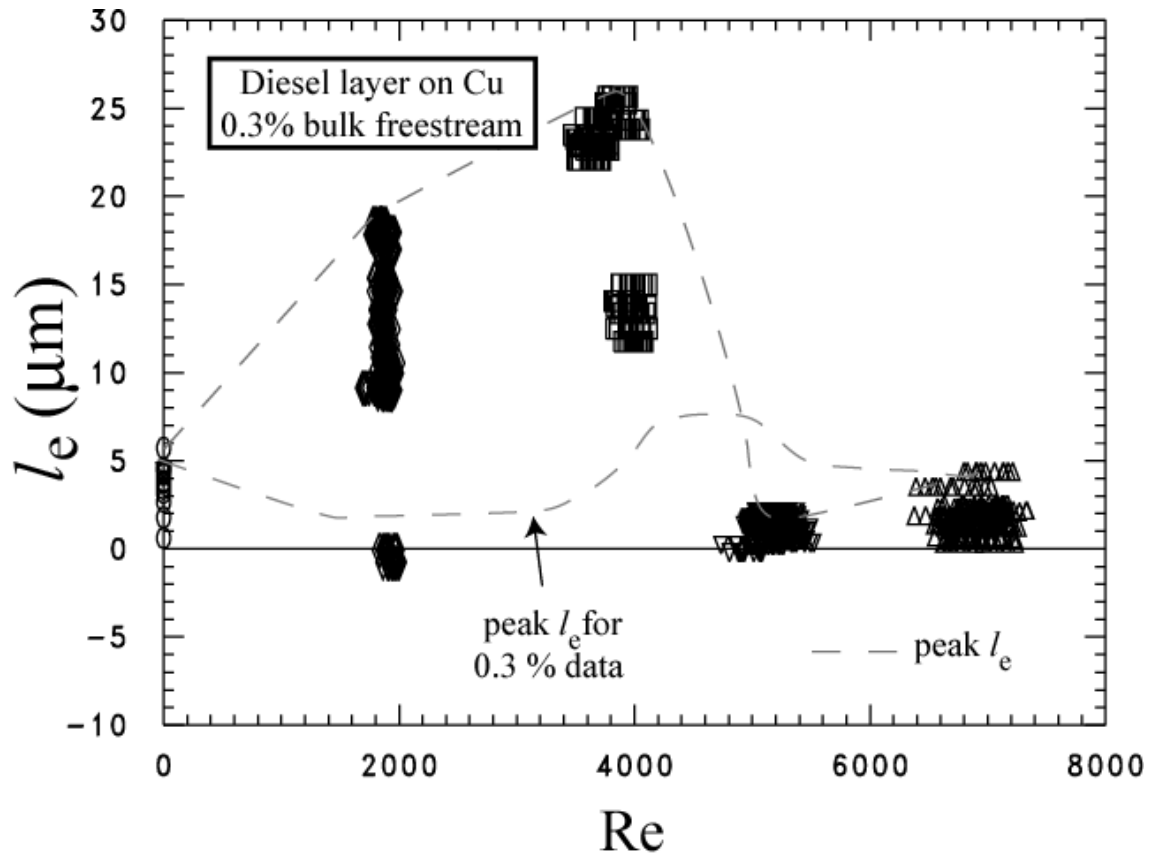


Fig. 11 Diesel excess layer thickness as a function of Re for water/diesel (99.7/0.3)

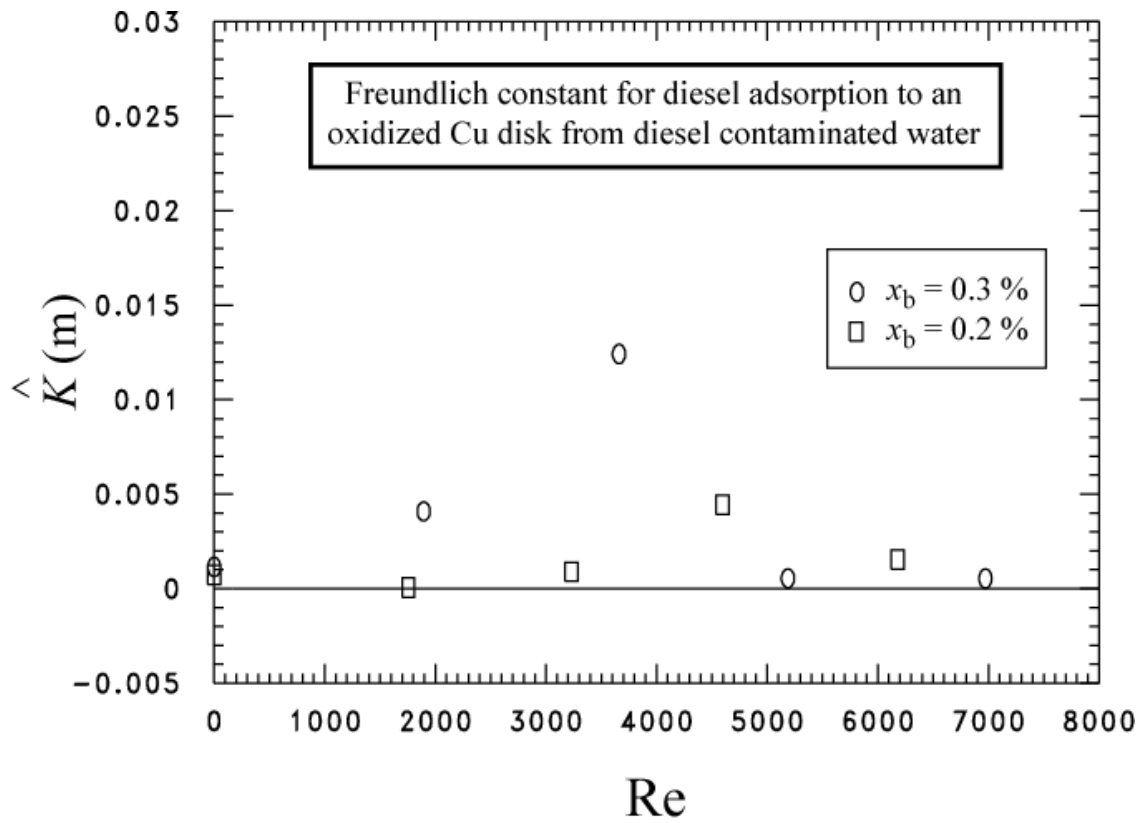


Fig. 12 Normalized Freundlich constants for diesel adsorption to an oxidized Cu disk from diesel contaminated water

APPENDIX A: EXCITATION AND EMISSION WAVELENGTHS

Appendix A describes the methodology used to select the excitation and emission wavelengths to ensure that a significant and measurable emission signal was obtained with no measurable overlap of the excitation and emission spectra.

The wavelengths for the excitation and emission light that gave the best compromise between emission intensity strength with minimal interference from the excitation were chosen based on the following analysis. Figure A.1 shows the analysis of the emission and excitation spectra of pure diesel in a cuvette. The test sample was placed directly in the sample chamber of the right angle spectrofluorometer. The excitation wavelength that produced the maximum fluorescence emission was iteratively found by scanning through both excitation and emission wavelengths. The excitation and emission wavelengths for diesel that produced the largest intensities were located approximately at 451 nm and 484 nm, respectively.

It is immediately apparent that filtering of both the excitation and the emission is required to reduce the overlap of the two spectra. Because of the parallel light configuration of the probe incident to the test surface, both excitation and emission light will be introduced to the detector if the light is not filtered. A 429 nm bandpass filter was chosen to filter the excitation before it got to the test surface. And a 490 nm bandpass filter was used to filter the emission intensity before it was sent to the detector. Figure A.2 shows the filtered spectra from the optical probe in a jar of diesel. The filtering process as successfully separated the emission and excitation peaks (485 nm and 435 nm, respectively) and removed the overlap of the two spectra. Because the interference filters have a finite bandwidth, an excitation filter centered at 450 nm would have resulted in some overlapping of the spectra. For this reason, a smaller wavelength was chosen for the excitation signal.

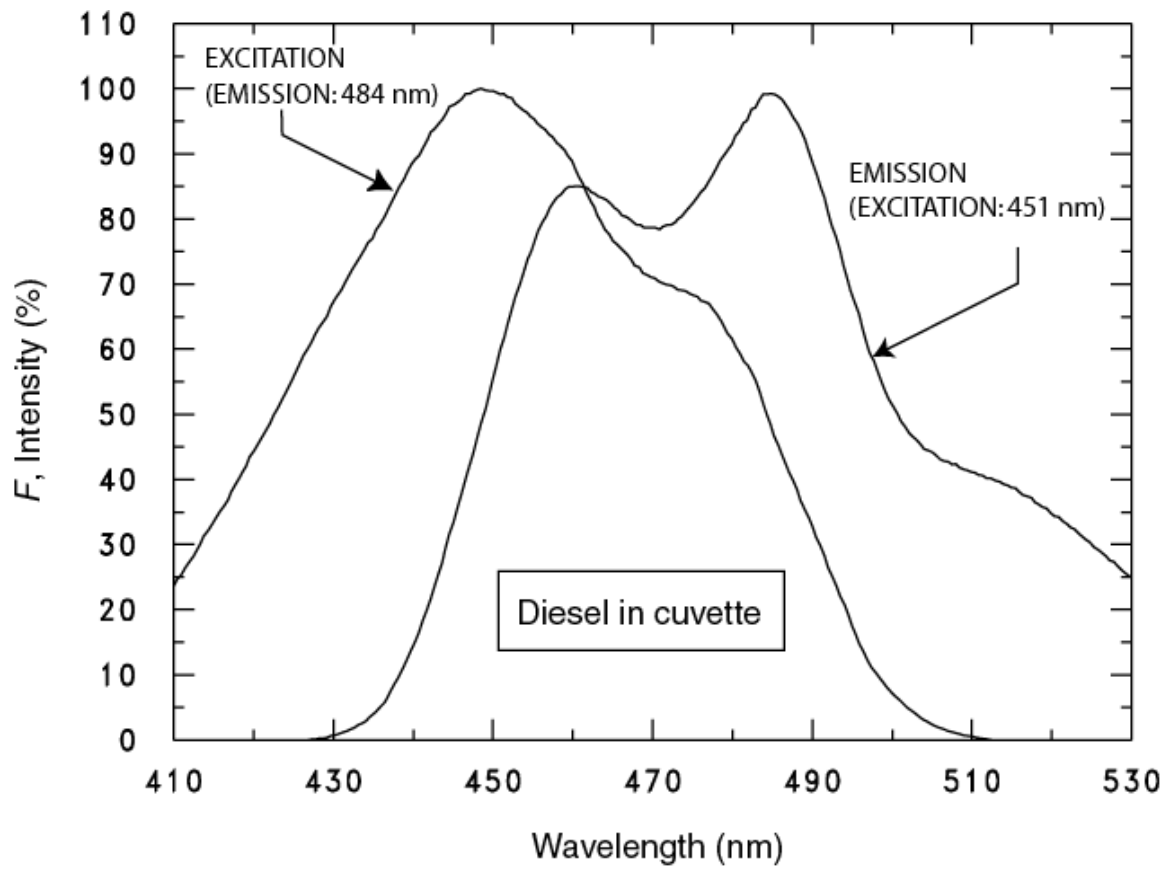


Fig. A.1 Emission and excitation spectra for diesel

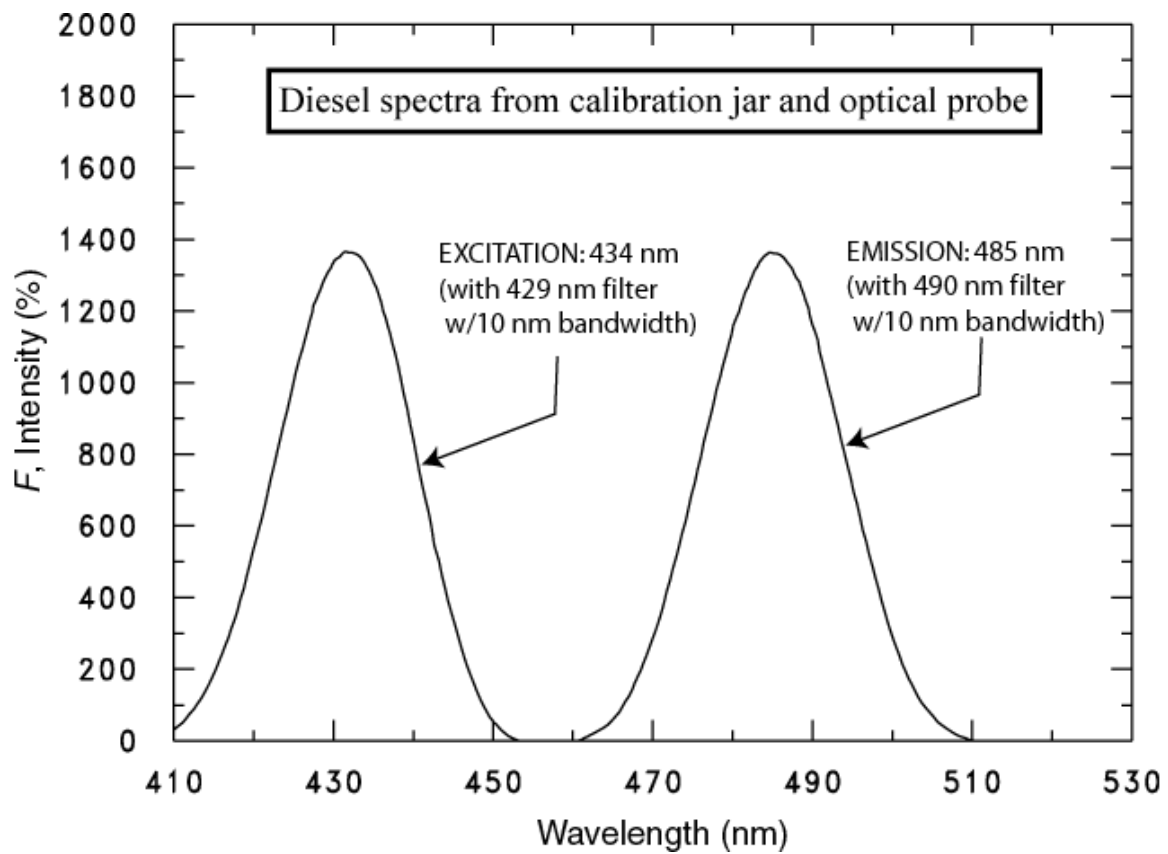


Fig. A.2 Filtered excitation and emission spectra for diesel

APPENDIX B: DIESEL PROPERTIES

This appendix presents the measurements and the correlation of the density (ρ_d) and the kinematic viscosity (ν_d) for the liquid #2 diesel fuel used in this experiment.

Liquid Density

The density of the liquid diesel was measured as a function of temperature with a glass pycnometer. The pycnometer was factory instrumented with a glass mercury thermometer with a range of 14°C to 38°C in 0.2° graduations, accurate to within ± 0.2 K. The pycnometer was filled with distilled water and its volume was calculated from the known density of water. The volume was found over five trails to be 9.84 mL with a standard uncertainty of 0.01 mL.

The pycnometer containing diesel was cooled in an ice bath and then removed from the bath and allowed to warm on the balance to room temperature over approximately one hour. The standard uncertainty of the balance was approximately 1 mg. The outside of the pycnometer was wiped clean before each measurement to remove the diesel that was expelled through the pipette due to volume expansion with temperature increase.

The Biot number for the warming pycnometer was estimated to be approximately 0.5, which is greater than the recommended limit of 0.1 (Incropera and Dewitt, 1985) for a uniform temperature in fluid. It is difficult to estimate the error introduced in the measurements due to temperature gradients that existed in the diesel. However, the data regression shows that the residuals are independent of temperature, which suggests that the error due to temperature gradients in the liquid had a negligible effect on the density measurements.

Table B.1 shows the recorded measurements for two days. Equation B.1 gives the fit of the liquid diesel density (ρ_d) in kg/m^3 versus temperature (T) in Kelvin:

$$\rho_d = 1056.29 - 0.700T \quad \text{B.1}$$

The expanded uncertainty of the fit was approximately $\pm 0.2 \text{ kg/m}^3$ for 95 % confidence.

Kinematic Viscosity

The kinematic viscosity of the liquid diesel (ν_d) was measured at room temperature (approximately 297.6 K) with a glass viscometer and found to be $3.93 \mu\text{m}^2/\text{s} \pm 0.024 \mu\text{m}^2/\text{s}$. Kinematic viscosity measurements from Simplex (2006) for #2 diesel fuel shown in Table B.2 were used to obtain the trend of viscosity with respect to temperature. This was done by using the same slope of the linear $\ln \nu$ versus T^{-1} fit for the Simplex (2006) data with an intercept that reproduced our single viscosity measurement. The following correlation reproduces the single room temperature value for our batch of diesel and temperature dependence of the Simplex (2006) diesel data:

$$\nu_d (\text{m}^2 / \text{s}) = 4.434 \times 10^{-9} e^{2020.17/T(K)} \quad \text{(B.2)}$$

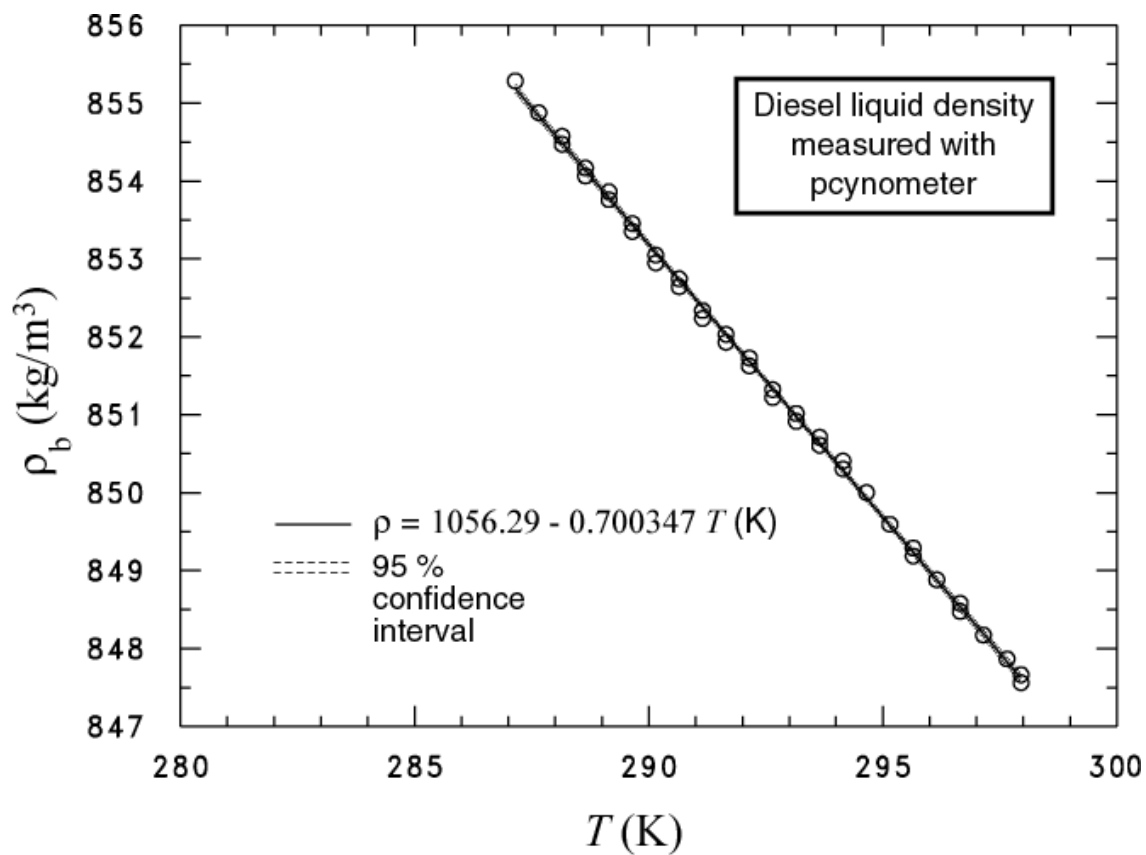


Fig. B.1 Measured liquid density of diesel and fit

Table B.1 Diesel liquid density measurements (file:DieDen.dat)

T (°C)	T (K)	diesel mass (g)	ρ_d (kg/m ³)
14.00	287.15	8.42	855.28
14.50	287.65	8.41	854.88
15.00	288.15	8.41	854.57
15.50	288.65	8.40	854.17
16.00	289.15	8.40	853.86
16.50	289.65	8.40	853.46
17.00	290.15	8.39	853.05
17.50	290.65	8.39	852.74
18.00	291.15	8.39	852.34
18.50	291.65	8.38	852.03
19.00	292.15	8.38	851.73
19.50	292.65	8.38	851.32
20.00	293.15	8.37	851.02
20.50	293.65	8.37	850.71
21.00	294.15	8.37	850.41
21.50	294.65	8.36	850.00
22.00	295.15	8.36	849.59
22.50	295.65	8.36	849.29
23.00	296.15	8.35	848.88
23.50	296.65	8.35	848.48
24.00	297.15	8.35	848.17
24.50	297.65	8.34	847.87
24.80	297.95	8.34	847.66
14.00	287.15	8.42	855.28
14.50	287.65	8.41	854.88
15.00	288.15	8.41	854.47
15.50	288.65	8.40	854.06
16.00	289.15	8.40	853.76
16.50	289.65	8.40	853.35
17.00	290.15	8.39	852.95
17.50	290.65	8.39	852.64
18.00	291.15	8.39	852.24
18.50	291.65	8.38	851.93
19.00	292.15	8.38	851.63
19.50	292.65	8.38	851.22
20.00	293.15	8.37	850.91
20.50	293.65	8.37	850.61
21.00	294.15	8.37	850.30
21.50	294.65	8.36	850.00
22.00	295.15	8.36	849.59
22.50	295.65	8.36	849.19
23.00	296.15	8.35	848.88
23.50	296.65	8.35	848.58
24.00	297.15	8.35	848.17
24.50	297.65	8.34	847.87
24.80	297.95	8.34	847.56

Table B.2 Diesel #2 liquid kinematic viscosity measurements (Simplex, 2006)

T (° F)	T (K)	ν_d (SUS)	ν_d (μm ² /s)
30	272.04	138	27.6
60	288.71	70	14
80	299.82	53.6	10.72
100	310.93	45.5	9.1
130	327.59	39	7.8

APPENDIX C: HYDROLYZED DIESEL

Figure C.1 compares the fluorescent emission spectrum for pure diesel to that of the hydrolyzed diesel in water mixture as taken from the reservoir of the test chamber. Both fluids were excited in quartz cuvettes at a wavelength of 451 nm with 2.5 nm slits in the spectrofluorometer. The fluid from the test reservoir was mostly the bulk phase of the water where the hydrolyzed diesel was stably suspended within the bulk water and at approximately 0.15 % mass fraction of diesel. The mass fraction was determined from the relative peak intensities of the reservoir fluid to that of the pure diesel for these cuvette tests. No interference filters were used in the sample chamber of the spectrofluorometer. Evidence for a chemical breakdown of the diesel is based on the fact that the peak fluorescence emission for the emulsified water diesel exists at a wavelength that is 25 nm greater than that of pure diesel.

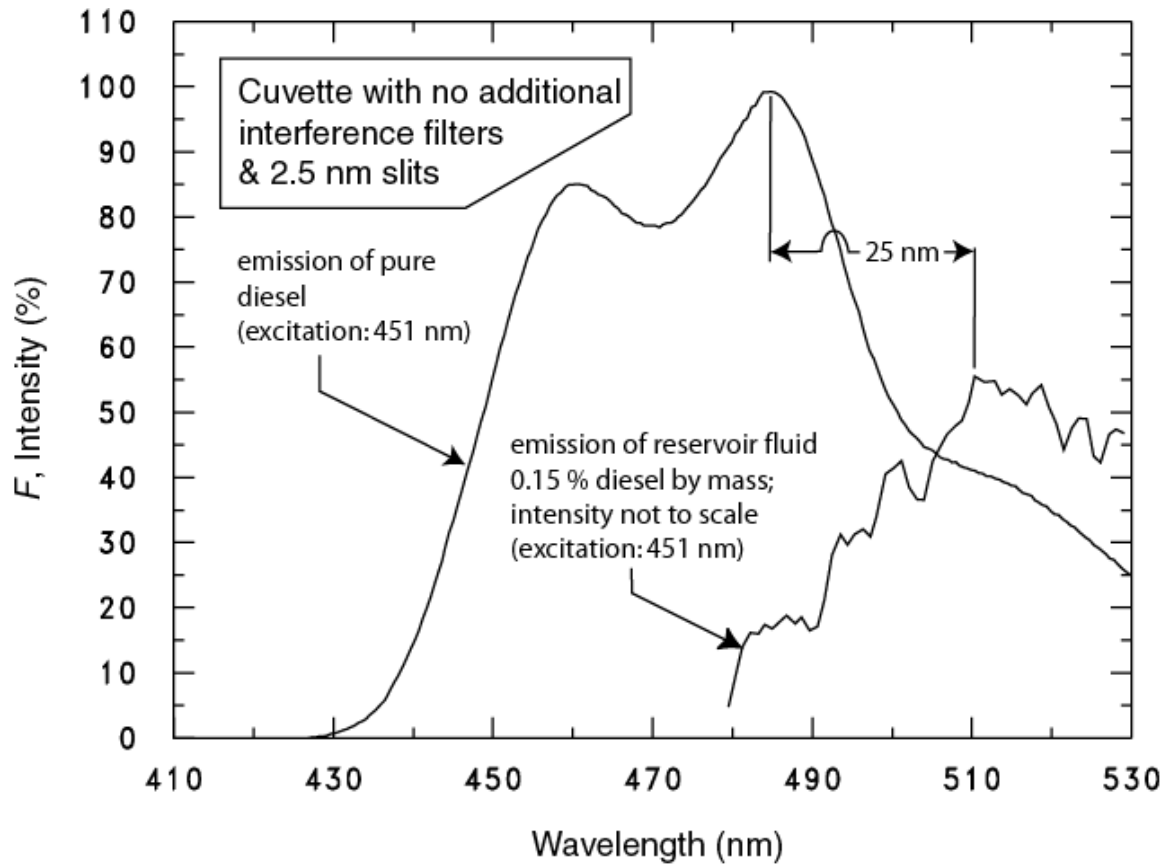


Fig. C.1 Fluorescent emission spectra for pure diesel and hydrolyzed reservoir test fluid

APPENDIX D: FLUORESCENT TEMPERATURE DEPENDENCE

This appendix presents the measurements and the methodology that were used to determine the coefficient of temperature dependence (β) for the fluorescent intensity of diesel (Kedzierski, 2003). All of the measurements and settings were made with the excitation set to 434 nm and the emission measured at 485 nm with the additional spectrofluorometer filters in place as described in Appendix A. Pure diesel was cooled from nominally 303 K to 279 K for two sets of 500 measurements in a temperature controlled liquid bath. The temperature of the mixture was measured with a sheathed thermocouple that was in the controlled temperature bath with the maximum- and zero-jars. The fluorescence intensity of the maximum-jar as a function of bath temperature is given in Fig. D.1.

The temperature dependence of the fluorescence can be expressed as the ratio of the fluorescence intensity at the bath temperature (F_{T_b}) to the intensity evaluated at the test section temperature (F_{T_T}) for all other variables held constant (Kedzierski, 2003):

$$\frac{F_{T_b}}{F_{T_T}} = e^{\beta(T_b - T_T)} \quad (\text{D.1})$$

where the coefficient of temperature dependence of the fluorescence (β) was found to be approximately 0.00156 for the diesel data set shown in Fig. D.1.

Equation D.1 is used to account for any difference between the temperature of the bath that holds the fluorescent standard jars and the temperature of the test section. The target test section fluid temperature for the contamination tests is the same as the fluorescent standard bath temperature. As a result, for approximately 85 % of the contamination measurements, the test section temperature differed no more than ± 1 K from the bath temperature, which would have resulted in an adjustment in the fluorescence with eq. (D.1) by no more than ± 0.2 %. The largest difference between the temperature of the jar bath and the average temperature of the test section for the contamination tests was approximately 4.5 K, which corresponds to a 0.3 % correction of the fluorescence intensity. Flushing tests required larger corrections via eq. (D.1). Flushing was done with house tap water that was as much as 10 K colder than the jar bath temperature, which resulted in a maximum correction of 1.5 % of the fluorescence intensity.

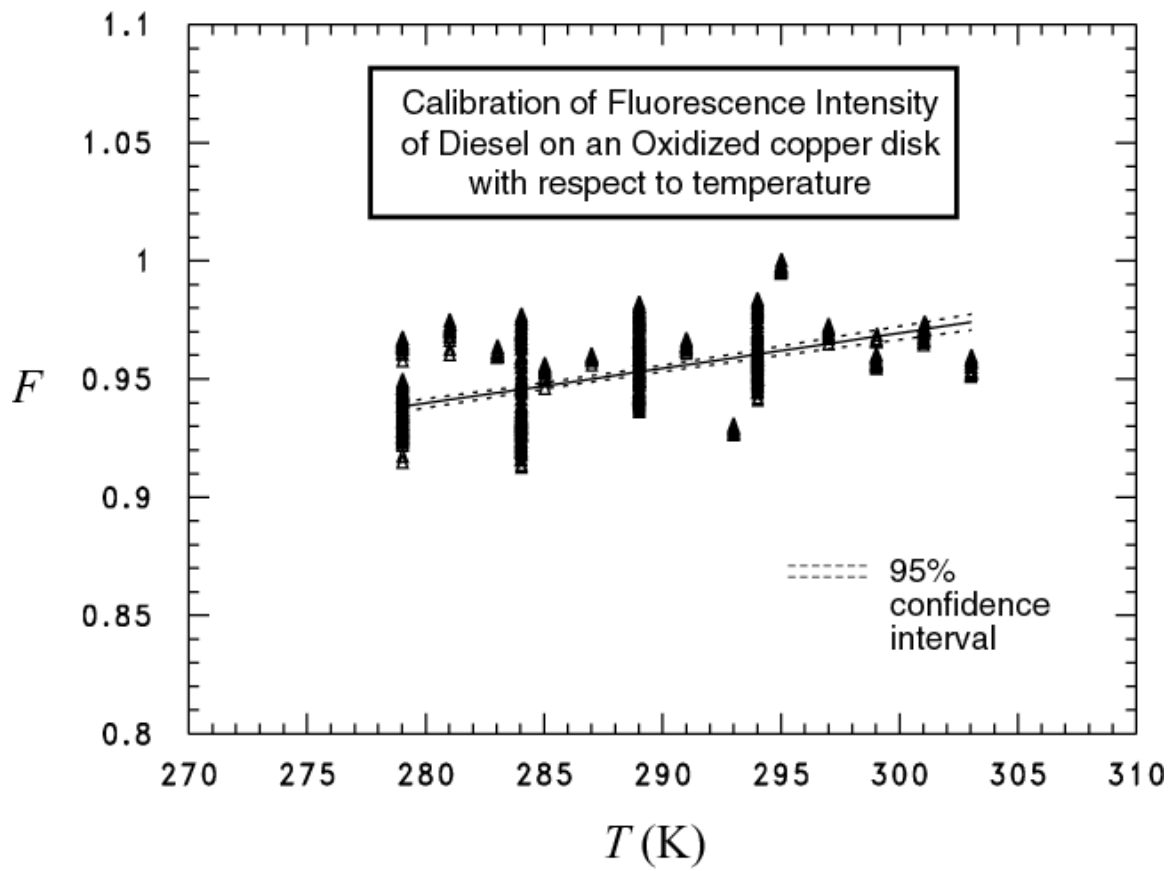


Fig. D.1 Temperature dependence of diesel fluorescence

APPENDIX E: FLUORESCENCE CALIBRATION

This appendix provides more detail on the procedure that was developed and used to calibrate the fluorescence intensity of diesel against mass fraction, path length, air gap, and fluid properties. All calibration measurements were done on a copper disk that was flattened from a pipe and evenly oxidized by electrolysis. Appendix I shows how the functionality of the spectrofluorometer was verified.

Figure E.1 shows the calibration of the fluorescence intensity of diesel against diesel mass fraction for fixed path length. The temperature of the diesel in the 150 mL calibration jar (shown in Fig. 6) was held constant at approximately 294 K. The diesel was mixed with non-fluorescent n-decane in order to dilute the diesel to the desired mass fraction. Unlike water, n-decane was miscible with diesel. The distance between the top of the calibration disk and the bottom of the quartz tube (the path length) was set and fixed with the aid of a 1.6 mm gauge block. For these conditions, the fluorescence intensity was fitted linearly with respect to the diesel mass fraction to within a residual standard deviation of $\pm 1.2\%$.

Figure E.2 shows the calibration of the fluorescence intensity of diesel against the path length through the diesel for neat diesel (for fixed $x_b = 1$). As in the previous mass fraction calibration described above, the temperature of the diesel was held constant at approximately 294 K. This second calibration method was used to determine the effect of the proximity of the incident light (I_o) via changing its path length (l). As shown in Fig. 2, a linear positioning device with a graduated knob was used to locate the quartz tube relative to the test surface and thus measure and set the path length of the incident light through the diesel. The measured fluorescent intensity versus the path length was non-linear as shown in Fig. E.2. The calibrations given in Figs. E.1 and E.2 were combined with an exponential representation of I_o as a function of l to give the total calibration as given in eq. (4).

Figure E.3 shows the calibration measurements that were used to determine the effect of an air gap above the test surface. This method served as a secondary measurement check because it was desired to have a technique that did not require the test section to be filled with test fluid. Because of the mismatch in the index of refraction between the quartz, the air, and the diesel film, the intensity incident to the diesel for when an air-gap existed differed from that for when fluid filled the space between the test surface and the bottom of the quartz probe. To determine the effect of incident intensity reflections from interfaces exposed by the air gap, the probe was traversed above a diesel film of fixed thickness. Because the amount of fluorescent material remained fixed for these tests, the magnitude of the measured intensity was attributed to change in the magnitude of the incident intensity due to its proximity to the diesel film.

Figure E.3. shows measurements with and without air gaps below the quartz probe. As expected, measurements with no air gap are shown to lie on the eq. (4) calibration. Measurements taken with an air gap reside to the right of the eq. (4) calibration in a stratum of nearly linear data grouped by different diesel film thickness. For these measurements, the intensity is shown to increase slightly as the probe approaches the diesel film. From the air-gap data, it was observed that $\frac{1}{F} \frac{dF}{dl}$ was approximately constant for all ranges of the F and l

traverse data for each group of fixed diesel film thickness. The value of F used in this product for each group was extrapolated to the calibration line for no-air-gap (F_{ng}). The gradient was calculated using the air-gap measurements, i.e., $\frac{dF_{ag}}{dl}$. The average ratio between F_{ng} and the air-gap gradient for all the groups was:

$$\frac{1}{F_{ng}} \frac{dF_{ag}}{dl} = -82.57 \text{m}^{-1} \quad (\text{E.1})$$

From the integration of eq. (E.1) it can be seen that the dependency of the intensity is exponential with path length. Considering that this dependency represents how I_o changes with proximity to the test surface, an exponential term with respect to path length was used to represent I_o in the full calibration eq. (4).

The diesel film thickness using the air-gap fluorescent gradient can be solved for by substituting eq. (4) into eq. (E.1) for the F_{ng} :

$$l_e = \frac{-0.0121 \text{m} \frac{dF_{ag}}{dl}}{2.3 I_o \Phi \epsilon M_c^{-1}} = \frac{-0.0115 \text{m}^{-1} \text{kg} \frac{dF_{ag}}{dl} e^{209.23 \text{m}^{-1} l}}{x_b \rho_b} \quad (\text{E.2})$$

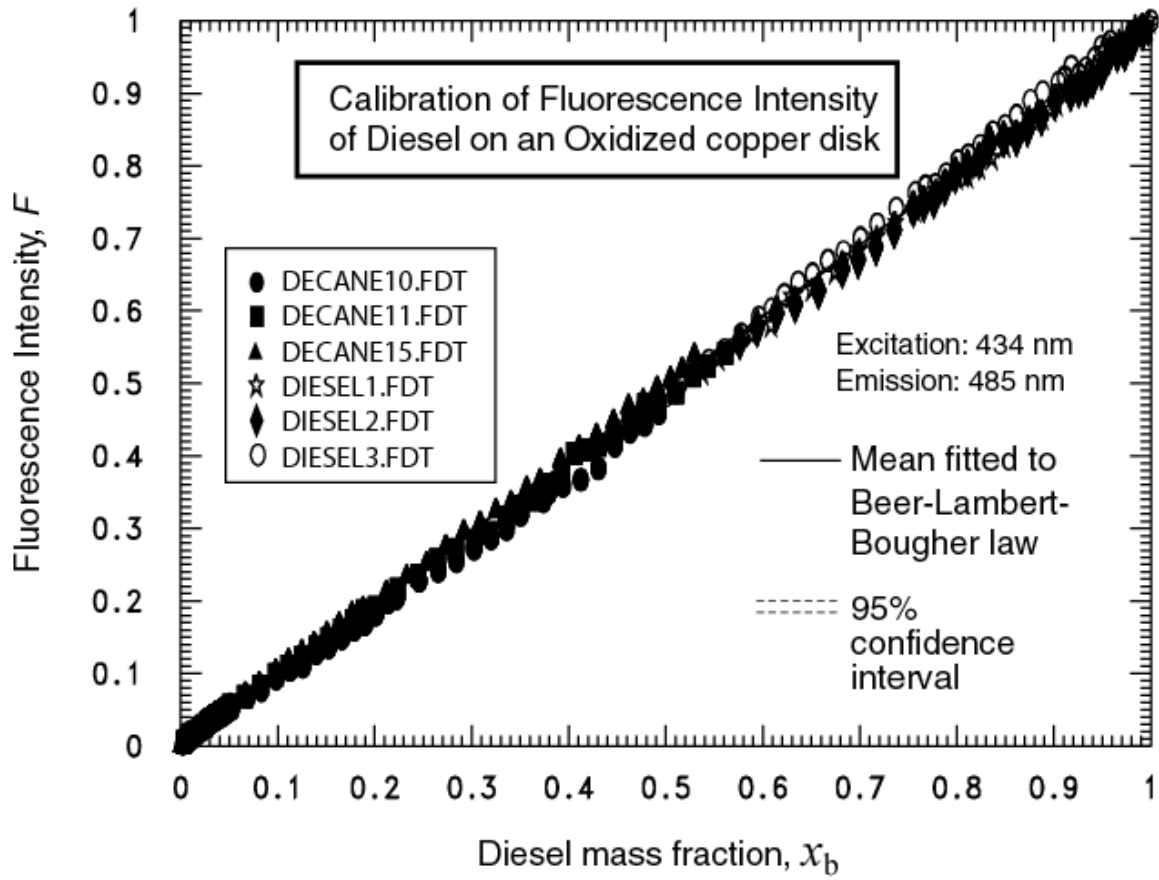


Fig. E.1 Calibration of diesel fluorescence against diesel mass fraction for different runs

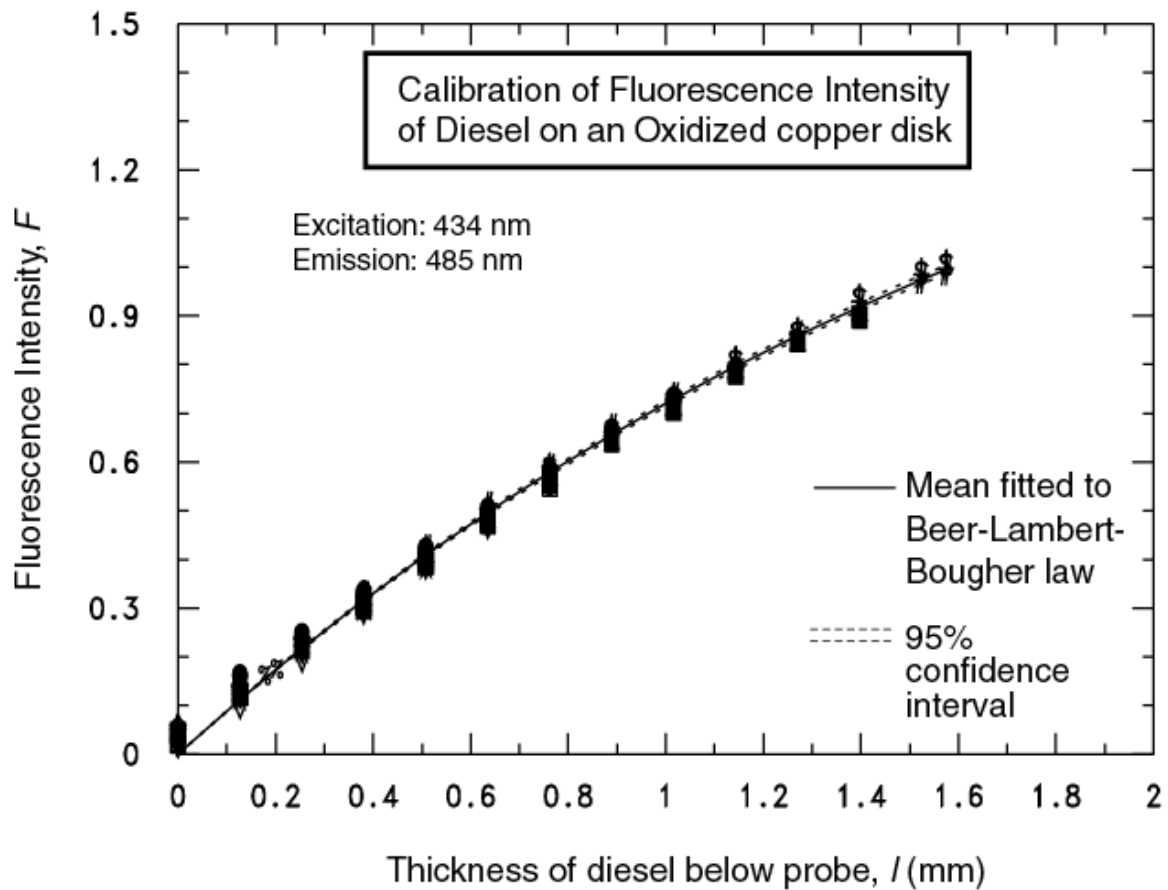


Fig. E.2 Calibration of fluorescence of diesel against path length for different runs

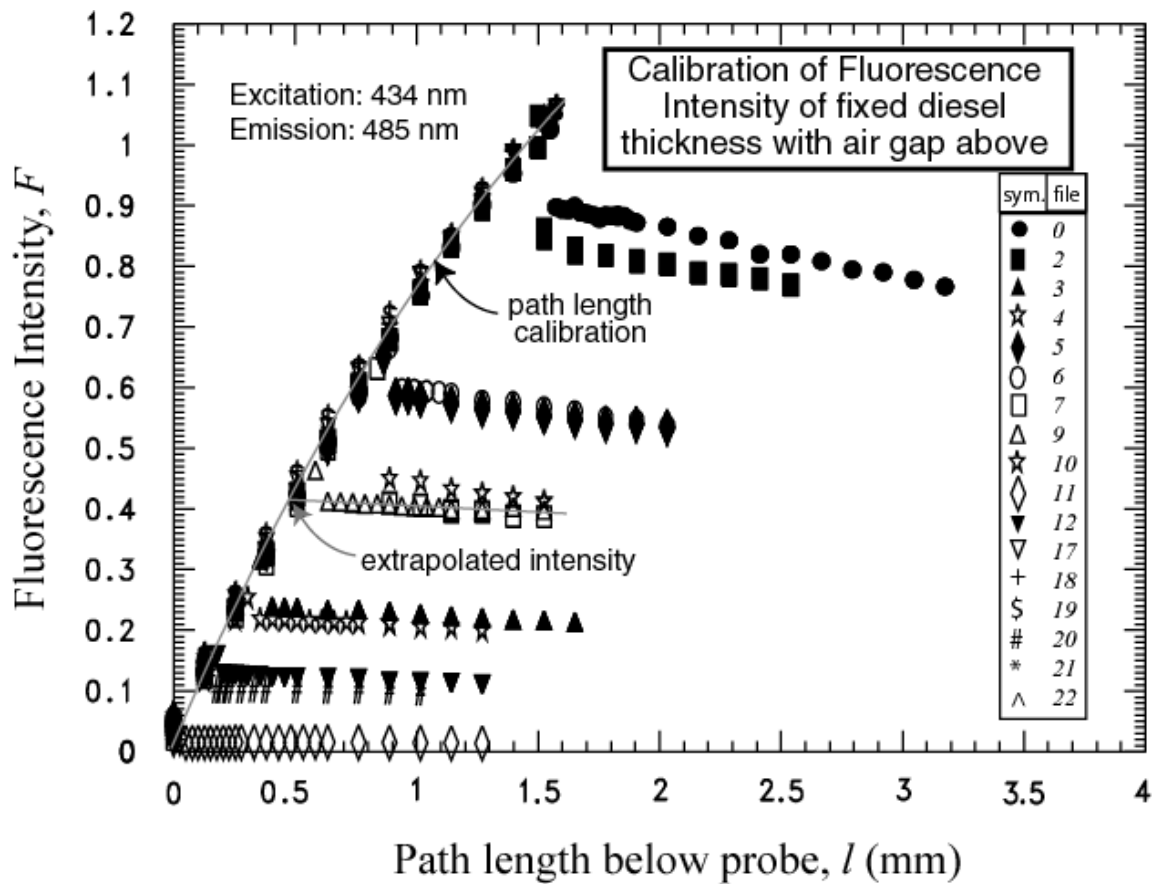


Fig. E.3 Calibration of diesel fluorescence intensity for fixed film thickness and air gap between quartz tube and liquid film

APPENDIX F: LINEAR BEER LAW

This appendix justifies the use of the linear form of the Beer-Lambert-Bouguer law (Amadeo et al., 1971) for the fluorescence calibration of the diesel mass. Regression of the calibration varied mass fraction measurements to the exponential and complete form of the Beer-Lambert-Bouguer law:

$$F = I_o \Phi(1 - 10^{-\epsilon cl}) \quad (\text{F.1})$$

resulted in a residual standard deviation between the measurements and the fit of 0.0156. Considering that the residual standard deviation of the linear fit (eq. 3) was marginally less (0.0151) than that of eq. (F.1), the linear model represents the calibration data just as well as the complete model.

Further justification for the use of eq. (F.1) can be obtained from the general knowledge of fluorescence characteristics. According to Herman (1998), fluorescence remains directly proportional to absorbance (ϵcl) as long as it is small, i.e., $\epsilon cl < 0.05$. Figure F.1 plots the absorbance against the mass fraction for both the mass fraction and the path length calibration measurements. The figure shows that mass fraction calibration measurements satisfy the linear criteria for mass fractions less than approximately 0.8. Similarly, the path length calibration measurements follow the linear Beer-Lambert-Bouguer law for absorption thicknesses (l) less than approximately 1.3 mm. Overall, approximately 78 % of the 936 calibration measurements fall within the linear criteria and none of the measurements exceeded an absorbance of 0.064.

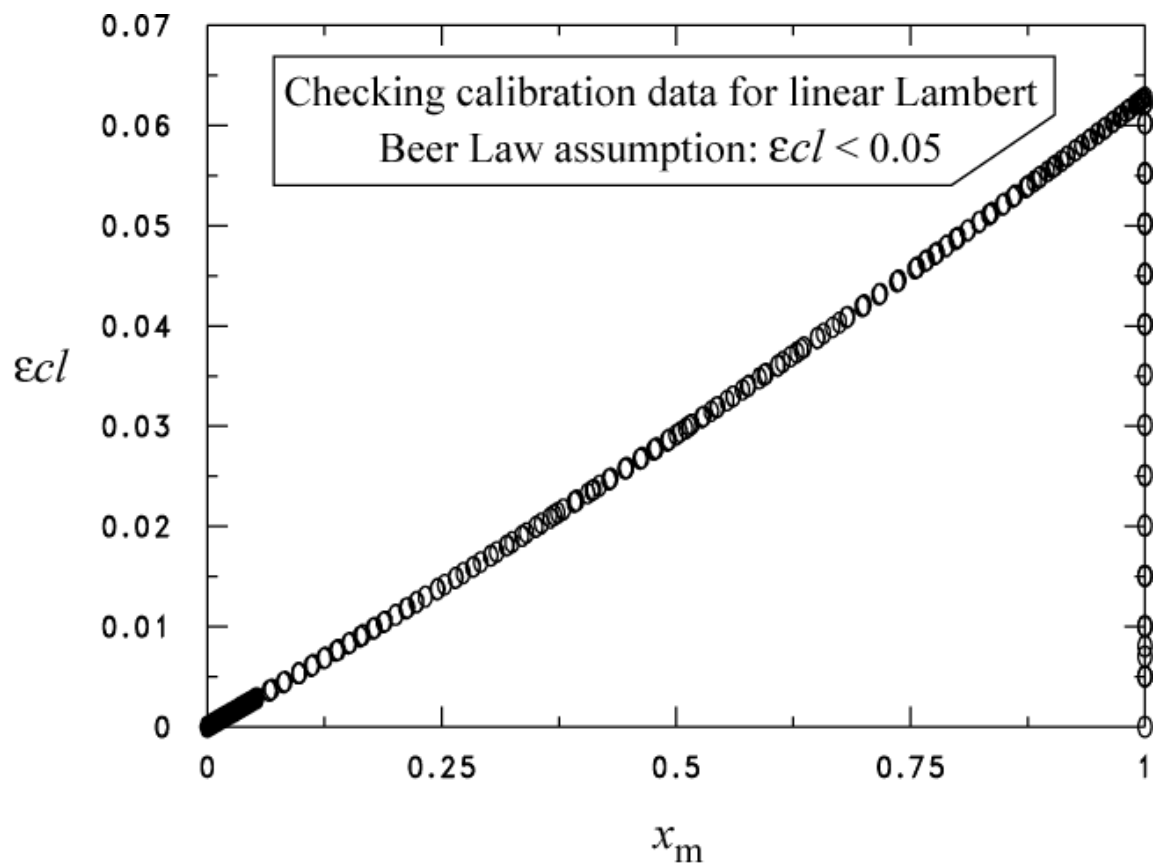


Fig. F.1 Absorbance of diesel for calibration measurements as a function of mass fraction

APPENDIX G: UNCERTAINTIES

Figure G.1 shows the relative (percent) uncertainty of the diesel excess layer thickness (U_{l_e}) as a function of l_e for a bulk mass fraction of nominally 0.2 %. Roughly 80 % of the l_e measurements for the 0.2 % bulk mass fraction have a relative uncertainty of less than 25 %. For measurements with an relative uncertainties less than 25 %, the average uncertainty of l_e is approximately ± 6 % of l_e . Overall, the average uncertainty of l_e on an absolute basis was approximately ± 0.1 μm .

Similarly, Fig. G.2 shows the relative (percent) uncertainty of the diesel excess layer thickness (U_{l_e}) as a function of l_e for a bulk mass fraction of nominally 0.3 %. Roughly 92 % of the l_e measurements have a relative uncertainty of less than 25 %. For these measurements the average uncertainty of l_e is approximately ± 8 % of l_e . Overall, the average uncertainty of l_e for the measurements with the 0.3 % bulk mass fraction was approximately ± 0.4 μm .

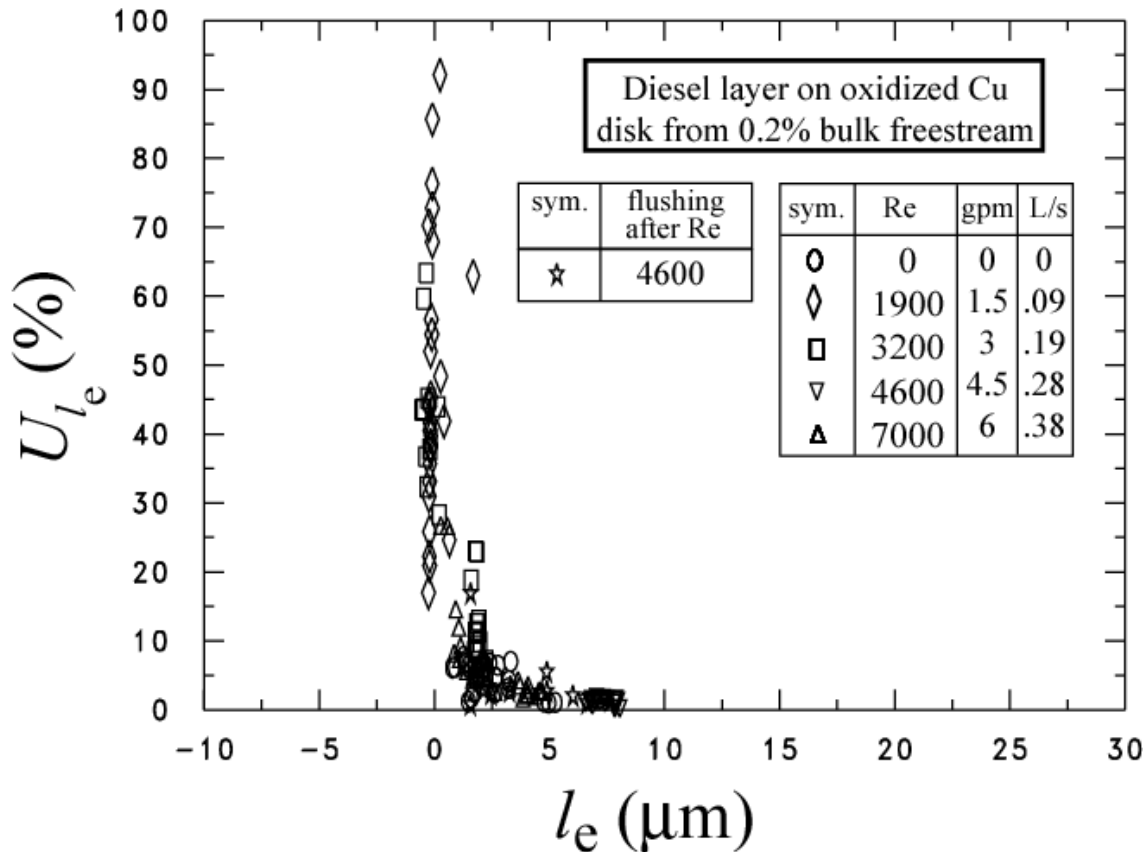


Fig. G.1 Relative uncertainty of l_e for 95 % confidence level and $x_b = 0.2$ %

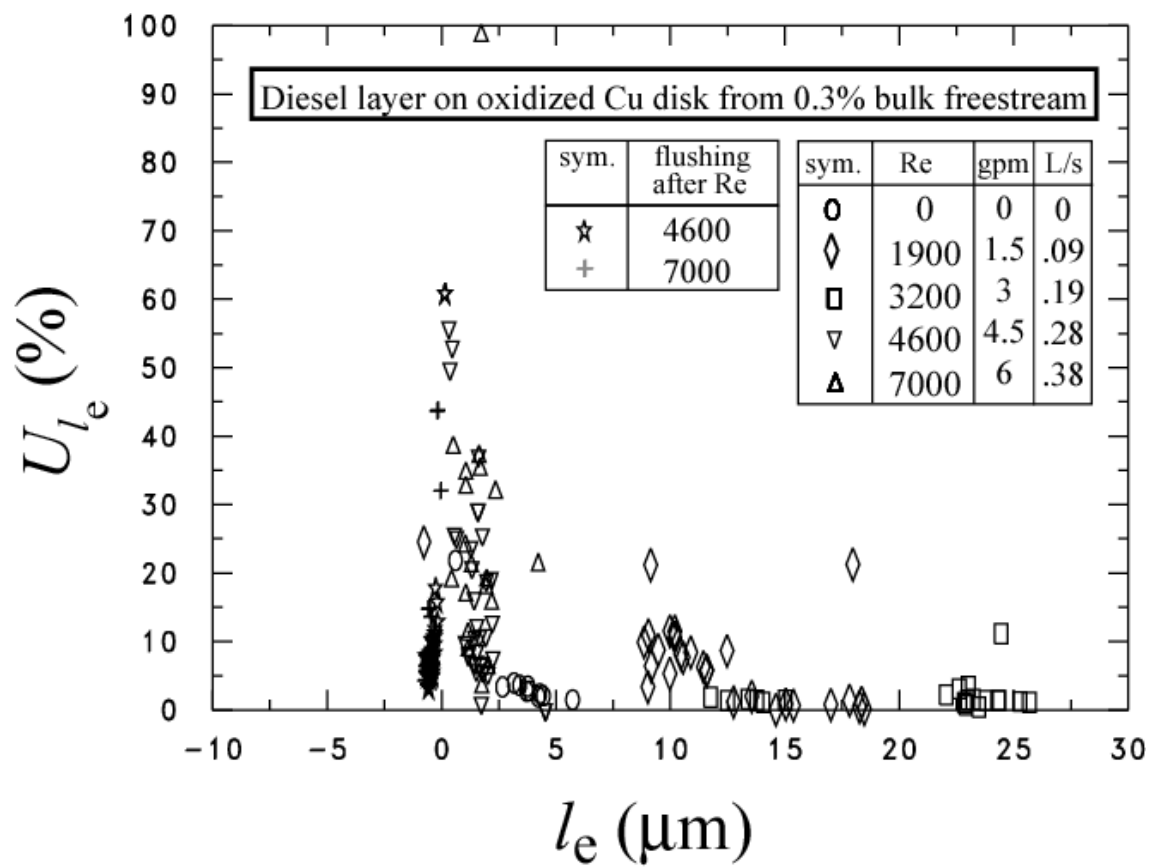


Fig. G.2 Relative uncertainty of l_e for 95 % confidence level and $x_b = 0.3 \%$

APPENDIX H: TABULATED MEASUREMENTS

This appendix provides both raw and reduced tabulated traverse measurements. The raw measurements for the fluorescent intensities used in eq. (2), the salient measured temperatures, the varied path length (l), the exposure time and the water/diesel mixture flow rate are presented in Tables H.1. The data is presented sequentially as blocks of traverse measurements (traverse of typically 13 measurements of l , and intensity while maintaining the flow rate and temperatures) which typically required approximately 10 min to complete. Each block or group of measurements was used to obtain a single value for the diesel excess surface density following the procedure illustrated in Fig. 7.

Reduced measurements including the excess layer thickness following the procedure demonstrated in Fig. 7 are given in Tables H.2. In addition, the excess surface density as calculated from eq. (1), the diesel mass fraction as calculated from eq. (9), the average test section fluid temperature, and the effect of temperature on fluorescence as calculated from eq. (D.1) are provided. The exposure time is the real time measured from the time starting when the clean surface was first exposed to the particular flow rate.

All tables present only a fraction of the measures and are given to provide only an example. Complete data files are available upon request.

Table H.1.1 Diesel contamination on oxidized copper surface for $Re = 0$ and $x_b = 0.2\%$

Diesel contamination on oxidized copper surface for $Re = 0$ and $x_b = 0.2\%$ (file: trv0con1.tbl)											
F (v)	F_r (v)	F_{100} (v)	F_0 (v)	T_{Ti} (K)	T_{To} (K)	T_a (K)	T_b (K)	l (mm)	Exposure time (s)	Turbine meter \dot{m}_w (kg/s)	Doppler meter \dot{m}_w (kg/s)
0.001242	0.001180	0.942909	0.000008	294.3	294.4	297.1	293.6	1.59	792.	0.0000	0.0625
0.001207	0.001147	0.942909	0.000008	294.3	294.5	296.7	293.6	1.52	842.	0.0000	0.0625
0.001249	0.001187	0.942909	0.000008	294.4	294.5	297.1	293.6	1.40	894.	0.0000	0.0625
0.001400	0.001330	0.942909	0.000008	294.4	294.6	297.1	293.6	1.27	945.	0.0000	0.0625
0.001449	0.001376	0.942909	0.000008	294.4	294.6	296.9	293.6	1.14	995.	0.0000	0.0625
0.001484	0.001409	0.942909	0.000008	294.5	294.7	297.2	293.6	1.02	1052.	0.0000	0.0625
0.001590	0.001510	0.942909	0.000008	294.5	294.7	296.9	293.6	0.89	1104.	0.0000	0.0625
0.001641	0.001558	0.942909	0.000008	294.5	294.7	296.9	293.6	0.76	1156.	0.0000	0.0625
0.001687	0.001602	0.942909	0.000008	294.6	294.8	297.0	293.6	0.64	1216.	0.0000	0.0697
0.001770	0.001679	0.942909	0.000008	294.6	294.8	296.8	293.6	0.51	1268.	0.0000	0.0738
0.001816	0.001724	0.942909	0.000008	294.6	294.9	297.1	293.6	0.38	1322.	0.0000	0.0697
0.001890	0.001794	0.942909	0.000008	294.6	294.9	297.0	293.6	0.25	1377.	0.0000	0.0800
0.001855	0.001760	0.942909	0.000008	294.7	294.9	296.9	293.6	0.13	1429.	0.0000	0.0853
0.002019	0.001910	0.935436	0.000017	294.8	295.1	297.1	293.6	1.59	1620.	0.0000	0.0625
0.001928	0.001825	0.935436	0.000017	294.8	295.1	297.0	293.6	1.52	1672.	0.0000	0.0624
0.002032	0.001922	0.935436	0.000017	294.8	295.1	297.3	293.6	1.40	1726.	0.0000	0.0625
0.002071	0.001959	0.935436	0.000017	294.8	295.1	297.0	293.6	1.27	1786.	0.0000	0.0625
0.002037	0.001927	0.935436	0.000017	294.8	295.1	297.1	293.6	1.14	1838.	0.0000	0.0624
0.002120	0.002005	0.935436	0.000017	294.9	295.2	297.0	293.6	1.02	1895.	0.0000	0.0625
0.002135	0.002019	0.935436	0.000017	294.9	295.2	297.1	293.6	0.89	1948.	0.0000	0.0625
0.002159	0.002042	0.935436	0.000017	294.9	295.2	297.3	293.6	0.76	2017.	0.0000	0.0739
0.002213	0.002093	0.935436	0.000017	294.9	295.2	297.0	293.6	0.64	2072.	0.0000	0.0781
0.002188	0.002069	0.935436	0.000017	294.9	295.3	297.2	293.6	0.51	2124.	0.0000	0.0745
0.002277	0.002152	0.935436	0.000017	295.0	295.3	297.2	293.6	0.38	2177.	0.0000	0.0625
0.002300	0.002175	0.935436	0.000017	295.0	295.3	297.1	293.6	0.25	2231.	0.0000	0.0625
0.002257	0.002134	0.935436	0.000017	295.0	295.3	297.0	293.6	0.13	2283.	0.0000	0.0709
0.001635	0.001631	0.985852	0.000013	295.5	296.0	297.2	293.6	1.59	6047.	0.0000	0.0625
0.001660	0.001655	0.985852	0.000013	295.5	296.0	296.9	293.6	1.52	6098.	0.0000	0.0624
0.001684	0.001679	0.985852	0.000013	295.5	296.0	297.0	293.6	1.40	6150.	0.0000	0.0625

Table H.1.2 Diesel contamination on oxidized copper surface for Re = 1900 and $x_b = 0.2\%$

Diesel contamination on oxidized copper surface for Re = 1900 and $x_b = 0.2\%$ (file: trv15con1.tbl)											
F (v)	F_r (v)	F_{100} (v)	F_0 (v)	T_{Ti} (K)	T_{To} (K)	T_a (K)	T_b (K)	l (mm)	Exposure time (s)	Turbine meter \dot{m}_w (kg/s)	Doppler meter \dot{m}_w (kg/s)
0.003617	0.003772	1.010201	0.000107	295.5	295.5	297.6	293.6	1.59	1008.	0.0763	0.1093
0.003411	0.003563	1.010201	0.000107	295.5	295.4	297.7	293.6	1.52	1065.	0.0737	0.1058
0.003222	0.003372	1.010201	0.000107	295.4	295.4	297.5	293.6	1.40	1135.	0.0759	0.1042
0.003004	0.003151	1.010201	0.000107	295.4	295.4	297.4	293.6	1.27	1179.	0.0742	0.1106
0.002763	0.002906	1.010201	0.000107	295.4	295.4	297.8	293.6	1.14	1258.	0.0750	0.1004
0.002261	0.002398	1.010201	0.000107	295.4	295.4	297.6	293.6	1.02	1321.	0.0755	0.1085
0.002154	0.002289	1.010201	0.000107	295.3	295.3	297.4	293.6	0.89	1392.	0.0712	0.1106
0.001791	0.001921	1.010201	0.000107	295.3	295.3	297.6	293.6	0.76	1492.	0.0732	0.1222
0.001876	0.002007	1.010201	0.000107	295.3	295.3	297.5	293.6	0.64	1536.	0.0742	0.1033
0.001588	0.001716	1.010201	0.000107	295.2	295.3	297.6	293.6	0.51	1574.	0.0745	0.1069
0.001351	0.001475	1.010201	0.000107	295.2	295.2	297.5	293.6	0.38	1617.	0.0710	0.1023
0.000918	0.001038	1.010201	0.000107	295.2	295.2	297.5	293.6	0.25	1661.	0.0720	0.1124
0.000574	0.000688	1.010201	0.000107	295.2	295.2	297.6	293.6	0.13	1705.	0.0747	0.1087
0.002523	0.002562	1.008425	0.000018	293.5	293.5	297.6	293.6	1.59	61523.	0.0844	0.1042
0.002449	0.002488	1.008425	0.000018	293.5	293.5	297.2	293.6	1.52	61568.	0.0874	0.1111
0.002293	0.002330	1.008425	0.000018	293.5	293.5	297.6	293.6	1.40	61614.	0.0864	0.1151
0.002095	0.002131	1.008425	0.000018	293.4	293.4	297.5	293.6	1.27	61656.	0.0869	0.1167
0.001901	0.001935	1.008425	0.000018	293.4	293.4	297.6	293.6	1.14	61697.	0.0870	0.1146
0.001768	0.001801	1.008425	0.000018	293.4	293.4	297.3	293.6	1.02	61743.	0.0877	0.1175
0.001607	0.001638	1.008425	0.000018	293.4	293.4	297.3	293.6	0.89	61782.	0.0833	0.1163
0.001453	0.001483	1.008425	0.000018	293.4	293.4	297.4	293.6	0.76	61823.	0.0866	0.1192
0.001238	0.001266	1.008425	0.000018	293.4	293.4	297.2	293.6	0.64	61865.	0.0853	0.1168
0.001073	0.001100	1.008425	0.000018	293.3	293.4	297.1	293.6	0.51	61905.	0.0827	0.1161
0.000963	0.000989	1.008425	0.000018	293.3	293.3	297.4	293.6	0.38	61946.	0.0866	0.1187
0.000763	0.000788	1.008425	0.000018	293.3	293.3	297.1	293.6	0.25	61987.	0.0858	0.1168
0.000609	0.000632	1.008425	0.000018	293.3	293.3	297.3	293.6	0.13	62026.	0.0875	0.1157
0.002626	0.002759	1.007386	0.000116	293.3	293.3	297.5	293.6	1.59	62198.	0.0833	0.1161
0.002493	0.002625	1.007386	0.000116	293.3	293.3	297.7	293.6	1.52	62241.	0.0848	0.1130
0.002345	0.002476	1.007386	0.000116	293.2	293.2	297.5	293.6	1.40	62282.	0.0870	0.1108
0.002184	0.002314	1.007386	0.000116	293.2	293.2	297.3	293.6	1.27	62324.	0.0853	0.1185
0.002013	0.002142	1.007386	0.000116	293.2	293.2	297.2	293.6	1.14	62367.	0.0833	0.1127
0.001872	0.002001	1.007386	0.000116	293.2	293.2	296.9	293.6	1.02	62409.	0.0872	0.1105
0.001720	0.001847	1.007386	0.000116	293.2	293.2	297.0	293.6	0.89	62454.	0.0852	0.1062
0.001540	0.001666	1.007386	0.000116	293.2	293.2	297.3	293.6	0.76	62498.	0.0858	0.1119
0.001507	0.001633	1.007386	0.000116	293.2	293.2	297.3	293.6	0.64	62539.	0.0829	0.1194
0.001393	0.001518	1.007386	0.000116	293.2	293.2	297.1	293.6	0.51	62581.	0.0862	0.1241
0.001258	0.001382	1.007386	0.000116	293.2	293.2	297.2	293.6	0.38	62622.	0.0863	0.1229
0.001078	0.001201	1.007386	0.000116	293.2	293.2	297.1	293.6	0.25	62664.	0.0868	0.1238
0.000830	0.000951	1.007386	0.000116	293.2	293.2	297.2	293.6	0.13	62707.	0.0843	0.1239
0.002796	0.002894	1.012094	0.000064	293.7	293.7	297.5	293.6	1.59	66387.	0.0870	0.1184
0.002666	0.002762	1.012094	0.000064	293.7	293.7	297.6	293.6	1.52	66427.	0.0862	0.1222
0.002592	0.002687	1.012094	0.000064	293.6	293.6	297.5	293.6	1.40	66469.	0.0845	0.1167
0.002529	0.002624	1.012094	0.000064	293.6	293.6	297.6	293.6	1.27	66509.	0.0883	0.1163
0.003842	0.003952	1.012094	0.000064	293.6	293.6	297.4	293.6	1.14	66551.	0.0877	0.1179
0.003831	0.003941	1.012094	0.000064	293.6	293.6	297.2	293.6	1.02	66592.	0.0877	0.1143
0.003148	0.003250	1.012094	0.000064	293.5	293.6	297.4	293.6	0.89	66632.	0.0865	0.1092
0.002608	0.002703	1.012094	0.000064	293.5	293.5	297.4	293.6	0.76	66709.	0.0816	0.1067
0.002231	0.002321	1.012094	0.000064	293.5	293.5	297.5	293.6	0.64	66749.	0.0836	0.1163
0.001971	0.002059	1.012094	0.000064	293.4	293.5	297.7	293.6	0.51	66788.	0.0864	0.1092
0.001619	0.001702	1.012094	0.000064	293.4	293.4	297.5	293.6	0.38	66829.	0.0829	0.1110
0.001524	0.001606	1.012094	0.000064	293.4	293.4	297.2	293.6	0.25	66869.	0.0872	0.1138
0.001461	0.001542	1.012094	0.000064	293.4	293.4	297.1	293.6	0.13	66910.	0.0850	0.1169
0.003188	0.003266	1.009252	0.000047	294.0	293.9	296.5	293.6	1.59	69847.	0.0853	0.1064
0.003181	0.003259	1.009252	0.000047	294.0	293.9	296.3	293.6	1.52	69884.	0.0834	0.1082
0.003045	0.003122	1.009252	0.000047	294.0	293.9	296.5	293.6	1.40	69926.	0.0857	0.1098
0.002962	0.003038	1.009252	0.000047	294.0	294.0	296.5	293.6	1.27	69967.	0.0859	0.1106
0.002824	0.002898	1.009252	0.000047	294.0	294.0	296.3	293.6	1.14	70009.	0.0862	0.1147

Table H.1.3 Diesel contamination on oxidized copper surface for Re = 3200 and $x_b = 0.2\%$

Diesel contamination on oxidized copper surface for Re = 3200 and $x_b = 0.2\%$ (file: trv3con1.tbl)											
F (v)	F_r (v)	F_{100} (v)	F_0 (v)	T_{Ti} (K)	T_{To} (K)	T_a (K)	T_b (K)	l (mm)	Exposure time (s)	Turbine meter \dot{m}_w (kg/s)	Doppler meter \dot{m}_w (kg/s)
0.003391	0.003385	1.002145	-0.0000260	296.2	296.1	296.1	293.6	1.59	1521.	0.1558	0.1596
0.003188	0.003182	1.002145	-0.000026	296.2	296.1	296.0	293.6	1.52	1563.	0.1512	0.1566
0.003292	0.003286	1.002145	-0.000026	296.2	296.1	296.0	293.6	1.40	1607.	0.1550	0.1613
0.003003	0.002996	1.002145	-0.000026	296.2	296.2	296.0	293.6	1.27	1706.	0.1531	0.1577
0.002738	0.002728	1.002145	-0.000026	296.2	296.2	295.9	293.6	1.14	1749.	0.1509	0.1601
0.002347	0.002335	1.002145	-0.000026	296.2	296.2	295.7	293.6	1.02	1789.	0.1476	0.1620
0.001922	0.001908	1.002145	-0.000026	296.2	296.2	295.3	293.6	0.89	1831.	0.1550	0.1634
0.001679	0.001663	1.002145	-0.000026	296.2	296.2	296.5	293.6	0.76	1873.	0.1453	0.1589
0.001387	0.001369	1.002145	-0.000026	296.2	296.2	296.2	293.6	0.64	1920.	0.1557	0.1587
0.001198	0.001179	1.002145	-0.000026	296.2	296.2	295.6	293.6	0.51	1966.	0.1535	0.1517
0.000929	0.000908	1.002145	-0.000026	296.2	296.2	295.8	293.6	0.38	2009.	0.1550	0.1509
0.000584	0.000561	1.002145	-0.000026	296.2	296.2	296.1	293.6	0.25	2051.	0.1542	0.1502
0.000082	0.000056	1.002145	-0.000026	296.2	296.2	296.0	293.6	0.13	2092.	0.1501	0.1581
0.003134	0.003115	1.006735	-0.000052	296.2	296.2	295.3	293.6	1.59	2224.	0.1470	0.1501
0.002885	0.002864	1.006735	-0.000052	296.2	296.2	295.2	293.6	1.52	2267.	0.1509	0.1669
0.002841	0.002819	1.006735	-0.000052	296.2	296.1	295.4	293.7	1.40	2310.	0.1550	0.1654
0.002923	0.002902	1.006735	-0.000052	296.2	296.1	295.9	293.6	1.27	2354.	0.1535	0.1563
0.002583	0.002558	1.006735	-0.000052	296.1	296.1	295.5	293.6	1.14	2401.	0.1480	0.1649
0.002263	0.002235	1.006735	-0.000052	296.1	296.1	296.0	293.6	1.02	2442.	0.1498	0.1600
0.001828	0.001795	1.006735	-0.000052	296.1	296.1	295.8	293.6	0.89	2482.	0.1546	0.1587
0.001410	0.001373	1.006735	-0.000052	296.1	296.1	295.4	293.6	0.76	2524.	0.1523	0.1517
0.001121	0.001081	1.006735	-0.000052	296.1	296.1	296.1	293.6	0.64	2569.	0.1516	0.1553
0.000973	0.000931	1.006735	-0.000052	296.1	296.0	295.6	293.6	0.51	2775.	0.1487	0.1572
0.000673	0.000628	1.006735	-0.000052	296.0	296.0	295.7	293.6	0.38	2819.	0.1487	0.1486
0.000397	0.000349	1.006735	-0.000052	296.0	296.0	295.8	293.6	0.25	2862.	0.1531	0.1543
0.000080	0.000029	1.006735	-0.000052	296.0	296.0	295.8	293.6	0.13	2903.	0.1466	0.1421
0.002741	0.002780	1.007206	0.000016	294.4	294.4	296.2	293.6	1.59	5441.	0.1543	0.1350
0.002670	0.002709	1.007206	0.000016	294.4	294.4	296.6	293.6	1.52	5486.	0.1535	0.1459
0.002594	0.002632	1.007206	0.000016	294.4	294.3	296.6	293.6	1.40	5531.	0.1550	0.1662
0.002476	0.002512	1.007206	0.000016	294.3	294.3	296.6	293.6	1.27	5572.	0.1562	0.1562
0.002236	0.002270	1.007206	0.000016	294.3	294.3	296.5	293.6	1.14	5619.	0.1509	0.1455
0.001912	0.001944	1.007206	0.000016	294.3	294.3	296.8	293.6	1.02	5660.	0.1532	0.1485
0.001566	0.001595	1.007206	0.000016	294.2	294.2	296.9	293.6	0.89	5702.	0.1488	0.1517
0.001214	0.001240	1.007206	0.000016	294.2	294.2	296.4	293.6	0.76	5744.	0.1528	0.1430
0.000993	0.001017	1.007206	0.000016	294.2	294.2	296.4	293.6	0.64	5783.	0.1488	0.1453
0.000791	0.000813	1.007206	0.000016	294.1	294.1	296.0	293.6	0.51	5824.	0.1477	0.1454
0.000601	0.000622	1.007206	0.000016	294.1	294.1	296.5	293.6	0.38	5866.	0.1554	0.1476
0.000331	0.000350	1.007206	0.000016	294.1	294.1	295.8	293.6	0.25	5909.	0.1539	0.1425
0.000083	0.000100	1.007206	0.000016	294.0	294.0	295.7	293.6	0.13	5957.	0.1481	0.1432
0.002855	0.002877	0.999473	0.000026	293.2	293.2	296.4	293.7	1.59	8736.	0.1562	0.1391
0.002723	0.002746	0.999473	0.000026	293.2	293.2	296.1	293.7	1.52	8776.	0.1562	0.1290
0.002447	0.002470	0.999473	0.000026	293.2	293.2	296.3	293.6	1.40	8821.	0.1570	0.1397
0.002283	0.002307	0.999473	0.000026	293.3	293.2	296.1	293.6	1.27	8865.	0.1524	0.1531
0.002136	0.002160	0.999473	0.000026	293.3	293.3	295.9	293.7	1.14	8906.	0.1502	0.1457
0.001921	0.001946	0.999473	0.000026	293.3	293.3	295.9	293.6	1.02	8946.	0.1547	0.1348
0.001659	0.001683	0.999473	0.000026	293.3	293.3	296.0	293.6	0.89	8988.	0.1513	0.1328
0.001420	0.001445	0.999473	0.000026	293.3	293.3	296.7	293.6	0.76	9028.	0.1521	0.1226
0.001140	0.001165	0.999473	0.000026	293.3	293.3	296.6	293.7	0.64	9070.	0.1528	0.1392
0.000918	0.000943	0.999473	0.000026	293.4	293.3	296.3	293.6	0.51	9116.	0.1578	0.1413
0.000610	0.000636	0.999473	0.000026	293.4	293.3	296.2	293.6	0.38	9162.	0.1547	0.1497
0.000373	0.000399	0.999473	0.000026	293.4	293.4	296.1	293.6	0.25	9204.	0.1502	0.1482
0.000174	0.000200	0.999473	0.000026	293.4	293.4	296.0	293.6	0.13	9244.	0.1506	0.1494
0.002669	0.002642	0.986360	0.000010	293.5	293.5	296.1	293.7	1.59	9383.	0.1559	0.1608
0.002560	0.002534	0.986360	0.000010	293.5	293.5	296.7	293.7	1.52	9424.	0.1510	0.1470
0.002486	0.002462	0.986360	0.000010	293.5	293.5	296.8	293.6	1.40	9465.	0.1543	0.1328
0.002299	0.002278	0.986360	0.000010	293.5	293.5	296.8	293.6	1.27	9506.	0.1543	0.1232
0.002114	0.002095	0.986360	0.000010	293.6	293.5	296.9	293.6	1.14	9548.	0.1562	0.1415
0.001922	0.001905	0.986360	0.000010	293.6	293.6	296.5	293.6	1.02	9592.	0.1558	0.1516

Table H.1.4 Diesel contamination on oxidized copper surface for Re = 4600 and $x_b = 0.2\%$

Diesel contamination on oxidized copper surface for Re = 4600 and $x_b = 0.2\%$ (file: trv45con1.tbl)											
F (v)	F_r (v)	F_{100} (v)	F_0 (v)	T_{Ti} (K)	T_{To} (K)	T_a (K)	T_b (K)	l (mm)	Exposure time (s)	Turbine meter \dot{m}_w (k g/s)	Doppler meter \dot{m}_w (k g/s)
0.0071260	0.007198	1.006097	0.000032	293.4	293.4	294.7	293.6	1.59	236041.	0.2280	0.2502
0.007096	0.007168	1.006097	0.000032	293.4	293.4	294.5	293.6	1.52	236081.	0.2305	0.2517
0.007047	0.007119	1.006097	0.000032	293.4	293.4	294.6	293.6	1.40	236122.	0.2191	0.2518
0.007094	0.007166	1.006097	0.000032	293.4	293.4	294.7	293.6	1.27	236166.	0.2280	0.2526
0.007073	0.007145	1.006097	0.000032	293.4	293.4	294.6	293.6	1.14	236207.	0.2264	0.2534
0.007054	0.007126	1.006097	0.000032	293.4	293.4	294.7	293.6	1.02	236249.	0.2238	0.2539
0.007076	0.007148	1.006097	0.000032	293.4	293.4	294.7	293.6	0.89	236293.	0.2255	0.2511
0.007170	0.007242	1.006097	0.000032	293.4	293.4	294.7	293.6	0.76	236338.	0.2169	0.2425
0.007069	0.007141	1.006097	0.000032	293.4	293.4	295.0	293.6	0.64	236382.	0.2264	0.2245
0.007079	0.007151	1.006097	0.000032	293.4	293.4	294.9	293.6	0.51	236423.	0.2199	0.2101
0.007225	0.007299	1.006097	0.000032	293.4	293.4	294.9	293.6	0.38	236464.	0.2222	0.1988
0.007117	0.007190	1.006097	0.000032	293.4	293.4	294.6	293.6	0.25	236505.	0.2176	0.1980
0.007247	0.007321	1.006097	0.000032	293.5	293.4	294.6	293.6	0.13	236554.	0.2246	0.1958
0.007107	0.007254	1.010847	0.000072	293.5	293.5	294.7	293.6	1.59	236711.	0.2215	0.2049
0.007058	0.007205	1.010847	0.000072	293.6	293.5	294.5	293.6	1.52	236754.	0.2246	0.2016
0.006926	0.007071	1.010847	0.000072	293.6	293.5	294.4	293.6	1.40	236797.	0.2215	0.2097
0.006983	0.007130	1.010847	0.000072	293.6	293.6	294.6	293.6	1.27	236838.	0.2215	0.2197
0.007073	0.007221	1.010847	0.000072	293.6	293.6	294.7	293.6	1.14	236883.	0.2223	0.2426
0.006951	0.007097	1.010847	0.000072	293.6	293.6	294.0	293.6	1.02	236931.	0.2184	0.2300
0.007007	0.007155	1.010847	0.000072	293.6	293.6	294.4	293.6	0.89	236982.	0.2176	0.2184
0.007060	0.007208	1.010847	0.000072	293.7	293.6	294.6	293.6	0.76	237026.	0.2146	0.2313
0.006998	0.007146	1.010847	0.000072	293.7	293.7	294.7	293.6	0.64	237070.	0.2288	0.2428
0.007111	0.007260	1.010847	0.000072	293.7	293.7	294.8	293.6	0.51	237111.	0.2161	0.2415
0.007065	0.007214	1.010847	0.000072	293.8	293.7	294.7	293.6	0.38	237152.	0.2154	0.2009
0.007105	0.007255	1.010847	0.000072	293.8	293.8	294.6	293.6	0.25	237198.	0.2231	0.2004
0.007172	0.007323	1.010847	0.000072	293.8	293.8	294.6	293.6	0.13	237241.	0.2314	0.1928
0.006849	0.007022	1.014358	0.000078	293.4	293.4	294.6	293.7	1.59	240174.	0.2232	0.2063
0.006815	0.006988	1.014358	0.000078	293.4	293.4	294.8	293.6	1.52	240224.	0.2185	0.2267
0.006847	0.007020	1.014358	0.000078	293.4	293.4	294.6	293.6	1.40	240267.	0.2184	0.2373
0.006850	0.007023	1.014358	0.000078	293.4	293.4	294.6	293.6	1.27	240313.	0.2200	0.2540
0.006814	0.006986	1.014358	0.000078	293.4	293.4	294.6	293.6	1.14	240355.	0.2192	0.2564
0.006853	0.007025	1.014358	0.000078	293.4	293.4	294.6	293.6	1.02	240396.	0.2185	0.2566
0.006883	0.007056	1.014358	0.000078	293.4	293.4	294.8	293.6	0.89	240460.	0.2263	0.2379
0.006854	0.007027	1.014358	0.000078	293.4	293.4	294.9	293.6	0.76	240502.	0.2264	0.2355
0.006924	0.007098	1.014358	0.000078	293.4	293.4	294.9	293.6	0.64	240546.	0.2192	0.2505
0.006944	0.007118	1.014358	0.000078	293.4	293.4	295.1	293.6	0.51	240591.	0.2255	0.2512
0.007005	0.007180	1.014358	0.000078	293.4	293.4	294.9	293.6	0.38	240635.	0.2169	0.2541
0.007047	0.007223	1.014358	0.000078	293.4	293.4	294.8	293.6	0.25	240679.	0.2232	0.2533
0.007078	0.007254	1.014358	0.000078	293.4	293.4	294.8	293.6	0.13	240723.	0.2154	0.2519
0.006790	0.006826	1.005077	-0.000003	294.1	294.0	295.3	293.6	1.59	243116.	0.2231	0.2427
0.006778	0.006814	1.005077	-0.000003	294.0	294.0	295.5	293.6	1.52	243163.	0.2296	0.2392
0.006690	0.006725	1.005077	-0.000003	294.0	294.0	295.7	293.6	1.40	243213.	0.2255	0.2352
0.006790	0.006825	1.005077	-0.000003	294.0	294.0	295.4	293.6	1.27	243257.	0.2215	0.2321
0.006798	0.006833	1.005077	-0.000003	294.0	294.0	295.1	293.6	1.14	243301.	0.2131	0.2323
0.006825	0.006860	1.005077	-0.000003	294.0	293.9	295.1	293.6	1.02	243345.	0.2231	0.2397
0.006816	0.006851	1.005077	-0.000003	294.0	293.9	295.0	293.6	0.89	243390.	0.2138	0.2493
0.006828	0.006863	1.005077	-0.000003	293.9	293.9	295.4	293.6	0.76	243433.	0.2296	0.2424
0.006875	0.006910	1.005077	-0.000003	293.9	293.9	295.3	293.6	0.64	243474.	0.2263	0.2402
0.006892	0.006927	1.005077	-0.000003	293.9	293.9	295.1	293.6	0.51	243515.	0.2255	0.2316
0.006982	0.007017	1.005077	-0.000003	293.9	293.9	295.0	293.6	0.38	243556.	0.2223	0.2139
0.006975	0.007010	1.005077	-0.000003	293.9	293.9	294.8	293.6	0.25	243596.	0.2177	0.2067
0.006999	0.007034	1.005077	-0.000003	293.9	293.9	294.8	293.6	0.13	243639.	0.2239	0.2073
0.006855	0.006929	1.005073	0.000038	293.8	293.8	295.2	293.6	1.59	243799.	0.2247	0.1886
0.006817	0.006890	1.005073	0.000038	293.8	293.8	295.1	293.6	1.52	243844.	0.2223	0.1999
0.006834	0.006907	1.005073	0.000038	293.8	293.8	295.0	293.6	1.40	243886.	0.2247	0.2027
0.006828	0.006901	1.005073	0.000038	293.8	293.7	294.9	293.6	1.27	243929.	0.2200	0.2222
0.006852	0.006925	1.005073	0.000038	293.7	293.7	294.9	293.6	1.14	243972.	0.2247	0.2475

Table H.1.5 Diesel contamination on oxidized copper surface for Re = 7000 and $x_b = 0.2\%$

Diesel contamination on oxidized copper surface for Re = 7000 and $x_b = 0.2\%$ (file:trv6con1.tbl)											
F (v)	F_r (v)	F_{100} (v)	F_0 (v)	T_{Ti} (K)	T_{To} (K)	T_a (K)	T_b (K)	l (mm)	Exposure time (s)	Turbine meter \dot{m}_w (kg/s)	Doppler meter \dot{m}_w (kg/s)
0.002504	0.002483	1.005823	-0.00005	297.5	297.4	296.8	293.7	1.59	4639.	0.3299	0.3423
0.002400	0.002378	1.005823	-0.000050	297.5	297.5	296.6	293.7	1.52	4684.	0.3265	0.3417
0.02268	0.002245	1.005823	-0.000050	297.6	297.5	297.0	293.7	1.40	4728.	0.3215	0.3391
0.002026	0.002000	1.005823	-0.000050	297.6	297.6	297.1	293.7	1.27	4771.	0.3167	0.3415
0.001853	0.001825	1.005823	-0.000050	297.6	297.6	296.9	293.7	1.14	4813.	0.3300	0.3453
0.001738	0.001709	1.005823	-0.000050	297.7	297.6	296.9	293.7	1.02	4857.	0.3181	0.3406
0.001519	0.001487	1.005823	-0.000050	297.7	297.7	296.8	293.7	0.89	4900.	0.3333	0.3420
0.001320	0.001285	1.005823	-0.000050	297.7	297.7	296.8	293.7	0.76	4943.	0.3214	0.3377
0.001150	0.001114	1.005823	-0.000050	297.8	297.7	296.9	293.6	0.64	4987.	0.3249	0.3425
0.000987	0.000949	1.005823	-0.000050	297.8	297.8	297.0	293.6	0.51	5029.	0.3282	0.3401
0.000803	0.000762	1.005823	-0.000050	297.8	297.8	297.1	293.7	0.38	5075.	0.3214	0.3392
0.000611	0.000568	1.005823	-0.000050	297.8	297.8	296.9	293.7	0.25	5122.	0.3133	0.3435
0.000479	0.000434	1.005823	-0.000050	297.9	297.8	297.1	293.7	0.13	5163.	0.3352	0.3391
0.002624	0.002647	1.006991	-0.000013	297.9	297.9	296.8	293.7	1.59	5325.	0.3232	0.3398
0.002535	0.002557	1.006991	-0.000013	297.9	297.9	297.0	293.7	1.52	5366.	0.3182	0.3404
0.002339	0.002358	1.006991	-0.000013	298.0	297.9	296.9	293.7	1.40	5412.	0.3181	0.3514
0.002156	0.002172	1.006991	-0.000013	298.0	297.9	297.0	293.7	1.27	5459.	0.3197	0.3590
0.001968	0.001982	1.006991	-0.000013	298.0	297.9	297.2	293.7	1.14	5511.	0.3231	0.3589
0.001751	0.001762	1.006991	-0.000013	298.0	297.9	297.0	293.7	1.02	5554.	0.3299	0.3511
0.001554	0.001562	1.006991	-0.000013	298.0	298.0	297.0	293.7	0.89	5600.	0.3317	0.3442
0.001390	0.001396	1.006991	-0.000013	298.0	298.0	296.8	293.7	0.76	5642.	0.3282	0.3571
0.001155	0.001158	1.006991	-0.000013	298.0	298.0	296.9	293.7	0.64	5685.	0.3165	0.3454
0.000955	0.000955	1.006991	-0.000013	298.0	298.0	297.0	293.7	0.51	5726.	0.3317	0.3504
0.000762	0.000759	1.006991	-0.000013	298.0	298.0	297.0	293.7	0.38	5771.	0.3299	0.3401
0.000603	0.000598	1.006991	-0.000013	298.0	298.0	296.9	293.7	0.25	5818.	0.3317	0.3394
.000443	0.000436	1.006991	-0.000013	298.0	298.0	297.0	293.7	0.13	5865.	0.3214	0.3467
.002757	0.002840	1.004241	0.000055	297.4	297.3	297.3	293.7	1.59	7893.	0.3316	0.3527
.002633	0.002714	1.004241	0.000055	297.3	297.3	297.5	293.7	1.52	7942.	0.3408	0.3492
.002596	0.002676	1.004241	0.000055	297.3	297.3	297.7	293.7	1.40	7988.	0.3249	0.3486
.002495	0.002574	1.004241	0.000055	297.3	297.3	297.4	293.7	1.27	8031.	0.3335	0.3486
.002276	0.002354	1.004241	0.000055	297.3	297.3	297.4	293.7	1.14	8072.	0.3370	0.3499
.002094	0.002169	1.004241	0.000055	297.2	297.2	297.3	293.7	1.02	8115.	0.3166	0.3528
.001767	0.001840	1.004241	0.000055	297.2	297.2	297.6	293.7	0.89	8159.	0.3282	0.3562
.001538	0.001608	1.004241	0.000055	297.2	297.2	297.5	293.7	0.76	8202.	0.3197	0.3500
.001401	0.001469	1.004241	0.000055	297.2	297.2	297.4	293.7	0.64	8245.	0.3264	0.3524
.001210	0.001276	1.004241	0.000055	297.2	297.1	297.5	293.7	0.51	8296.	0.3335	0.3529
.001021	0.001086	1.004241	0.000055	297.1	297.1	297.4	293.7	0.38	8341.	0.3266	0.3500
.000822	0.000884	1.004241	0.000055	297.1	297.1	297.5	293.7	0.25	8392.	0.3248	0.3483
.000718	0.000780	1.004241	0.000055	297.1	297.1	297.6	293.7	0.13	8449.	0.3335	0.3437
.003012	0.003122	1.010220	0.000071	295.4	295.4	297.5	293.7	1.59	11766.	0.3337	0.3416
.002916	0.003025	1.010220	0.000071	295.4	295.4	297.5	293.7	1.52	11806.	0.3319	0.3414
.002828	0.002936	1.010220	0.000071	295.4	295.4	297.6	293.7	1.40	11848.	0.3372	0.3358
.002715	0.002821	1.010220	0.000071	295.4	295.4	297.4	293.7	1.27	11894.	0.3372	0.3367
.002608	0.002713	1.010220	0.000071	295.3	295.3	297.5	293.7	1.14	11937.	0.3184	0.3550
.002429	0.002531	1.010220	0.000071	295.3	295.3	297.6	293.7	1.02	11984.	0.3266	0.3483
.002213	0.002313	1.010220	0.000071	295.3	295.3	297.6	293.7	0.89	12032.	0.3250	0.3441
.002003	0.002100	1.010220	0.000071	295.3	295.3	297.5	293.7	0.76	12082.	0.3354	0.3192
.001850	0.001945	1.010220	0.000071	295.3	295.3	297.4	293.7	0.64	12124.	0.3374	0.3216
.001622	0.001714	1.010220	0.000071	295.2	295.2	297.5	293.7	0.51	12168.	0.3337	0.3134
.001473	0.001564	1.010220	0.000071	295.2	295.2	297.7	293.7	0.38	12208.	0.3216	0.3164
.001245	0.001333	1.010220	0.000071	295.2	295.2	297.4	293.7	0.25	12252.	0.3284	0.3298
.001071	0.001156	1.010220	0.000071	295.2	295.2	297.6	293.7	0.13	12298.	0.3284	0.3386
.003126	0.003182	1.005162	0.000033	295.1	295.1	297.4	293.7	1.59	12461.	0.3266	0.3588
.003037	0.003092	1.005162	0.000033	295.1	295.1	297.4	293.7	1.52	12506.	0.3216	0.3555
.002849	0.002903	1.005162	0.000033	295.1	295.1	297.5	293.7	1.40	12550.	0.3354	0.3592
.002710	0.002763	1.005162	0.000033	295.0	295.0	297.3	293.7	1.27	12595.	0.3185	0.3491
.002642	0.002694	1.005162	0.000033	295.0	295.0	297.6	293.7	1.14	12637.	0.3267	0.3426

Table H.1.6 Tap water flushing after Re = 4600 contamination tests at $x_b = 0.2 \%$

Tap water flushing after Re = 4600 contamination tests at $x_b = 0.2 \%$ (file:flsh45c1.tbl)											
F (v)	F_r (v)	F_{100} (v)	F_0 (v)	T_{Ti} (K)	T_{To} (K)	T_a (K)	T_b (K)	l (mm)	Exposure time (s)	Turbine meter \dot{m}_w (kg/s)	Doppler meter \dot{m}_w (kg/s)
0.004939	0.004940	0.996651	-0.000033	300.0	300.1	295.2	293.6	1.59	2413.	N/A	N/A
0.004815	0.004814	0.996651	-0.000033	299.9	300.0	295.5	293.6	1.52	2467.	N/A	N/A
0.004740	0.004738	0.996651	-0.000033	299.9	299.9	295.3	293.6	1.40	2522.	N/A	N/A
0.004705	0.004703	0.996651	-0.000033	299.9	299.9	295.6	293.6	1.27	2574.	N/A	N/A
0.004696	0.004693	0.996651	-0.000033	299.8	299.8	295.6	293.6	1.14	2634.	N/A	N/A
0.004677	0.004674	0.996651	-0.000033	299.8	299.8	295.5	293.6	1.02	2686.	N/A	N/A
0.004686	0.004683	0.996651	-0.000033	299.7	299.7	295.4	293.6	0.89	2744.	N/A	N/A
0.004756	0.004753	0.996651	-0.000033	299.7	299.6	295.6	293.6	0.76	2796.	N/A	N/A
0.004820	0.004817	0.996651	-0.000033	299.6	299.6	295.3	293.5	0.64	2849.	N/A	N/A
0.004874	0.004870	0.996651	-0.000033	299.5	299.5	295.2	293.6	0.51	2898.	N/A	N/A
0.004914	0.004909	0.996651	-0.000033	299.4	299.4	295.3	293.6	0.38	2953.	N/A	N/A
0.004973	0.004968	0.996651	-0.000033	299.4	299.3	295.4	293.6	0.25	3000.	N/A	N/A
0.004295	0.004363	0.994784	0.000053	299.1	299.1	295.7	293.6	1.59	3214.	N/A	N/A
0.004260	0.004327	0.994784	0.000053	299.0	299.0	295.7	293.6	1.40	3271.	N/A	N/A
0.004307	0.004374	0.994784	0.000053	299.0	298.9	295.7	293.6	1.14	3326.	N/A	N/A
0.004450	0.004518	0.994784	0.000053	298.9	298.9	295.8	293.6	0.89	3380.	N/A	N/A
0.004456	0.004524	0.994784	0.000053	298.9	298.8	295.8	293.6	0.76	3430.	N/A	N/A
0.004555	0.004622	0.994784	0.000053	298.8	298.8	295.7	293.6	0.64	3481.	N/A	N/A
0.004656	0.004723	0.994784	0.000053	298.8	298.7	295.7	293.6	0.51	3530.	N/A	N/A
0.004733	0.004799	0.994784	0.000053	298.7	298.7	295.8	293.6	0.38	3581.	N/A	N/A
0.004788	0.004854	0.994784	0.000053	298.7	298.6	296.0	293.6	0.25	3631.	N/A	N/A
0.004939	0.005006	0.994784	0.000053	298.6	298.6	296.0	293.6	0.13	3684.	N/A	N/A
0.003415	0.003450	1.009424	0.000007	292.8	292.7	295.3	293.6	1.59	25131.	N/A	N/A
0.003385	0.003419	1.009424	0.000007	292.8	292.7	295.4	293.6	1.40	25189.	N/A	N/A
0.003506	0.003542	1.009424	0.000007	292.8	292.7	295.3	293.6	1.14	25244.	N/A	N/A
0.003575	0.003611	1.009424	0.000007	292.8	292.7	295.3	293.6	0.89	25297.	N/A	N/A
0.003776	0.003814	1.009424	0.000007	292.8	292.7	295.4	293.6	0.64	25351.	N/A	N/A
0.003805	0.003843	1.009424	0.000007	292.8	292.7	295.3	293.6	0.51	25403.	N/A	N/A
0.003859	0.003897	1.009424	0.000007	292.8	292.7	295.4	293.6	0.38	25455.	N/A	N/A
0.004004	0.004044	1.009424	0.000007	292.8	292.7	295.5	293.6	0.25	25506.	N/A	N/A
0.004149	0.004189	1.009424	0.000007	292.8	292.7	295.5	293.6	0.13	25557.	N/A	N/A
0.003426	0.003475	1.007668	0.000027	292.9	292.8	295.5	293.6	1.59	25789.	N/A	N/A
0.003328	0.003377	1.007668	0.000027	292.9	292.8	295.4	293.6	1.40	25844.	N/A	N/A
0.003477	0.003527	1.007668	0.000027	292.9	292.8	295.6	293.6	1.14	25894.	N/A	N/A
0.003526	0.003576	1.007668	0.000027	292.9	292.8	295.5	293.6	0.89	25951.	N/A	N/A
0.003649	0.003700	1.007668	0.000027	292.9	292.8	295.3	293.6	0.64	26010.	N/A	N/A
0.003825	0.003878	1.007668	0.000027	292.9	292.9	295.5	293.6	0.38	26058.	N/A	N/A
0.004136	0.004190	1.007668	0.000027	292.9	292.9	295.4	293.6	0.13	26106.	N/A	N/A
0.002337	0.002309	1.001896	0.000868	293.9	293.9	295.2	293.6	1.59	83821.	N/A	N/A
0.002272	0.002414	1.002567	0.000135	294.0	293.9	295.4	293.6	1.52	84083.	N/A	N/A
0.002263	0.002405	1.002567	0.000135	293.9	293.9	295.4	293.6	1.40	84145.	N/A	N/A
0.002284	0.002426	1.002567	0.000135	294.0	293.9	295.6	293.6	1.27	84204.	N/A	N/A
0.002328	0.002470	1.002567	0.000135	294.0	293.9	295.5	293.6	1.14	84256.	N/A	N/A
0.002313	0.002455	1.002567	0.000135	294.0	293.9	295.4	293.6	1.02	84311.	N/A	N/A
0.002436	0.002578	1.002567	0.000135	293.9	293.9	295.5	293.6	0.89	84369.	N/A	N/A
0.002417	0.002559	1.002567	0.000135	293.9	293.9	295.5	293.6	0.76	84456.	N/A	N/A
0.002492	0.002635	1.002567	0.000135	293.9	293.9	295.6	293.6	0.64	84513.	N/A	N/A
0.002559	0.002702	1.002567	0.000135	293.9	293.9	295.4	293.6	0.51	84590.	N/A	N/A
0.002583	0.002725	1.002567	0.000135	294.0	293.9	295.5	293.6	0.38	84641.	N/A	N/A
0.002656	0.002799	1.002567	0.000135	293.9	293.9	295.6	293.6	0.25	84697.	N/A	N/A
0.002766	0.002909	1.002567	0.000135	294.0	293.9	295.5	293.6	0.13	84755.	N/A	N/A
0.002256	0.002399	1.002415	0.000137	294.1	294.0	295.6	293.6	1.59	85420.	N/A	N/A
0.002223	0.002366	1.002415	0.000137	294.1	294.0	295.4	293.6	1.52	85482.	N/A	N/A
0.002229	0.002373	1.002415	0.000137	294.1	294.0	295.4	293.6	1.40	85542.	N/A	N/A
0.002258	0.002402	1.002415	0.000137	294.1	294.0	295.4	293.6	1.27	85595.	N/A	N/A
0.002341	0.002485	1.002415	0.000137	294.1	294.0	295.5	293.6	1.14	85648.	N/A	N/A
0.002334	0.002478	1.002415	0.000137	294.1	294.0	295.5	293.6	1.02	85697.	N/A	N/A

Table H.1.7 Diesel contamination on oxidized copper surface for Re = 0 and $x_b = 0.3\%$

Diesel contamination on oxidized copper surface for Re = 0 and $x_b = 0.3\%$ (file:trv0con2.tbl)											
F (v)	F_r (v)	F_{100} (v)	F_0 (v)	T_{Ti} (K)	T_{To} (K)	T_a (K)	T_b (K)	l (mm)	Exposure time (s)	Turbine meter \dot{m}_w (kg/s)	Doppler meter \dot{m}_w (kg/s)
0.004440	0.004456	1.007538	-0.000029	295.4	295.4	294.5	293.7	1.59	2476.	0.0000	0.0626
0.004311	0.004326	1.007538	-0.000029	295.4	295.4	294.6	293.7	1.52	2532.	0.0000	0.0627
0.004040	0.004052	1.007538	-0.000029	295.4	295.3	294.5	293.7	1.40	2592.	0.0000	0.0626
0.003770	0.003779	1.007538	-0.000029	295.4	295.3	294.4	293.7	1.27	2647.	0.0000	0.0626
0.003469	0.003475	1.007538	-0.000029	295.4	295.3	294.5	293.7	1.14	2702.	0.0000	0.0626
0.003200	0.003204	1.007538	-0.000029	295.3	295.3	294.5	293.7	1.02	2763.	0.0000	0.0627
0.002949	0.002949	1.007538	-0.000029	295.3	295.3	294.4	293.7	0.89	2823.	0.0000	0.0626
0.002672	0.002670	1.007538	-0.000029	295.3	295.3	294.4	293.7	0.76	2880.	0.0000	0.0626
0.002325	0.002319	1.007538	-0.000029	295.3	295.3	294.4	293.7	0.64	2939.	0.0000	0.0626
0.002060	0.002052	1.007538	-0.000029	295.3	295.2	294.4	293.7	0.51	3000.	0.0000	0.0626
0.001739	0.001727	1.007538	-0.000029	295.3	295.2	294.4	293.7	0.38	3056.	0.0000	0.0626
0.001418	0.001404	1.007538	-0.000029	295.3	295.2	294.5	293.7	0.25	3118.	0.0000	0.0627
0.001074	0.001055	1.007538	-0.000029	295.3	295.2	294.6	293.7	0.13	3178.	0.0000	0.0626
0.004750	0.004793	1.009045	-0.000006	294.4	294.8	294.1	293.7	1.59	406841.	0.0000	0.0713
0.004606	0.004648	1.009045	-0.000006	294.4	294.7	294.1	293.7	1.52	406899.	0.0000	0.0792
0.004393	0.004432	1.009045	-0.000006	294.4	294.8	294.1	293.7	1.40	406954.	0.0000	0.0741
0.004173	0.004211	1.009045	-0.000006	294.4	294.8	294.1	293.7	1.27	407010.	0.0000	0.0734
0.003978	0.004013	1.009045	-0.000006	294.4	294.7	294.1	293.7	1.14	407065.	0.0000	0.0807
0.003783	0.003816	1.009045	-0.000006	294.4	294.8	294.1	293.7	1.02	407122.	0.0000	0.0793
0.003533	0.003564	1.009045	-0.000006	294.4	294.8	294.2	293.7	0.89	407178.	0.0000	0.0808
0.003261	0.003289	1.009045	-0.000006	294.4	294.8	294.1	293.7	0.76	407234.	0.0000	0.0738
0.003042	0.003067	1.009045	-0.000006	294.4	294.8	294.1	293.7	0.64	407289.	0.0000	0.0788
0.002831	0.002854	1.009045	-0.000006	294.4	294.8	294.1	293.7	0.51	407354.	0.0000	0.0823
0.002561	0.002581	1.009045	-0.000006	294.4	294.8	294.1	293.7	0.38	407410.	0.0000	0.0779
0.002334	0.002352	1.009045	-0.000006	294.4	294.8	294.1	293.7	0.25	407466.	0.0000	0.0794
0.001987	0.002001	1.009045	-0.000006	294.4	294.8	294.1	293.7	0.13	407521.	0.0000	0.0817
0.005085	0.005157	1.000987	0.000058	294.5	294.9	294.3	293.7	1.59	410253.	0.0000	0.0793
0.005006	0.005077	1.000987	0.000058	294.5	294.9	294.2	293.7	1.52	410306.	0.0000	0.0785
0.004853	0.004923	1.000987	0.000058	294.5	294.9	294.3	293.7	1.40	410359.	0.0000	0.0755
0.004663	0.004733	1.000987	0.000058	294.5	294.9	294.2	293.7	1.27	410412.	0.0000	0.0803
0.004474	0.004544	1.000987	0.000058	294.5	294.9	294.2	293.7	1.14	410468.	0.0000	0.0799
0.004302	0.004371	1.000987	0.000058	294.5	294.9	294.3	293.7	1.02	410522.	0.0000	0.0747
0.004080	0.004149	1.000987	0.000058	294.5	294.9	294.2	293.7	0.89	410577.	0.0000	0.0721
0.003813	0.003881	1.000987	0.000058	294.5	294.9	294.2	293.7	0.76	410632.	0.0000	0.0768
0.003700	0.003768	1.000987	0.000058	294.5	294.9	294.3	293.7	0.64	410685.	0.0000	0.0627
0.003460	0.003527	1.000987	0.000058	294.5	294.9	294.3	293.7	0.51	410739.	0.0000	0.0627
0.003296	0.003363	1.000987	0.000058	294.5	294.9	294.3	293.7	0.38	410798.	0.0000	0.0627
0.003000	0.003066	1.000987	0.000058	294.5	294.9	294.3	293.7	0.25	410853.	0.0000	0.0627
0.002693	0.002758	1.000987	0.000058	294.5	294.9	294.3	293.7	0.13	410915.	0.0000	0.0627
0.005401	0.005435	1.003869	0.000004	294.6	295.1	294.2	293.7	1.59	414268.	0.0000	0.0740
0.005254	0.005287	1.003869	0.000004	294.6	295.1	294.2	293.7	1.52	414324.	0.0000	0.0789
0.005067	0.005099	1.003869	0.000004	294.6	295.1	294.2	293.7	1.40	414380.	0.0000	0.0780
0.004929	0.004961	1.003869	0.000004	294.6	295.1	294.2	293.7	1.27	414435.	0.0000	0.0705
0.004675	0.004706	1.003869	0.000004	294.6	295.1	294.2	293.7	1.14	414494.	0.0000	0.0691
0.004599	0.004629	1.003869	0.000004	294.6	295.1	294.2	293.7	1.02	414545.	0.0000	0.0627
0.004409	0.004438	1.003869	0.000004	294.6	295.1	294.2	293.7	0.89	414605.	0.0000	0.0724
0.004208	0.004236	1.003869	0.000004	294.6	295.1	294.2	293.7	0.76	414662.	0.0000	0.0627
0.004000	0.004026	1.003869	0.000004	294.6	295.1	294.2	293.7	0.64	414717.	0.0000	0.0627
0.003820	0.003845	1.003869	0.000004	294.6	295.1	294.2	293.7	0.51	414775.	0.0000	0.0691
0.003647	0.003672	1.003869	0.000004	294.6	295.1	294.2	293.7	0.38	414834.	0.0000	0.0727
0.003382	0.003405	1.003869	0.000004	294.6	295.1	294.2	293.7	0.25	414889.	0.0000	0.0698
0.003199	0.003221	1.003869	0.000004	294.6	295.1	294.2	293.7	0.13	414947.	0.0000	0.0627
0.005584	0.005656	1.003422	0.000044	294.6	295.1	294.3	293.7	1.59	418388.	0.0000	0.0627
0.005722	0.005796	1.003422	0.000044	294.6	295.1	294.3	293.7	1.52	418457.	0.0000	0.0627
0.005533	0.005605	1.003422	0.000044	294.6	295.1	294.3	293.7	1.40	418510.	0.0000	0.0627
0.005359	0.005431	1.003422	0.000044	294.6	295.1	294.3	293.7	1.27	418565.	0.0000	0.0627
0.005183	0.005254	1.003422	0.000044	294.6	295.1	294.2	293.7	1.14	418620.	0.0000	0.0627
0.005061	0.005131	1.003422	0.000044	294.6	295.1	294.2	293.7	1.02	418674.	0.0000	0.0627

Table H.1.8 Diesel contamination on oxidized copper surface for Re = 2000 and $x_b = 0.3\%$

Diesel contamination on oxidized copper surface for Re = 2000 and $x_b = 0.3\%$ (file:trv15con2.tbl)											
F (v)	F_r (v)	F_{100} (v)	F_0 (v)	T_{Ti} (K)	T_{To} (K)	T_a (K)	T_b (K)	l (mm)	Exposure time (s)	Turbine meter \dot{m}_w (kg/s)	Doppler meter \dot{m}_w (kg/s)
0.0035970	0.0036550	1.005509	0.0000330	294.6	294.4	294.3	293.7	1.59	613.	0.0906	0.0623
0.003322	0.003378	1.005509	0.000033	294.6	294.4	294.7	293.7	1.52	749.	0.0931	0.0623
0.003042	0.003096	1.005509	0.000033	294.6	294.4	294.4	293.7	1.40	792.	0.0942	0.0623
0.002723	0.002775	1.005509	0.000033	294.6	294.4	294.8	293.7	1.27	837.	0.0904	0.0623
0.002429	0.002479	1.005509	0.000033	294.6	294.4	294.6	293.7	1.14	881.	0.0909	0.0623
0.002193	0.002241	1.005509	0.000033	294.5	294.4	294.7	293.7	1.02	922.	0.0942	0.0623
0.001812	0.001857	1.005509	0.000033	294.5	294.4	294.7	293.6	0.89	966.	0.0952	0.0623
0.001578	0.001622	1.005509	0.000033	294.5	294.4	294.6	293.7	0.76	1008.	0.0935	0.0623
0.001261	0.001303	1.005509	0.000033	294.5	294.4	294.4	293.7	0.64	1054.	0.0920	0.0623
0.000910	0.000949	1.005509	0.000033	294.5	294.4	294.4	293.7	0.51	1097.	0.0943	0.0623
0.000618	0.000656	1.005509	0.000033	294.5	294.4	294.3	293.7	0.38	1138.	0.0887	0.0623
0.000226	0.000261	1.005509	0.000033	294.4	294.4	294.7	293.7	0.25	1181.	0.0952	0.0623
-0.000086	-0.000054	1.005509	0.000033	294.4	294.4	294.2	293.7	0.13	1226.	0.0926	0.0623
0.003653	0.003637	1.003232	-0.000032	294.4	294.3	294.5	293.7	1.59	1374.	0.0933	0.0623
0.003463	0.003446	1.003232	-0.000032	294.4	294.3	294.3	293.7	1.52	1422.	0.0900	0.0623
0.003191	0.003172	1.003232	-0.000032	294.3	294.3	294.5	293.7	1.40	1468.	0.0942	0.0623
0.002991	0.002972	1.003232	-0.000032	294.3	294.3	294.0	293.7	1.27	1513.	0.0945	0.0623
0.002751	0.002730	1.003232	-0.000032	294.3	294.2	294.7	293.7	1.14	1557.	0.0896	0.0623
0.002472	0.002451	1.003232	-0.000032	294.3	294.2	294.6	293.6	1.02	1606.	0.0906	0.0623
0.002169	0.002146	1.003232	-0.000032	294.2	294.2	294.4	293.7	0.89	1652.	0.0939	0.0623
0.001908	0.001884	1.003232	-0.000032	294.2	294.2	294.4	293.7	0.76	1694.	0.0934	0.0623
0.001576	0.001550	1.003232	-0.000032	294.2	294.1	294.4	293.7	0.64	1739.	0.0914	0.0623
0.001306	0.001279	1.003232	-0.000032	294.2	294.1	294.2	293.7	0.51	1786.	0.0916	0.0623
0.001026	0.000998	1.003232	-0.000032	294.1	294.1	294.2	293.6	0.38	1831.	0.0879	0.0623
0.000778	0.000749	1.003232	-0.000032	294.1	294.1	294.4	293.7	0.25	1875.	0.0936	0.0623
0.000533	0.000503	1.003232	-0.000032	294.1	294.1	294.5	293.7	0.13	1919.	0.0892	0.0623
0.012290	0.012345	1.004488	0.000009	293.3	293.2	294.2	293.7	1.59	5348.	0.0890	0.0623
0.012646	0.012703	1.004488	0.000009	293.3	293.2	294.2	293.7	1.52	5391.	0.0890	0.0623
0.012457	0.012514	1.004488	0.000009	293.3	293.2	294.1	293.7	1.40	5440.	0.0909	0.0623
0.012575	0.012632	1.004488	0.000009	293.3	293.3	294.2	293.7	1.27	5485.	0.0846	0.0623
0.013596	0.013657	1.004488	0.000009	293.3	293.3	294.6	293.6	1.14	5528.	0.0882	0.0623
0.012922	0.012981	1.004488	0.000009	293.3	293.3	294.1	293.7	1.02	5573.	0.0835	0.0623
0.011067	0.011119	1.004488	0.000009	293.4	293.3	294.2	293.7	0.89	5620.	0.0877	0.0623
0.009262	0.009308	1.004488	0.000009	293.4	293.3	294.0	293.6	0.76	5667.	0.0891	0.0623
0.009017	0.009061	1.004488	0.000009	293.4	293.3	294.6	293.7	0.64	5712.	0.0857	0.0623
0.009151	0.009196	1.004488	0.000009	293.4	293.4	294.6	293.7	0.51	5756.	0.0839	0.0623
0.009208	0.009254	1.004488	0.000009	293.4	293.4	294.5	293.7	0.38	5804.	0.0856	0.0623
0.009529	0.009577	1.004488	0.000009	293.4	293.4	294.3	293.7	0.25	5855.	0.0873	0.0623
0.010371	0.010423	1.004488	0.000009	293.5	293.4	294.6	293.7	0.13	5910.	0.0827	0.0623
0.018959	0.019067	1.005701	0.000000	293.7	293.6	294.4	293.7	1.59	11545.	0.0909	0.0623
0.019063	0.019172	1.005701	0.000000	293.7	293.7	294.2	293.7	1.52	11590.	0.0906	0.0623
0.019103	0.019213	1.005701	0.000000	293.7	293.7	294.2	293.7	1.40	11635.	0.0905	0.0623
0.019066	0.019176	1.005701	0.000000	293.7	293.7	294.5	293.7	1.27	11678.	0.0897	0.0623
0.019079	0.019190	1.005701	0.000000	293.8	293.7	294.6	293.7	1.14	11723.	0.0905	0.0623
0.018951	0.019062	1.005701	0.000000	293.8	293.8	294.4	293.6	1.02	11769.	0.0909	0.0623
0.017200	0.017301	1.005701	0.000000	293.8	293.8	294.2	293.7	0.89	11820.	0.0919	0.0623
0.015048	0.015137	1.005701	0.000000	293.8	293.8	294.4	293.7	0.76	11885.	0.0907	0.0623
0.013818	0.013900	1.005701	0.000000	293.9	293.8	294.6	293.6	0.64	11937.	0.0925	0.0623
0.013441	0.013522	1.005701	0.000000	293.9	293.8	294.3	293.7	0.51	11982.	0.0910	0.0623
0.013486	0.013567	1.005701	0.000000	293.9	293.9	294.2	293.6	0.38	12028.	0.0872	0.0623
0.013593	0.013675	1.005701	0.000000	293.9	293.9	294.6	293.6	0.25	12073.	0.0865	0.0623
0.013592	0.013673	1.005701	0.000000	293.9	293.9	294.5	293.7	0.13	12118.	0.0895	0.0623
0.013199	0.013298	1.004021	0.000041	293.9	293.9	294.2	293.7	1.59	12289.	0.0925	0.0623
0.013292	0.013391	1.004021	0.000041	293.9	293.9	294.8	293.6	1.52	12336.	0.0868	0.0623
0.013225	0.013324	1.004021	0.000041	293.9	293.9	294.7	293.6	1.40	12382.	0.0901	0.0623
0.013196	0.013295	1.004021	0.000041	293.9	293.9	294.8	293.7	1.27	12433.	0.0901	0.0623

Table H.1.9 Diesel contamination on oxidized copper surface for Re = 4000 and $x_b = 0.3 \%$

Diesel contamination on oxidized copper surface for Re = 4000 and $x_b = 0.3 \%$ (file:trv3con2.tbl)											
F (v)	F_r (v)	F_{100} (v)	F_0 (v)	T_{Ti} (K)	T_{To} (K)	T_a (K)	T_b (K)	l (mm)	Exposure time (s)	Turbine meter \dot{m}_w (kg/s)	Doppler meter \dot{m}_w (kg/s)
0.011072	0.011157	1.004420	0.000033	293.9	293.9	293.9	293.7	1.59	64840.	0.1899	0.1835
0.010992	0.011077	1.004420	0.000033	293.9	293.9	293.9	293.7	1.52	64910.	0.1952	0.1842
0.010911	0.010995	1.004420	0.000033	293.9	293.9	293.9	293.7	1.40	64953.	0.1946	0.1841
0.010948	0.011031	1.004420	0.000033	293.8	293.8	293.9	293.7	1.27	65012.	0.1887	0.1821
0.010886	0.010968	1.004420	0.000033	293.8	293.8	293.9	293.7	1.14	65079.	0.1922	0.1690
0.010847	0.010929	1.004420	0.000033	293.8	293.8	293.9	293.7	1.02	65125.	0.1927	0.1730
0.010797	0.010878	1.004420	0.000033	293.8	293.8	293.9	293.7	0.89	65175.	0.1940	0.1940
0.010634	0.010714	1.004420	0.000033	293.8	293.8	294.1	293.7	0.76	65229.	0.1934	0.2099
0.010665	0.010745	1.004420	0.000033	293.7	293.7	293.9	293.7	0.64	65299.	0.1983	0.2010
0.010695	0.010775	1.004420	0.000033	293.7	293.7	294.0	293.7	0.51	65349.	0.1922	0.1997
0.010746	0.010825	1.004420	0.000033	293.6	293.6	294.0	293.7	0.38	65421.	0.1910	0.2042
0.010743	0.010821	1.004420	0.000033	293.6	293.6	293.9	293.7	0.25	65505.	0.1977	0.1811
0.010748	0.010825	1.004420	0.000033	293.5	293.5	293.9	293.7	0.13	65555.	0.1887	0.1470
0.011404	0.011431	1.003228	-0.000015	294.0	293.9	293.9	293.7	1.59	68691.	0.1910	0.1550
0.011317	0.011343	1.003228	-0.000015	293.9	293.9	293.9	293.7	1.52	68759.	0.1958	0.1605
0.011275	0.011301	1.003228	-0.000015	293.9	293.9	293.9	293.7	1.40	68808.	0.1989	0.1385
0.011285	0.011311	1.003228	-0.000015	293.9	293.9	293.9	293.7	1.27	68854.	0.1910	0.1457
0.011252	0.011278	1.003228	-0.000015	293.9	293.9	293.9	293.7	1.14	68898.	0.1853	0.1799
0.011261	0.011286	1.003228	-0.000015	293.9	293.9	294.0	293.7	1.02	68943.	0.1964	0.1686
0.011191	0.011215	1.003228	-0.000015	293.8	293.8	294.0	293.7	0.89	69033.	0.1934	0.1802
0.011306	0.011331	1.003228	-0.000015	293.8	293.8	293.9	293.7	0.76	69084.	0.1893	0.1982
0.011366	0.011390	1.003228	-0.000015	293.8	293.8	293.9	293.7	0.64	69132.	0.1940	0.1949
0.011243	0.011266	1.003228	-0.000015	293.8	293.8	293.9	293.7	0.51	69177.	0.1916	0.1955
0.011259	0.011282	1.003228	-0.000015	293.8	293.7	294.0	293.7	0.38	69225.	0.1843	0.2035
0.011345	0.011368	1.003228	-0.000015	293.7	293.7	293.9	293.7	0.25	69274.	0.1922	0.2078
0.011269	0.011292	1.003228	-0.000015	293.7	293.7	294.0	293.7	0.13	69322.	0.1910	0.2029
0.011701	0.011696	1.006369	-0.000084	293.9	293.9	294.1	293.7	1.59	72093.	0.1922	0.1646
0.011799	0.011796	1.006369	-0.000084	293.9	293.9	294.1	293.7	1.52	72139.	0.1946	0.1650
0.011717	0.011713	1.006369	-0.000084	293.9	293.9	294.1	293.7	1.40	72186.	0.1945	0.1533
0.011791	0.011788	1.006369	-0.000084	293.9	293.9	294.1	293.7	1.27	72236.	0.1893	0.1609
0.011637	0.011633	1.006369	-0.000084	294.0	293.9	294.1	293.7	1.14	72284.	0.1951	0.1636
0.011679	0.011675	1.006369	-0.000084	294.0	293.9	294.1	293.7	1.02	72331.	0.1952	0.1873
0.011720	0.011717	1.006369	-0.000084	294.0	293.9	294.1	293.7	0.89	72379.	0.1853	0.2214
0.011621	0.011617	1.006369	-0.000084	294.0	294.0	294.1	293.7	0.76	72428.	0.1927	0.2032
0.011719	0.011716	1.006369	-0.000084	294.0	293.9	294.1	293.7	0.64	72482.	0.1865	0.1756
0.011645	0.011641	1.006369	-0.000084	294.0	293.9	294.0	293.7	0.51	72531.	0.1945	0.1689
0.011779	0.011776	1.006369	-0.000084	294.0	294.0	294.0	293.7	0.38	72577.	0.1881	0.1765
0.011726	0.011723	1.006369	-0.000084	293.9	293.9	294.0	293.7	0.25	72621.	0.1977	0.1734
0.011862	0.011860	1.006369	-0.000084	293.9	293.9	294.0	293.7	0.13	72668.	0.1904	0.1744
0.012166	0.012227	1.008294	-0.000045	294.0	293.9	294.1	293.7	1.59	76231.	0.1945	0.1881
0.012174	0.012236	1.008294	-0.000045	294.0	293.9	294.1	293.7	1.52	76278.	0.1922	0.1710
0.012214	0.012276	1.008294	-0.000045	294.0	293.9	294.1	293.7	1.40	76326.	0.1837	0.1822
0.012061	0.012121	1.008294	-0.000045	294.0	294.0	294.1	293.7	1.27	76375.	0.1898	0.1925
0.012127	0.012188	1.008294	-0.000045	294.0	293.9	294.1	293.7	1.14	76421.	0.1910	0.1880
0.012160	0.012222	1.008294	-0.000045	294.0	293.9	294.1	293.7	1.02	76475.	0.1934	0.1821
0.012168	0.012230	1.008294	-0.000045	294.0	294.0	294.2	293.7	0.89	76523.	0.1934	0.1814
0.012160	0.012222	1.008294	-0.000045	294.0	293.9	294.1	293.7	0.76	76568.	0.1853	0.1850
0.012271	0.012333	1.008294	-0.000045	294.0	293.9	294.1	293.7	0.64	76613.	0.1859	0.1863
0.012255	0.012318	1.008294	-0.000045	294.0	293.9	294.2	293.7	0.51	76659.	0.1934	0.1865
0.012299	0.012361	1.008294	-0.000045	294.0	293.9	294.1	293.7	0.38	76707.	0.1983	0.1735
0.012432	0.012495	1.008294	-0.000045	293.9	293.9	294.1	293.7	0.25	76755.	0.1983	0.1723
0.012438	0.012501	1.008294	-0.000045	293.9	293.9	294.2	293.7	0.13	76826.	0.1934	0.1663
0.012171	0.012131	1.004779	-0.000097	293.6	293.5	294.3	293.7	1.59	79482.	0.1952	0.1872
0.012184	0.012144	1.004779	-0.000097	293.6	293.5	294.3	293.7	1.52	79525.	0.1899	0.1769
0.012254	0.012216	1.004779	-0.000097	293.6	293.6	294.2	293.7	1.40	79573.	0.1910	0.1438
0.012222	0.012183	1.004779	-0.000097	293.6	293.6	294.2	293.7	1.27	79620.	0.1848	0.1511

Table H.1.10 Diesel contamination on oxidized copper surface for Re = 5000 and $x_b = 0.3 \%$

Diesel contamination on oxidized copper surface for Re = 5000 and $x_b = 0.3 \%$ (file:trv45con2.tbl)											
F (v)	F_r (v)	F_{100} (v)	F_0 (v)	T_{Ti} (K)	T_{To} (K)	T_a (K)	T_b (K)	l (mm)	Exposure time (s)	Turbine meter \dot{m}_w (kg/s)	Doppler meter \dot{m}_w (kg/s)
0.004208	0.004205	0.993235	00.000034	292.4	292.4	295.4	293.7	1.59	4061.	0.2420	0.2266
0.004008	0.004007	0.993235	0.000034	292.4	292.4	295.3	293.7	1.52	4103.	0.2488	0.2322
0.003698	0.003700	0.993235	0.000034	292.5	292.5	295.2	293.7	1.40	4144.	0.2488	0.2378
0.003431	0.003435	0.993235	0.000034	292.5	292.5	294.6	293.7	1.27	4187.	0.2497	0.2440
0.003121	0.003128	0.993235	0.000034	292.6	292.5	294.4	293.7	1.14	4229.	0.2420	0.2478
0.002796	0.002806	0.993235	0.000034	292.6	292.6	294.9	293.7	1.02	4271.	0.2458	0.2502
0.002473	0.002486	0.993235	0.000034	292.6	292.6	295.4	293.7	0.89	4315.	0.2458	0.2462
0.002210	0.002226	0.993235	0.000034	292.7	292.6	295.1	293.7	0.76	4360.	0.2507	0.2210
0.001853	0.001871	0.993235	0.000034	292.7	292.7	295.7	293.7	0.64	4402.	0.2528	0.2271
0.001530	0.001551	0.993235	0.000034	292.8	292.7	295.8	293.7	0.51	4444.	0.2449	0.2448
0.001180	0.001204	0.993235	0.000034	292.8	292.8	295.6	293.7	0.38	4488.	0.2401	0.2488
0.000923	0.000950	0.993235	0.000034	292.8	292.8	295.5	293.7	0.25	4530.	0.2338	0.2444
0.000681	0.000709	0.993235	0.000034	292.9	292.9	295.7	293.7	0.13	4574.	0.2508	0.2383
0.004110	0.004058	0.989872	-0.000007	293.1	293.0	294.7	293.7	1.59	4733.	0.2497	0.2248
0.003916	0.003865	0.989872	-0.000007	293.1	293.1	295.0	293.7	1.52	4776.	0.2487	0.2322
0.003659	0.003612	0.989872	-0.000007	293.1	293.1	296.1	293.7	1.40	4819.	0.2401	0.2489
0.003347	0.003304	0.989872	-0.000007	293.2	293.1	295.7	293.7	1.27	4862.	0.2458	0.2416
0.003064	0.003024	0.989872	-0.000007	293.2	293.2	296.3	293.7	1.14	4903.	0.2392	0.2417
0.002810	0.002772	0.989872	-0.000007	293.2	293.2	296.2	293.7	1.02	4948.	0.2478	0.2329
0.002424	0.002391	0.989872	-0.000007	293.3	293.3	295.4	293.7	0.89	4990.	0.2402	0.2246
0.002123	0.002093	0.989872	-0.000007	293.3	293.3	295.2	293.7	0.76	5032.	0.2478	0.2041
0.001808	0.001782	0.989872	-0.000007	293.4	293.3	294.8	293.7	0.64	5077.	0.2402	0.2124
0.001516	0.001493	0.989872	-0.000007	293.4	293.4	296.0	293.7	0.51	5121.	0.2468	0.2318
0.001248	0.001228	0.989872	-0.000007	293.4	293.4	295.8	293.6	0.38	5163.	0.2402	0.2284
0.000887	0.000871	0.989872	-0.000007	293.5	293.4	295.8	293.7	0.25	5205.	0.2339	0.2381
0.000559	0.000546	0.989872	-0.000007	293.5	293.5	295.9	293.7	0.13	5247.	0.2467	0.2513
0.004139	0.004004	0.984469	-0.000074	294.4	294.4	295.9	293.7	1.59	7217.	0.2383	0.2167
0.004077	0.003944	0.984469	-0.000074	294.4	294.4	295.8	293.7	1.52	7260.	0.2374	0.2182
0.003855	0.003725	0.984469	-0.000074	294.3	294.3	295.9	293.7	1.40	7312.	0.2497	0.2093
0.003594	0.003468	0.984469	-0.000074	294.3	294.3	295.9	293.7	1.27	7363.	0.2401	0.2119
0.003310	0.003187	0.984469	-0.000074	294.3	294.3	295.8	293.7	1.14	7418.	0.2448	0.2173
0.002939	0.002822	0.984469	-0.000074	294.3	294.3	295.8	293.7	1.02	7466.	0.2497	0.2195
0.002658	0.002545	0.984469	-0.000074	294.3	294.3	296.1	293.7	0.89	7510.	0.2476	0.2221
0.002330	0.002222	0.984469	-0.000074	294.3	294.3	296.0	293.7	0.76	7553.	0.2467	0.2251
0.002069	0.001965	0.984469	-0.000074	294.3	294.2	296.0	293.7	0.64	7596.	0.2497	0.2678
0.001724	0.001625	0.984469	-0.000074	294.3	294.2	296.1	293.7	0.51	7638.	0.2497	0.2355
0.001494	0.001398	0.984469	-0.000074	294.2	294.2	295.7	293.7	0.38	7682.	0.2517	0.2429
0.001162	0.001071	0.984469	-0.000074	294.2	294.2	295.3	293.7	0.25	7724.	0.2400	0.2493
0.000913	0.000826	0.984469	-0.000074	294.2	294.2	295.9	293.7	0.13	7767.	0.2429	0.2530
0.003987	0.004049	1.005697	0.000037	294.1	294.0	296.5	293.7	1.59	72772.	0.2558	0.2324
0.003930	0.003992	1.005697	0.000037	294.1	294.0	296.3	293.7	1.52	72816.	0.2558	0.2511
0.003774	0.003835	1.005697	0.000037	294.1	294.0	296.4	293.6	1.40	72863.	0.2569	0.2579
0.003574	0.003634	1.005697	0.000037	294.1	294.1	296.7	293.7	1.27	72904.	0.2476	0.2651
0.003399	0.003458	1.005697	0.000037	294.1	294.1	296.4	293.7	1.14	72945.	0.2622	0.2697
0.003093	0.003149	1.005697	0.000037	294.1	294.1	296.4	293.7	1.02	72988.	0.2601	0.2501
0.002719	0.002774	1.005697	0.000037	294.1	294.1	296.3	293.7	0.89	73030.	0.2548	0.2617
0.002359	0.002411	1.005697	0.000037	294.1	294.1	296.3	293.7	0.76	73071.	0.2569	0.2594
0.002145	0.002196	1.005697	0.000037	294.1	294.1	296.4	293.7	0.64	73115.	0.2548	0.2626
0.001927	0.001977	1.005697	0.000037	294.1	294.1	296.4	293.7	0.51	73157.	0.2590	0.2634
0.001635	0.001683	1.005697	0.000037	294.1	294.1	296.4	293.7	0.38	73202.	0.2611	0.2676
0.001386	0.001432	1.005697	0.000037	294.1	294.1	296.6	293.7	0.25	73245.	0.2458	0.2695
0.001104	0.001149	1.005697	0.000037	294.1	294.1	296.5	293.7	0.13	73286.	0.2537	0.2679
0.004063	0.004069	1.008256	-0.000031	294.1	294.1	296.8	293.7	1.59	73421.	0.2477	0.2603
0.003791	0.003794	1.008256	-0.000031	294.1	294.1	296.5	293.7	1.52	73462.	0.2634	0.2560
0.003890	0.003893	1.008256	-0.000031	294.1	294.1	296.3	293.7	1.40	73506.	0.2611	0.2613
0.003280	0.003278	1.008256	-0.000031	294.1	294.1	296.5	293.7	1.27	73548.	0.2506	0.2641
0.003152	0.003149	1.008256	-0.000031	294.1	294.0	296.6	293.7	1.14	73591.	0.2487	0.2619

Table H.1.11 Diesel contamination on oxidized copper surface for Re = 7000 and $x_b = 0.3 \%$

Diesel contamination on oxidized copper surface for Re = 7000 and $x_b = 0.3 \%$ (file:trv6con2.tbl)											
F (v)	F_r (v)	F_{100} (v)	F_0 (v)	T_{Ti} (K)	T_{To} (K)	T_a (K)	T_b (K)	l (mm)	Exposure time (s)	Turbine meter \dot{m}_w (kg/s)	Doppler meter \dot{m}_w (kg/s)
0.013240	0.013403	1.004572	0.000105	293.6	293.6	294.5	293.7	1.59	63545.	0.3372	0.0624
0.015901	0.016076	1.004572	0.000105	293.6	293.6	294.5	293.7	1.52	63592.	0.3354	0.0624
0.013409	0.013573	1.004572	0.000105	293.6	293.6	294.6	293.7	1.40	63638.	0.3372	0.3744
0.010815	0.010968	1.004572	0.000105	293.7	293.6	294.5	293.7	1.27	63685.	0.3198	0.0625
0.012913	0.013076	1.004572	0.000105	293.7	293.7	294.5	293.7	1.14	63734.	0.3182	0.0624
0.009349	0.009496	1.004572	0.000105	293.7	293.7	294.5	293.7	1.02	63782.	0.3150	0.0654
0.009588	0.009737	1.004572	0.000105	293.8	293.7	294.6	293.7	0.89	63831.	0.3265	0.0624
0.007571	0.007712	1.004572	0.000105	293.8	293.8	294.6	293.7	0.76	63880.	0.3248	0.0624
0.006367	0.006503	1.004572	0.000105	293.8	293.8	294.6	293.7	0.64	63929.	0.3389	0.0624
0.006039	0.006174	1.004572	0.000105	293.9	293.8	294.5	293.6	0.51	63980.	0.3102	0.0624
0.004005	0.004130	1.004572	0.000105	293.9	293.9	294.6	293.7	0.38	64031.	0.3299	0.3531
0.003336	0.003458	1.004572	0.000105	293.9	293.9	294.6	293.6	0.25	64083.	0.3407	0.0624
0.004463	0.004590	1.004572	0.000105	293.9	293.9	294.5	293.6	0.13	64129.	0.3198	0.0624
0.014031	0.014287	1.009780	0.000126	293.5	293.5	294.6	293.7	1.59	67123.	0.3246	0.0624
0.015226	0.015493	1.009780	0.000126	293.5	293.5	294.6	293.7	1.52	67170.	0.3248	0.0624
0.011928	0.012165	1.009780	0.000126	293.4	293.4	294.6	293.7	1.40	67218.	0.3231	0.0625
0.011950	0.012186	1.009780	0.000126	293.4	293.4	294.6	293.7	1.27	67262.	0.3353	0.3073
0.013350	0.013599	1.009780	0.000126	293.4	293.4	294.6	293.7	1.14	67309.	0.3353	0.0624
0.009006	0.009215	1.009780	0.000126	293.4	293.4	294.6	293.7	1.02	67355.	0.3246	0.0626
0.009475	0.009688	1.009780	0.000126	293.4	293.4	294.5	293.7	0.89	67405.	0.3371	0.0624
0.007716	0.007913	1.009780	0.000126	293.4	293.4	294.4	293.7	0.76	67453.	0.3281	0.0624
0.006117	0.006299	1.009780	0.000126	293.4	293.4	294.4	293.7	0.64	67505.	0.3182	0.0628
0.005736	0.005914	1.009780	0.000126	293.4	293.4	294.5	293.7	0.51	67553.	0.3317	0.3902
0.004038	0.004201	1.009780	0.000126	293.4	293.4	294.3	293.7	0.38	67601.	0.3317	0.3837
0.003438	0.003595	1.009780	0.000126	293.4	293.4	294.4	293.7	0.25	67648.	0.3133	0.0624
0.002834	0.002986	1.009780	0.000126	293.4	293.4	294.4	293.7	0.13	67693.	0.3389	0.3960
0.006600	0.006756	1.007389	0.000107	293.7	293.7	294.2	293.7	1.59	71007.	0.3183	0.3181
0.006594	0.006749	1.007389	0.000107	293.6	293.6	294.1	293.7	1.52	71064.	0.3486	0.3096
0.006078	0.006229	1.007389	0.000107	293.6	293.6	294.2	293.7	1.40	71120.	0.3267	0.3206
0.005643	0.005791	1.007389	0.000107	293.6	293.6	294.0	293.7	1.27	71171.	0.3392	0.3277
0.005132	0.005276	1.007389	0.000107	293.6	293.6	294.1	293.7	1.14	71215.	0.3430	0.3223
0.004617	0.004757	1.007389	0.000107	293.5	293.5	294.1	293.7	1.02	71261.	0.3251	0.3223
0.004079	0.004215	1.007389	0.000107	293.5	293.5	294.2	293.7	0.89	71313.	0.3392	0.3417
0.003558	0.003690	1.007389	0.000107	293.5	293.5	294.4	293.7	0.76	71362.	0.3234	0.3463
0.003162	0.003291	1.007389	0.000107	293.5	293.5	294.1	293.7	0.64	71407.	0.3320	0.3249
0.002323	0.002447	1.007389	0.000107	293.5	293.5	294.0	293.7	0.51	71457.	0.3354	0.3325
0.002056	0.002178	1.007389	0.000107	293.4	293.4	294.4	293.7	0.38	71502.	0.3320	0.3336
0.001764	0.001884	1.007389	0.000107	293.4	293.4	294.1	293.7	0.25	71548.	0.3392	0.3316
0.001366	0.001482	1.007389	0.000107	293.4	293.4	294.4	293.7	0.13	71593.	0.3217	0.3290
0.006422	0.006540	1.005913	0.000077	294.0	294.0	294.3	293.7	1.59	74448.	0.3392	0.3111
0.006279	0.006396	1.005913	0.000077	294.0	294.0	294.1	293.7	1.52	74495.	0.3185	0.3107
0.005683	0.005796	1.005913	0.000077	294.0	294.0	294.0	293.7	1.40	74538.	0.3429	0.2996
0.005293	0.005404	1.005913	0.000077	294.0	294.0	294.2	293.7	1.27	74584.	0.3392	0.3098
0.004710	0.004817	1.005913	0.000077	294.0	293.9	294.3	293.7	1.14	74629.	0.3338	0.3120
0.004242	0.004345	1.005913	0.000077	294.0	293.9	294.2	293.7	1.02	74679.	0.3447	0.3138
0.003850	0.003951	1.005913	0.000077	293.9	293.9	294.1	293.7	0.89	74725.	0.3268	0.3178
0.003439	0.003537	1.005913	0.000077	293.9	293.9	294.4	293.7	0.76	74768.	0.3374	0.3251
0.002879	0.002974	1.005913	0.000077	293.9	293.9	294.4	293.7	0.64	74816.	0.3410	0.3271
0.002648	0.002741	1.005913	0.000077	293.9	293.9	294.1	293.7	0.51	74862.	0.3429	0.3340
0.002338	0.002429	1.005913	0.000077	293.9	293.9	294.0	293.7	0.38	74908.	0.3410	0.3447
0.002140	0.002230	1.005913	0.000077	293.8	293.8	294.4	293.7	0.25	74956.	0.3268	0.3455
0.002386	0.002477	1.005913	0.000077	293.8	293.8	294.3	293.7	0.13	75002.	0.3320	0.3456
0.004443	0.004531	1.014729	0.000021	293.9	293.9	294.3	293.7	1.59	79055.	0.3302	0.3190
0.004224	0.004308	1.014729	0.000021	293.9	293.9	294.4	293.7	1.52	79101.	0.3485	0.3097
0.003983	0.004064	1.014729	0.000021	293.9	293.9	294.4	293.7	1.40	79145.	0.3216	0.3186
0.003816	0.003894	1.014729	0.000021	293.9	293.8	294.3	293.7	1.27	79190.	0.3391	0.3295
0.003562	0.003636	1.014729	0.000021	293.8	293.8	294.3	293.7	1.14	79238.	0.3267	0.3324

Table H.1.12 Tap water flushing after Re = 5000 contamination tests at $x_b = 0.3 \%$

Tap water flushing after Re = 5000 contamination tests at $x_b = 0.3 \%$ (file:flsh45c2.tbl)											
F (v)	F_r (v)	F_{100} (v)	F_0 (v)	T_{Ti} (K)	T_{To} (K)	T_a (K)	T_b (K)	l (mm)	Exposure time (s)	Turbine meter \dot{m}_w (kg/s)	Doppler meter \dot{m}_w (kg/s)
00.000048	00.000113	1.007885	00.000065	293.3	293.1	297.0	293.7	1.59	402.	N/A	N/A
-0.000054	0.000010	1.007885	0.000065	292.7	292.5	297.2	293.7	1.52	453.	N/A	N/A
0.000103	0.000169	1.007885	0.000065	292.1	291.9	297.1	293.7	1.40	506.	N/A	N/A
0.000066	0.000131	1.007885	0.000065	291.6	291.4	297.0	293.7	1.27	557.	N/A	N/A
0.000034	0.000099	1.007885	0.000065	291.1	290.9	297.0	293.7	1.14	610.	N/A	N/A
0.000180	0.000245	1.007885	0.000065	290.6	290.5	296.9	293.7	1.02	663.	N/A	N/A
0.000047	0.000111	1.007885	0.000065	290.2	290.0	296.9	293.7	0.89	719.	N/A	N/A
0.000019	0.000083	1.007885	0.000065	289.7	289.5	296.7	293.7	0.76	775.	N/A	N/A
0.000044	0.000108	1.007885	0.000065	289.3	289.1	296.8	293.7	0.64	832.	N/A	N/A
0.000029	0.000093	1.007885	0.000065	289.0	288.8	296.9	293.7	0.51	886.	N/A	N/A
0.000113	0.000177	1.007885	0.000065	288.7	288.6	296.9	293.7	0.38	938.	N/A	N/A
0.000299	0.000363	1.007885	0.000065	288.5	288.4	297.0	293.7	0.25	995.	N/A	N/A
0.000638	0.000702	1.007885	0.000065	288.4	288.3	297.0	293.7	0.13	1053.	N/A	N/A
0.000061	0.000048	1.006992	-0.000012	286.4	286.4	297.0	293.7	1.59	3736.	N/A	N/A
-0.000004	-0.000016	1.006992	-0.000012	286.4	286.4	296.8	293.7	1.52	3787.	N/A	N/A
0.000019	0.000006	1.006992	-0.000012	286.4	286.4	297.0	293.7	1.40	3842.	N/A	N/A
0.000000	-0.000012	1.006992	-0.000012	286.4	286.4	297.2	293.7	1.27	3902.	N/A	N/A
0.000025	0.000013	1.006992	-0.000012	286.4	286.3	297.1	293.7	1.14	3958.	N/A	N/A
0.000029	0.000016	1.006992	-0.000012	286.4	286.4	297.0	293.7	1.02	4013.	N/A	N/A
0.000017	0.000005	1.006992	-0.000012	286.4	286.4	297.0	293.7	0.89	4070.	N/A	N/A
0.000038	0.000026	1.006992	-0.000012	286.4	286.4	297.1	293.7	0.76	4124.	N/A	N/A
0.000029	0.000016	1.006992	-0.000012	286.4	286.4	297.4	293.7	0.64	4180.	N/A	N/A
0.000049	0.000037	1.006992	-0.000012	286.4	286.4	297.0	293.7	0.51	4234.	N/A	N/A
0.000018	0.000006	1.006992	-0.000012	286.4	286.3	297.0	293.7	0.38	4294.	N/A	N/A
0.000023	0.000011	1.006992	-0.000012	286.4	286.4	297.2	293.7	0.25	4349.	N/A	N/A
-0.000002	-0.000014	1.006992	-0.000012	286.4	286.3	297.3	293.7	0.13	4406.	N/A	N/A
-0.000262	-0.000424	1.006313	-0.000164	287.3	287.3	295.0	293.7	1.59	64014.	N/A	N/A
-0.000287	-0.000449	1.006313	-0.000164	287.3	287.3	295.0	293.7	1.52	64064.	N/A	N/A
-0.000282	-0.000443	1.006313	-0.000164	287.3	287.3	295.1	293.6	1.40	64118.	N/A	N/A
-0.000297	-0.000459	1.006313	-0.000164	287.3	287.3	295.0	293.7	1.27	64176.	N/A	N/A
-0.000306	-0.000468	1.006313	-0.000164	287.3	287.3	295.0	293.7	1.14	64239.	N/A	N/A
-0.000310	-0.000471	1.006313	-0.000164	287.3	287.3	295.0	293.7	1.02	64292.	N/A	N/A
-0.000308	-0.000469	1.006313	-0.000164	287.3	287.3	295.1	293.7	0.89	64346.	N/A	N/A
-0.000289	-0.000451	1.006313	-0.000164	287.3	287.3	295.1	293.7	0.76	64398.	N/A	N/A
-0.000298	-0.000460	1.006313	-0.000164	287.3	287.3	295.3	293.7	0.64	64452.	N/A	N/A
-0.000302	-0.000464	1.006313	-0.000164	287.3	287.3	295.4	293.6	0.51	64508.	N/A	N/A
-0.000305	-0.000467	1.006313	-0.000164	287.3	287.3	295.1	293.7	0.38	64560.	N/A	N/A
-0.000313	-0.000474	1.006313	-0.000164	287.3	287.3	295.2	293.7	0.25	64612.	N/A	N/A
-0.000311	-0.000472	1.006313	-0.000164	287.3	287.3	295.1	293.7	0.13	64667.	N/A	N/A
-0.000130	-0.000221	1.003946	-0.000093	287.4	287.3	295.3	293.7	1.59	64866.	N/A	N/A
-0.000142	-0.000233	1.003946	-0.000093	287.4	287.3	295.0	293.7	1.52	64920.	N/A	N/A
-0.000145	-0.000237	1.003946	-0.000093	287.4	287.3	295.3	293.7	1.40	64975.	N/A	N/A
-0.000119	-0.000211	1.003946	-0.000093	287.4	287.3	295.3	293.7	1.27	65027.	N/A	N/A
-0.000142	-0.000234	1.003946	-0.000093	287.4	287.3	295.1	293.7	1.14	65082.	N/A	N/A
-0.000162	-0.000253	1.003946	-0.000093	287.4	287.3	295.1	293.7	1.02	65135.	N/A	N/A
-0.000138	-0.000229	1.003946	-0.000093	287.4	287.3	295.0	293.6	0.89	65188.	N/A	N/A
-0.000132	-0.000224	1.003946	-0.000093	287.4	287.3	295.3	293.7	0.76	65245.	N/A	N/A
-0.000127	-0.000218	1.003946	-0.000093	287.4	287.3	295.2	293.6	0.64	65300.	N/A	N/A
-0.000144	-0.000235	1.003946	-0.000093	287.4	287.3	295.3	293.7	0.51	65351.	N/A	N/A
-0.000139	-0.000230	1.003946	-0.000093	287.4	287.3	295.2	293.6	0.38	65405.	N/A	N/A
-0.000136	-0.000227	1.003946	-0.000093	287.4	287.3	295.1	293.7	0.25	65458.	N/A	N/A
-0.000135	-0.000226	1.003946	-0.000093	287.4	287.3	295.4	293.7	0.13	65513.	N/A	N/A
-0.000254	-0.000184	1.008369	0.000071	287.5	287.5	295.2	293.7	1.59	67977.	N/A	N/A
-0.000289	-0.000218	1.008369	0.000071	287.5	287.5	295.3	293.7	1.52	68028.	N/A	N/A
-0.000286	-0.000216	1.008369	0.000071	287.5	287.5	295.4	293.7	1.40	68086.	N/A	N/A
-0.000299	-0.000228	1.008369	0.000071	287.5	287.5	295.2	293.7	1.27	68139.	N/A	N/A
-0.000294	-0.000224	1.008369	0.000071	287.5	287.5	295.2	293.7	1.14	68190.	N/A	N/A
-0.000283	-0.000213	1.008369	0.000071	287.5	287.5	295.1	293.7	1.02	68242.	N/A	N/A

Table H.1.13 Tap water flushing after Re = 7000 contamination tests at $x_b = 0.3 \%$

Tap water flushing after Re = 7000 contamination tests at $x_b = 0.3 \%$ (file:flsh6c2.tbl)											
F (v)	F_r (v)	F_{100} (v)	F_0 (v)	T_{Ti} (K)	T_{To} (K)	T_a (K)	T_b (K)	l (mm)	Exposure time (s)	Turbine meter \dot{m}_w (kg/s)	Doppler meter \dot{m}_w (kg/s)
-	-	1.005803	0.000064	296.9	296.8	295.4	293.7	1.59	0.	N/A	N/A
00.000236	00.000174										
-0.000369	-0.000308	1.005803	0.000064	296.0	295.9	295.4	293.7	1.52	56.	N/A	N/A
-0.000370	-0.000309	1.005803	0.000064	295.5	295.4	295.4	293.7	1.40	110.	N/A	N/A
-0.000406	-0.000345	1.005803	0.000064	294.9	294.8	295.4	293.7	1.27	165.	N/A	N/A
-0.000409	-0.000347	1.005803	0.000064	294.3	294.1	295.4	293.7	1.14	218.	N/A	N/A
-0.000421	-0.000359	1.005803	0.000064	293.6	293.5	295.4	293.7	1.02	276.	N/A	N/A
-0.000425	-0.000363	1.005803	0.000064	293.0	292.8	295.4	293.7	0.89	328.	N/A	N/A
-0.000423	-0.000360	1.005803	0.000064	292.1	291.8	295.4	293.7	0.76	383.	N/A	N/A
-0.000438	-0.000375	1.005803	0.000064	290.9	290.7	295.4	293.7	0.64	439.	N/A	N/A
-0.000438	-0.000375	1.005803	0.000064	290.0	289.7	295.4	293.7	0.51	492.	N/A	N/A
-0.000453	-0.000389	1.005803	0.000064	289.2	288.9	295.4	293.7	0.38	544.	N/A	N/A
-0.000411	-0.000347	1.005803	0.000064	288.5	288.3	295.4	293.7	0.25	600.	N/A	N/A
-0.000442	-0.000377	1.005803	0.000064	288.0	287.7	295.4	293.7	0.13	654.	N/A	N/A
0.000007	0.000068	1.010679	0.000062	284.3	284.2	296.1	293.7	1.59	11606.	N/A	N/A
-0.000037	0.000025	1.010679	0.000062	284.3	284.2	296.1	293.7	1.52	11662.	N/A	N/A
-0.000023	0.000038	1.010679	0.000062	284.3	284.2	296.0	293.7	1.40	11753.	N/A	N/A
-0.000025	0.000036	1.010679	0.000062	284.2	284.2	296.0	293.7	1.27	11809.	N/A	N/A
-0.000035	0.000026	1.010679	0.000062	284.2	284.2	296.1	293.7	1.14	11862.	N/A	N/A
-0.000033	0.000029	1.010679	0.000062	284.2	284.2	296.0	293.7	1.02	11918.	N/A	N/A
0.000006	0.000067	1.010679	0.000062	284.2	284.1	296.1	293.7	0.89	11974.	N/A	N/A
-0.000007	0.000054	1.010679	0.000062	284.2	284.2	296.1	293.7	0.76	12030.	N/A	N/A
-0.000025	0.000036	1.010679	0.000062	284.2	284.1	296.1	293.7	0.64	12091.	N/A	N/A
0.000000	0.000061	1.010679	0.000062	284.2	284.1	296.1	293.7	0.51	12143.	N/A	N/A
-0.000012	0.000050	1.010679	0.000062	284.2	284.1	296.1	293.7	0.38	12197.	N/A	N/A
-0.000037	0.000024	1.010679	0.000062	284.2	284.1	296.1	293.7	0.25	12250.	N/A	N/A
-0.000042	0.000019	1.010679	0.000062	284.2	284.1	296.1	293.7	0.13	12305.	N/A	N/A
-0.000055	0.00002	1.003075	0.000057	283.7	283.6	295.6	293.7	1.59	15484.	N/A	N/A
-0.000104	-0.000047	1.003075	0.000057	283.7	283.7	295.8	293.7	1.52	15541.	N/A	N/A
-0.000149	-0.000091	1.003075	0.000057	283.7	283.7	295.7	293.7	1.40	15599.	N/A	N/A
-0.000141	-0.000084	1.003075	0.000057	283.7	283.6	295.7	293.7	1.27	15652.	N/A	N/A
-0.000123	-0.000066	1.003075	0.000057	283.7	283.7	295.4	293.7	1.14	15722.	N/A	N/A
-0.000129	-0.000072	1.003075	0.000057	283.7	283.7	295.5	293.7	1.02	15778.	N/A	N/A
-0.000098	-0.000041	1.003075	0.000057	283.7	283.7	295.7	293.7	0.89	15835.	N/A	N/A
-0.000129	-0.000072	1.003075	0.000057	283.8	283.7	295.8	293.7	0.76	15890.	N/A	N/A
-0.000126	-0.000069	1.003075	0.000057	283.7	283.7	295.3	293.7	0.64	15953.	N/A	N/A
-0.000152	-0.000094	1.003075	0.000057	283.7	283.6	295.2	293.7	0.51	16008.	N/A	N/A
-0.000127	-0.000070	1.003075	0.000057	283.7	283.6	295.7	293.7	0.38	16065.	N/A	N/A
-0.000187	-0.000129	1.003075	0.000057	283.7	283.7	295.4	293.7	0.25	16120.	N/A	N/A
-0.000173	-0.000115	1.003075	0.000057	283.7	283.6	295.4	293.7	0.13	16191.	N/A	N/A
-0.000298	-0.000403	1.005909	-0.000108	285.3	285.3	294.0	293.7	1.59	77260.	N/A	N/A
-0.000334	-0.000438	1.005909	-0.000108	285.3	285.3	294.0	293.7	1.52	77315.	N/A	N/A
-0.000319	-0.000423	1.005909	-0.000108	285.3	285.3	294.2	293.7	1.40	77369.	N/A	N/A
-0.000357	-0.000461	1.005909	-0.000108	285.3	285.3	294.1	293.7	1.27	77421.	N/A	N/A
-0.000316	-0.000421	1.005909	-0.000108	285.3	285.3	294.0	293.7	1.14	77475.	N/A	N/A
-0.000364	-0.000468	1.005909	-0.000108	285.3	285.3	293.9	293.7	1.02	77526.	N/A	N/A
-0.000340	-0.000444	1.005909	-0.000108	285.3	285.3	294.0	293.7	0.89	77580.	N/A	N/A
-0.000316	-0.000420	1.005909	-0.000108	285.3	285.3	294.0	293.7	0.76	77632.	N/A	N/A
-0.000324	-0.000429	1.005909	-0.000108	285.3	285.3	294.1	293.7	0.64	77682.	N/A	N/A
-0.000313	-0.000417	1.005909	-0.000108	285.3	285.3	293.9	293.7	0.51	77735.	N/A	N/A
-0.000346	-0.000450	1.005909	-0.000108	285.3	285.3	294.0	293.7	0.38	77789.	N/A	N/A
-0.000366	-0.000470	1.005909	-0.000108	285.3	285.3	294.0	293.7	0.25	77841.	N/A	N/A
-0.000355	-0.000458	1.005909	-0.000108	285.3	285.3	293.9	293.7	0.13	77895.	N/A	N/A
-0.000385	-0.000396	1.004326	-0.000015	285.3	285.3	294.0	293.7	1.59	78063.	N/A	N/A
-0.000418	-0.000429	1.004326	-0.000015	285.3	285.3	294.0	293.7	1.52	78114.	N/A	N/A
-0.000463	-0.000474	1.004326	-0.000015	285.3	285.2	293.9	293.7	1.40	78168.	N/A	N/A
-0.000453	-0.000463	1.004326	-0.000015	285.3	285.2	294.0	293.7	1.27	78219.	N/A	N/A
-0.000406	-0.000417	1.004326	-0.000015	285.2	285.2	293.9	293.7	1.14	78274.	N/A	N/A

Table H.2.6 Tap water flushing after Re = 4600 contamination tests at $x_b = 0.2\%$
(file:flsh45c1.tb2)

l_c (μm)	Γ (kg/m^2) $\times 10^5$	x_b (%)	Exposure Time (s)	\bar{T}_{T_i} (K)	$T_b - \bar{T}_{T_i}$ (K)	$\frac{F_{T_b}}{F_{T_i}}$
6.62	560.	0.077	2413.	300.1	-6.5	0.99
6.62	560.	0.077	2467.	299.9	-6.4	0.99
6.62	560.	0.077	2522.	299.9	-6.3	0.99
6.62	560.	0.077	2574.	299.9	-6.3	0.99
6.62	560.	0.077	2634.	299.8	-6.3	0.99
6.62	560.	0.077	2686.	299.8	-6.2	0.99
6.62	560.	0.077	2744.	299.7	-6.2	0.99
6.62	560.	0.077	2796.	299.7	-6.1	0.99
6.62	560.	0.077	2849.	299.6	-6.0	0.99
6.62	560.	0.077	2898.	299.5	-5.9	0.99
6.62	560.	0.077	2953.	299.4	-5.8	0.99
6.62	560.	0.077	3000.	299.3	-5.8	0.99
6.02	509.	0.037	3214.	299.1	-5.5	0.99
6.02	509.	0.037	3271.	299.0	-5.5	0.99
6.02	509.	0.037	3326.	298.9	-5.4	0.99
6.02	509.	0.037	3380.	298.9	-5.3	0.99
6.02	509.	0.037	3430.	298.8	-5.3	0.99
6.02	509.	0.037	3481.	298.8	-5.2	0.99
6.02	509.	0.037	3530.	298.7	-5.2	0.99
6.02	509.	0.037	3581.	298.7	-5.1	0.99
6.02	509.	0.037	3631.	298.6	-5.1	0.99
6.02	509.	0.037	3684.	298.6	-5.0	0.99
4.89	416.	0.040	25131.	292.7	0.8	1.00
4.89	416.	0.040	25189.	292.7	0.8	1.00
4.89	416.	0.040	25244.	292.7	0.8	1.00
4.89	416.	0.040	25297.	292.7	0.8	1.00
4.89	416.	0.040	25351.	292.8	0.8	1.00
4.89	416.	0.040	25403.	292.8	0.8	1.00
4.89	416.	0.040	25455.	292.8	0.8	1.00
4.89	416.	0.040	25506.	292.8	0.8	1.00
4.89	416.	0.040	25557.	292.8	0.8	1.00
4.88	415.	0.047	25789.	292.8	0.7	1.00
4.88	415.	0.047	25844.	292.8	0.7	1.00
4.88	415.	0.047	25894.	292.9	0.7	1.00
4.88	415.	0.047	25951.	292.9	0.7	1.00
4.88	415.	0.047	26010.	292.9	0.7	1.00
4.88	415.	0.047	26058.	292.9	0.7	1.00
4.88	415.	0.047	26106.	292.9	0.7	1.00
3.29	280.	0.009	83821.	293.9	-0.3	1.00
3.29	280.	0.009	84083.	293.9	-0.4	1.00
3.29	280.	0.009	84145.	293.9	-0.4	1.00
3.29	280.	0.009	84204.	293.9	-0.4	1.00
3.29	280.	0.009	84256.	293.9	-0.4	1.00
3.29	280.	0.009	84311.	293.9	-0.4	1.00
3.29	280.	0.009	84369.	293.9	-0.4	1.00
3.29	280.	0.009	84456.	293.9	-0.4	1.00
3.29	280.	0.009	84513.	293.9	-0.3	1.00
3.29	280.	0.009	84590.	293.9	-0.4	1.00
3.29	280.	0.009	84641.	293.9	-0.4	1.00
3.29	280.	0.009	84697.	293.9	-0.4	1.00
3.29	280.	0.009	84755.	293.9	-0.4	1.00
3.27	278.	0.022	85420.	294.0	-0.5	1.00
3.27	278.	0.022	85482.	294.0	-0.5	1.00
3.27	278.	0.022	85542.	294.0	-0.5	1.00
3.27	278.	0.022	85595.	294.0	-0.5	1.00
3.27	278.	0.022	85648.	294.0	-0.5	1.00
3.27	278.	0.022	85697.	294.0	-0.5	1.00

3.27	278.	0.022	85750.	294.1	-0.5	1.00
3.27	278.	0.022	85808.	294.0	-0.5	1.00
3.27	278.	0.022	85861.	294.1	-0.5	1.00
3.27	278.	0.022	85913.	294.0	-0.5	1.00
3.27	278.	0.022	85962.	294.0	-0.5	1.00
3.27	278.	0.022	86023.	294.1	-0.5	1.00
3.27	278.	0.022	86073.	294.1	-0.5	1.00
2.46	209.	0.012	111672.	294.0	-0.5	1.00
2.46	209.	0.012	111735.	294.0	-0.5	1.00
2.46	209.	0.012	111793.	294.0	-0.5	1.00
2.46	209.	0.012	111862.	294.0	-0.5	1.00
2.46	209.	0.012	111923.	294.0	-0.5	1.00
2.46	209.	0.012	111976.	294.0	-0.5	1.00
2.46	209.	0.012	112026.	294.0	-0.5	1.00
2.46	209.	0.012	112079.	294.0	-0.5	1.00
2.46	209.	0.012	112131.	294.0	-0.5	1.00
2.46	209.	0.012	112178.	294.0	-0.5	1.00
2.46	209.	0.012	112226.	294.0	-0.5	1.00
2.46	209.	0.012	112269.	294.0	-0.5	1.00
2.46	209.	0.012	112318.	294.0	-0.5	1.00
2.50	212.	0.020	112462.	294.0	-0.5	1.00
2.50	212.	0.020	112513.	294.0	-0.5	1.00
2.50	212.	0.020	112562.	294.0	-0.5	1.00
2.50	212.	0.020	112607.	294.0	-0.5	1.00
2.50	212.	0.020	112651.	294.0	-0.5	1.00
1.94	165.	0.014	169806.	295.0	-1.4	1.00
1.94	165.	0.014	169865.	295.0	-1.4	1.00
1.94	165.	0.014	169922.	295.0	-1.4	1.00
1.94	165.	0.014	169977.	294.9	-1.4	1.00
1.94	165.	0.014	170036.	295.0	-1.4	1.00
1.94	165.	0.014	170093.	294.9	-1.4	1.00
1.94	165.	0.014	170147.	295.0	-1.4	1.00
1.94	165.	0.014	170205.	294.9	-1.4	1.00
1.94	165.	0.014	170261.	295.0	-1.4	1.00
1.94	165.	0.014	170312.	294.9	-1.4	1.00
1.94	165.	0.014	170367.	295.0	-1.4	1.00
1.94	165.	0.014	170416.	294.9	-1.4	1.00
1.94	165.	0.014	170470.	294.9	-1.4	1.00
2.13	181.	0.012	170928.	294.9	-1.4	1.00
2.13	181.	0.012	170986.	294.9	-1.4	1.00
2.13	181.	0.012	171035.	294.9	-1.4	1.00
2.13	181.	0.012	171087.	294.9	-1.4	1.00
2.13	181.	0.012	171142.	294.9	-1.4	1.00
2.13	181.	0.012	171194.	294.9	-1.4	1.00
2.13	181.	0.012	171235.	294.9	-1.4	1.00
2.13	181.	0.012	171288.	294.9	-1.4	1.00
2.13	181.	0.012	171334.	294.9	-1.3	1.00
2.13	181.	0.012	171389.	294.9	-1.3	1.00
2.13	181.	0.012	171429.	294.9	-1.3	1.00
2.13	181.	0.012	171476.	294.9	-1.3	1.00
2.13	181.	0.012	171520.	294.9	-1.3	1.00
1.57	134.	0.027	197155.	294.2	-0.7	1.00
1.57	134.	0.027	197198.	294.2	-0.7	1.00
1.57	134.	0.027	197247.	294.3	-0.7	1.00
1.57	134.	0.027	197290.	294.3	-0.7	1.00
1.57	134.	0.027	197343.	294.3	-0.8	1.00
1.58	134.	0.004	197498.	294.4	-0.8	1.00
1.58	134.	0.004	197541.	294.4	-0.8	1.00
1.58	134.	0.004	197581.	294.4	-0.8	1.00

Table H.2.13 Tap water flushing after Re = 7000 contamination tests at $x_b = 0.3$ %
(file:flsh6c2.tb2)

l_c (μm)	Γ (kg/m^2) $\times 10^5$	x_b (%)	Exposure Time (s)	\bar{T}_{T_1} (K)	$T_b - \bar{T}_{T_1}$ (K)	$\frac{F_{T_1}}{F_T}$
-0.54	-46.	0.003	0.	296.8	-3.1	1.00
-0.54	-46.	0.003	56.	296.0	-2.3	1.00
-0.54	-46.	0.003	110.	295.5	-1.8	1.00
-0.54	-46.	0.003	165.	294.9	-1.1	1.00
-0.54	-46.	0.003	218.	294.2	-0.5	1.00
-0.54	-46.	0.003	276.	293.5	0.1	1.00
-0.54	-46.	0.003	328.	292.9	0.8	1.00
-0.54	-46.	0.003	383.	291.9	1.7	1.00
-0.54	-46.	0.003	439.	290.8	2.9	1.00
-0.54	-46.	0.003	492.	289.9	3.8	1.01
-0.54	-46.	0.003	544.	289.1	4.6	1.01
-0.54	-46.	0.003	600.	288.4	5.3	1.01
-0.54	-46.	0.003	654.	287.9	5.8	1.01
-0.03	-2.	0.006	11606.	284.2	9.5	1.01
-0.03	-2.	0.006	11662.	284.2	9.5	1.01
-0.03	-2.	0.006	11753.	284.2	9.5	1.01
-0.03	-2.	0.006	11809.	284.2	9.5	1.01
-0.03	-2.	0.006	11862.	284.2	9.5	1.01
-0.03	-2.	0.006	11918.	284.2	9.5	1.01
-0.03	-2.	0.006	11974.	284.2	9.5	1.01
-0.03	-2.	0.006	12030.	284.2	9.5	1.01
-0.03	-2.	0.006	12091.	284.2	9.5	1.01
-0.03	-2.	0.006	12143.	284.2	9.5	1.01
-0.03	-2.	0.006	12197.	284.2	9.5	1.01
-0.03	-2.	0.006	12250.	284.2	9.5	1.01
-0.03	-2.	0.006	12305.	284.1	9.5	1.01
-0.17	-15.	0.005	15484.	283.7	10.0	1.02
-0.17	-15.	0.005	15541.	283.7	10.0	1.02
-0.17	-15.	0.005	15599.	283.7	10.0	1.02
-0.17	-15.	0.005	15652.	283.7	10.0	1.02
-0.17	-15.	0.005	15722.	283.7	10.0	1.02
-0.17	-15.	0.005	15778.	283.7	10.0	1.02
-0.17	-15.	0.005	15835.	283.7	10.0	1.02
-0.17	-15.	0.005	15890.	283.7	10.0	1.02
-0.17	-15.	0.005	15953.	283.7	10.0	1.02
-0.17	-15.	0.005	16008.	283.7	10.0	1.02
-0.17	-15.	0.005	16065.	283.7	10.0	1.02
-0.17	-15.	0.005	16120.	283.7	10.0	1.02
-0.17	-15.	0.005	16191.	283.7	10.0	1.02
-0.45	-39.	0.000	77260.	285.3	8.4	1.01
-0.45	-39.	0.000	77315.	285.3	8.4	1.01
-0.45	-39.	0.000	77369.	285.3	8.4	1.01
-0.45	-39.	0.000	77421.	285.3	8.4	1.01
-0.45	-39.	0.000	77475.	285.3	8.4	1.01
-0.45	-39.	0.000	77526.	285.3	8.4	1.01
-0.45	-39.	0.000	77580.	285.3	8.4	1.01
-0.45	-39.	0.000	77632.	285.3	8.4	1.01
-0.45	-39.	0.000	77682.	285.3	8.4	1.01
-0.45	-39.	0.000	77735.	285.3	8.4	1.01
-0.45	-39.	0.000	77789.	285.3	8.4	1.01
-0.45	-39.	0.000	77841.	285.3	8.4	1.01
-0.45	-39.	0.000	77895.	285.3	8.4	1.01
-0.58	-50.	-0.009	78063.	285.3	8.4	1.01
-0.58	-50.	-0.009	78114.	285.3	8.4	1.01
-0.58	-50.	-0.009	78168.	285.2	8.4	1.01
-0.58	-50.	-0.009	78219.	285.2	8.5	1.01
-0.58	-50.	-0.009	78274.	285.2	8.5	1.01
-0.58	-50.	-0.009	78327.	285.2	8.5	1.01
-0.58	-50.	-0.009	78381.	285.2	8.5	1.01
-0.58	-50.	-0.009	78433.	285.2	8.5	1.01
-0.58	-50.	-0.009	78485.	285.2	8.5	1.01
-0.58	-50.	-0.009	78539.	285.2	8.5	1.01
-0.58	-50.	-0.009	78593.	285.2	8.5	1.01
-0.58	-50.	-0.009	78647.	285.2	8.5	1.01
-0.58	-50.	-0.009	78701.	285.2	8.5	1.01
-0.66	-56.	-0.013	82130.	285.0	8.7	1.01
-0.66	-56.	-0.013	82181.	285.0	8.8	1.01
-0.66	-56.	-0.013	82238.	285.0	8.7	1.01
-0.66	-56.	-0.013	82292.	284.9	8.8	1.01
-0.66	-56.	-0.013	82350.	284.9	8.8	1.01
-0.66	-56.	-0.013	82404.	284.9	8.8	1.01
-0.66	-56.	-0.013	82457.	284.9	8.8	1.01
-0.66	-56.	-0.013	82512.	284.9	8.8	1.01
-0.66	-56.	-0.013	82565.	284.9	8.8	1.01
-0.66	-56.	-0.013	82616.	284.9	8.8	1.01
-0.66	-56.	-0.013	82670.	284.9	8.8	1.01
-0.66	-56.	-0.013	82723.	284.9	8.8	1.01

-0.66	-56.	-0.013	82774.	284.9	8.8	1.01
-0.58	-50.	-0.005	86376.	284.1	9.6	1.01
-0.58	-50.	-0.005	86430.	284.1	9.6	1.01
-0.58	-50.	-0.005	86481.	284.1	9.6	1.01
-0.58	-50.	-0.005	86533.	284.2	9.5	1.01
-0.58	-50.	-0.005	86587.	284.2	9.5	1.01
-0.58	-50.	-0.005	86642.	284.1	9.5	1.01
-0.58	-50.	-0.005	86701.	284.2	9.5	1.01
-0.58	-50.	-0.005	86757.	284.2	9.5	1.01
-0.58	-50.	-0.005	86811.	284.2	9.5	1.01
-0.58	-50.	-0.005	86865.	284.2	9.5	1.01
-0.58	-50.	-0.005	86918.	284.2	9.5	1.01
-0.58	-50.	-0.005	86972.	284.1	9.5	1.01
-0.58	-50.	-0.005	87025.	284.2	9.5	1.01
-0.56	-48.	-0.007	87172.	284.1	9.6	1.01
-0.56	-48.	-0.007	87225.	284.1	9.5	1.01
-0.56	-48.	-0.007	87278.	284.1	9.6	1.01
-0.56	-48.	-0.007	87335.	284.1	9.6	1.02
-0.56	-48.	-0.007	87400.	284.1	9.6	1.01
-0.56	-48.	-0.007	87456.	284.1	9.6	1.01
-0.56	-48.	-0.007	87513.	284.1	9.6	1.01
-0.56	-48.	-0.007	87565.	284.1	9.6	1.01
-0.56	-48.	-0.007	87621.	284.1	9.6	1.02
-0.56	-48.	-0.007	87672.	284.1	9.6	1.02
-0.56	-48.	-0.007	87727.	284.1	9.6	1.02
-0.56	-48.	-0.007	87780.	284.1	9.6	1.02
-0.56	-48.	-0.007	87832.	284.1	9.6	1.02
-0.50	-43.	-0.003	87988.	284.1	9.6	1.02
-0.50	-43.	-0.003	88044.	284.1	9.6	1.02
-0.50	-43.	-0.003	88098.	284.0	9.7	1.02
-0.50	-43.	-0.003	88154.	284.0	9.7	1.02
-0.50	-43.	-0.003	88207.	284.0	9.7	1.02
-0.50	-43.	-0.003	88265.	284.1	9.6	1.02
-0.50	-43.	-0.003	88318.	284.1	9.6	1.02
-0.50	-43.	-0.003	88371.	284.0	9.6	1.02
-0.50	-43.	-0.003	88426.	284.0	9.7	1.02
-0.50	-43.	-0.003	88480.	284.0	9.7	1.02
-0.50	-43.	-0.003	88538.	284.0	9.6	1.02
-0.50	-43.	-0.003	88593.	284.0	9.7	1.02
-0.50	-43.	-0.003	88648.	284.0	9.7	1.02
-0.66	-57.	-0.011	95135.	284.2	9.6	1.01
-0.66	-57.	-0.011	95191.	284.2	9.6	1.01
-0.66	-57.	-0.011	95245.	284.2	9.5	1.01
-0.66	-57.	-0.011	95298.	284.2	9.5	1.01
-0.66	-57.	-0.011	95357.	284.2	9.5	1.01
-0.66	-57.	-0.011	95413.	284.2	9.5	1.01
-0.66	-57.	-0.011	95472.	284.2	9.4	1.01
-0.66	-57.	-0.011	95529.	284.2	9.4	1.01
-0.66	-57.	-0.011	95584.	284.3	9.4	1.01
-0.66	-57.	-0.011	95635.	284.3	9.4	1.01
-0.66	-57.	-0.011	95691.	284.3	9.4	1.01
-0.66	-57.	-0.011	95746.	284.3	9.4	1.01
-0.66	-57.	-0.011	95801.	284.3	9.4	1.01
-0.52	-44.	-0.011	100071.	284.3	9.4	1.01
-0.52	-44.	-0.011	100129.	284.3	9.4	1.01
-0.52	-44.	-0.011	100183.	284.3	9.4	1.01
-0.52	-44.	-0.011	100237.	284.3	9.4	1.01
-0.52	-44.	-0.011	100290.	284.3	9.4	1.01
-0.52	-44.	-0.011	100344.	284.2	9.4	1.01
-0.52	-44.	-0.011	100398.	284.3	9.4	1.01
-0.52	-44.	-0.011	100453.	284.2	9.4	1.01
-0.52	-44.	-0.011	100515.	284.2	9.5	1.01
-0.52	-44.	-0.011	100575.	284.2	9.5	1.01
-0.52	-44.	-0.011	100631.	284.1	9.6	1.01
-0.52	-44.	-0.011	100689.	284.1	9.5	1.01
-0.52	-44.	-0.011	100744.	284.2	9.5	1.01
-0.71	-61.	-0.010	166191.	285.9	7.8	1.01
-0.71	-61.	-0.010	166248.	285.8	7.8	1.01
-0.71	-61.	-0.010	166302.	285.9	7.8	1.01
-0.71	-61.	-0.010	166356.	285.9	7.8	1.01
-0.71	-61.	-0.010	166410.	285.9	7.8	1.01
-0.71	-61.	-0.010	166464.	285.9	7.8	1.01
-0.71	-61.	-0.010	166518.	285.9	7.8	1.01
-0.71	-61.	-0.010	166574.	285.9	7.8	1.01
-0.71	-61.	-0.010	166626.	285.9	7.8	1.01
-0.71	-61.	-0.010	166676.	285.9	7.8	1.01
-0.71	-61.	-0.010	166727.	285.9	7.8	1.01
-0.71	-61.	-0.010	166779.	285.9	7.8	1.01
-0.71	-61.	-0.010	166832.	285.9	7.8	1.01
-0.56	-48.	-0.007	168424.	285.4	8.3	1.01

APPENDIX I: SPECTROFLUOROMETER CHECK

This appendix discusses how the emission and excitation wavelength measurements were verified with a mercury standard and a "crossover peak" from the excitation. The emission wavelength measurement obtained from the spectrofluorometer without the glass filter was checked against a mercury vapor light. Figure I.1 and Table I.1 show a comparison of the published values of the peak wavelengths for mercury (Reader et al., 1980) to those obtained from the spectrofluorometer. The absolute difference between the measured and published wavelengths was approximately within 10 nm.

The excitation wavelength measurement obtained from the spectrofluorometer was checked with a "crossover peak" from the excitation. In other words, the excitation monochromator was set to a specific wavelength with no specimen in the sample chamber. Under these conditions, the emission intensity should peak at the excitation wavelength. The wavelength of the emission peaked at the excitation wavelength to within the resolution of the digital display (± 1 nm) for the wavelengths that were tested.

Table I.1 Calibration check of spectrofluorometer against Mercury lamp

Published ¹ wavelength (nm)	Measured wavelength (nm)	Absolute difference (nm)	Relative Difference (%)
312.567	307	5	1.6
365.015	358	7	1.9
404.656	398	7	1.7
435.833	427	9	2.1
546.074	540	6	1.1
576.960	569	8	1.4

¹Reader et al. (1980)

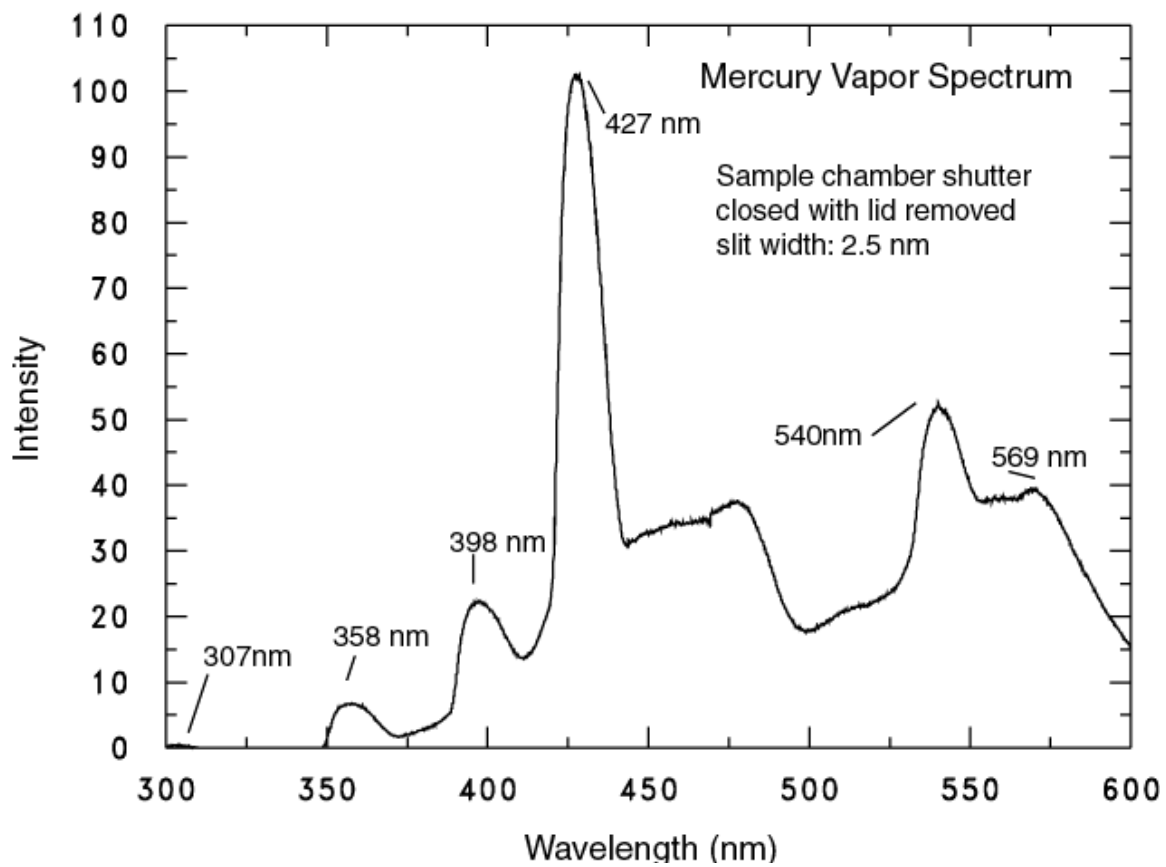


Fig. I.1 Verification of spectrofluorometer wavelength with Mercury standard